OPTIMAL ANALYSIS OF A SUBSURFACE BARRIER FOR SALTWATER INTRUSION CONTROL

BY

MUNDZIR HASAN BASRI

A Thesis
Submitted to the Faculty of Graduate Studies
in Partial Fulfillment of the Requirements
for the Degree of

MASTER OF SCIENCE

Department of Civil & Geological Engineering
University of Manitoba
Winnipeg, Manitoba

ISBN 0-315-99050-3

Name _____

Dissertation Abstracts International is arranged by broad, general subject categories. Please select the one subject which most nearly describes the content of your dissertation. Enter the corresponding four-digit code in the spaces provided.

CIVIL — SUBJECT TERM

0543 — SUBJECT CODE

U·M·I

Subject Categories

THE HUMANITIES AND SOCIAL SCIENCES

COMMUNICATIONS AND THE ARTS
Architecture 0729
Art History 0377
Cinema 0900
Dance 0378
Fine Arts 0357
Information Science 0723
Journalism 0391
Library Science 0399
Mass Communications 0708
Music 0413
Speech Communication 0459
Theater 0465

EDUCATION
General 0515
Administration 0514
Adult and Continuing 0516
Agricultural 0517
Art 0273
Bilingual and Multicultural 0282
Business 0688
Community College 0275
Curriculum and Instruction 0727
Early Childhood 0518
Elementary 0524
Finance 0277
Guidance and Counseling 0519
Health 0680
Higher 0745
History of 0520
Home Economics 0278
Industrial 0521
Language and Literature 0279
Mathematics 0280
Music 0522
Philosophy of 0998
Physical 0523
Psychology 0525
Reading 0535
Religious 0527
Sciences 0714
Secondary 0533
Social Sciences 0534
Sociology of 0340
Special 0529
Teacher Training 0530
Technology 0710
Tests and Measurements 0288
Vocational 0747

LANGUAGE, LITERATURE AND LINGUISTICS
Language
- General 0679
- Ancient 0289
- Linguistics 0290
- Modern 0291

Literature
- General 0401
- Classical 0294
- Comparative 0295
- Medieval 0297
- Modern 0298
- African 0316
- American 0591
- Asian 0305
- Canadian (English) 0352
- Canadian (French) 0355
- English 0593
- Germanic 0311
- Latin American 0312
- Middle Eastern 0315
- Romance 0313
- Slavic and East European 0314

PHILOSOPHY, RELIGION AND THEOLOGY
Philosophy 0422
Religion
- General 0318
- Biblical Studies 0321
- Clergy 0319
- History of 0320
- Philosophy of 0322

Theology 0469

SOCIAL SCIENCES
American Studies 0323
Anthropology
- Archaeology 0324
- Cultural 0326
- Physical 0327

Business Administration
- General 0310
- Accounting 0272
- Banking 0770
- Management 0454
- Marketing 0338

Canadian Studies 0385
Economics
- General 0501
- Agricultural 0503
- Commerce-Business 0505
- Finance 0508
- History 0509
- Labor 0510
- Theory 0511

Folklore 0358
Geography 0366
Gerontology 0351
History
- General 0578
- Ancient 0579
- Medieval 0581
- Modern 0582
- Black 0328
- African 0331
- Asia, Australia and Oceania 0332
- Canadian 0334
- European 0335
- Latin American 0336
- Middle Eastern 0333
- United States 0337

History of Science 0585
Law 0398
Political Science
- General 0615
- International Law and Relations 0616
- Public Administration 0617

Recreation 0814
Social Work 0452
Sociology
- General 0626
- Criminology and Penology 0627
- Demography 0938
- Ethnic and Racial Studies 0631
- Individual and Family Studies 0628
- Industrial and Labor Relations 0629
- Public and Social Welfare 0630
- Social Structure and Development 0700
- Theory and Methods 0344

Transportation 0709
Urban and Regional Planning 0999
Women's Studies 0453

THE SCIENCES AND ENGINEERING

BIOLOGICAL SCIENCES
Agriculture
- General 0473
- Agronomy 0285
- Animal Culture and Nutrition 0475
- Animal Pathology 0476
- Food Science and Technology 0359
- Forestry and Wildlife 0478
- Plant Culture 0479
- Plant Pathology 0480
- Plant Physiology 0817
- Range Management 0777
- Wood Technology 0746

Biology
- General 0306
- Anatomy 0287
- Biostatistics 0308
- Botany 0309
- Cell 0379
- Ecology 0329
- Entomology 0353
- Genetics 0369
- Limnology 0793
- Microbiology 0410
- Molecular 0307
- Neuroscience 0317
- Oceanography 0416
- Physiology 0433
- Radiation 0821
- Veterinary Science 0778
- Zoology 0472

Biophysics
- General 0786
- Medical 0760

EARTH SCIENCES
Biogeochemistry 0425
Geochemistry 0996
Geodesy 0370
Geology 0372
Geophysics 0373
Hydrology 0388
Mineralogy 0411
Paleobotany 0345
Paleoecology 0426
Paleontology 0418
Paleozoology 0985
Palynology 0427
Physical Geography 0368
Physical Oceanography 0415

HEALTH AND ENVIRONMENTAL SCIENCES
Environmental Sciences 0768
Health Sciences
- General 0566
- Audiology 0300
- Chemotherapy 0992
- Dentistry 0567
- Education 0350
- Hospital Management 0769
- Human Development 0758
- Immunology 0982
- Medicine and Surgery 0564
- Mental Health 0347
- Nursing 0569
- Nutrition 0570
- Obstetrics and Gynecology 0380
- Occupational Health and Therapy 0354
- Ophthalmology 0381
- Pathology 0571
- Pharmacology 0419
- Pharmacy 0572
- Physical Therapy 0382
- Public Health 0573
- Radiology 0574
- Recreation 0575
- Speech Pathology 0460
- Toxicology 0383

Home Economics 0386

PHYSICAL SCIENCES

Pure Sciences
Chemistry
- General 0485
- Agricultural 0749
- Analytical 0486
- Biochemistry 0487
- Inorganic 0488
- Nuclear 0738
- Organic 0490
- Pharmaceutical 0491
- Physical 0494
- Polymer 0495
- Radiation 0754

Mathematics 0405
Physics
- General 0605
- Acoustics 0986
- Astronomy and Astrophysics 0606
- Atmospheric Science 0608
- Atomic 0748
- Electronics and Electricity 0607
- Elementary Particles and High Energy 0798
- Fluid and Plasma 0759
- Molecular 0609
- Nuclear 0610
- Optics 0752
- Radiation 0756
- Solid State 0611

Statistics 0463

Applied Sciences
Applied Mechanics 0346
Computer Science 0984
Engineering
- General 0537
- Aerospace 0538
- Agricultural 0539
- Automotive 0540
- Biomedical 0541
- Chemical 0542
- Civil 0543
- Electronics and Electrical 0544
- Heat and Thermodynamics 0348
- Hydraulic 0545
- Industrial 0546
- Marine 0547
- Materials Science 0794
- Mechanical 0548
- Metallurgy 0743
- Mining 0551
- Nuclear 0552
- Packaging 0549
- Petroleum 0765
- Sanitary and Municipal 0554
- System Science 0790

Geotechnology 0428
Operations Research 0796
Plastics Technology 0795
Textile Technology 0994

PSYCHOLOGY
General 0621
Behavioral 0384
Clinical 0622
Developmental 0620
Experimental 0623
Industrial 0624
Personality 0625
Physiological 0989
Psychobiology 0349
Psychometrics 0632
Social 0451

Nom _____

Dissertation Abstracts International est organisé en catégories de sujets. Veuillez s.v.p. choisir le sujet qui décrit le mieux votre thèse et inscrivez le code numérique approprié dans l'espace réservé ci-dessous.

SUJET	CODE DE SUJET

U·M·I

Catégories par sujets

HUMANITÉS ET SCIENCES SOCIALES

COMMUNICATIONS ET LES ARTS
Architecture 0729
Beaux-arts 0357
Bibliothéconomie 0399
Cinéma 0900
Communication verbale 0459
Communications 0708
Danse 0378
Histoire de l'art 0377
Journalisme 0391
Musique 0413
Sciences de l'information 0723
Théâtre 0465

ÉDUCATION
Généralités 515
Administration 0514
Art 0273
Collèges communautaires 0275
Commerce 0688
Économie domestique 0278
Éducation permanente 0516
Éducation préscolaire 0518
Éducation sanitaire 0680
Enseignement agricole 0517
Enseignement bilingue et multiculturel 0282
Enseignement industriel 0521
Enseignement primaire. 0524
Enseignement professionnel 0747
Enseignement religieux 0527
Enseignement secondaire 0533
Enseignement spécial 0529
Enseignement supérieur 0745
Évaluation 0288
Finances 0277
Formation des enseignants 0530
Histoire de l'éducation 0520
Langues et littérature 0279
Lecture 0535
Mathématiques 0280
Musique 0522
Orientation et consultation 0519
Philosophie de l'éducation 0998
Physique 0523
Programmes d'études et enseignement 0727
Psychologie 0525
Sciences 0714
Sciences sociales 0534
Sociologie de l'éducation 0340
Technologie 0710

LANGUE, LITTÉRATURE ET LINGUISTIQUE
Langues
- Généralités 0679
- Anciennes 0289
- Linguistique 0290
- Modernes 0291

Littérature
- Généralités 0401
- Anciennes 0294
- Comparée 0295
- Médiévale 0297
- Moderne 0298
- Africaine 0316
- Américaine 0591
- Anglaise 0593
- Asiatique 0305
- Canadienne (Anglaise) 0352
- Canadienne (Française) 0355
- Germanique 0311
- Latino-américaine 0312
- Moyen-orientale 0315
- Romane 0313
- Slave et est-européenne 0314

PHILOSOPHIE, RELIGION ET THÉOLOGIE
Philosophie 0422
Religion
- Généralités 0318
- Clergé 0319
- Études bibliques 0321
- Histoire des religions 0320
- Philosophie de la religion 0322

Théologie 0469

SCIENCES SOCIALES
Anthropologie
- Archéologie 0324
- Culturelle 0326
- Physique 0327

Droit 0398
Économie
- Généralités 0501
- Commerce-Affaires 0505
- Économie agricole 0503
- Économie du travail 0510
- Finances 0508
- Histoire 0509
- Théorie 0511

Études américaines 0323
Études canadiennes 0385
Études féministes 0453
Folklore 0358
Géographie 0366
Gérontologie 0351
Gestion des affaires
- Généralités 0310
- Administration 0454
- Banques 0770
- Comptabilité 0272
- Marketing 0338

Histoire
- Histoire générale 0578
- Ancienne 0579
- Médiévale 0581
- Moderne 0582
- Histoire des noirs 0328
- Africaine 0331
- Canadienne 0334
- États-Unis 0337
- Européenne 0335
- Moyen-orientale 0333
- Latino-américaine 0336
- Asie, Australie et Océanie 0332

Histoire des sciences 0585
Loisirs 0814
Planification urbaine et régionale 0999
Science politique
- Généralités 0615
- Administration publique 0617
- Droit et relations internationales 0616

Sociologie
- Généralités 0626
- Aide et bien-être social 0630
- Criminologie et établissements pénitentiaires 0627
- Démographie 0938
- Études de l' individu et de la famille 0628
- Études des relations interethniques et des relations raciales 0631
- Structure et développement social 0700
- Théorie et méthodes. 0344
- Travail et relations industrielles 0629

Transports 0709
Travail social 0452

SCIENCES ET INGÉNIERIE

SCIENCES BIOLOGIQUES
Agriculture
- Généralités 0473
- Agronomie. 0285
- Alimentation et technologie alimentaire 0359
- Culture 0479
- Élevage et alimentation 0475
- Exploitation des pâturages 0777
- Pathologie animale 0476
- Pathologie végétale 0480
- Physiologie végétale 0817
- Sylviculture et faune 0478
- Technologie du bois 0746

Biologie
- Généralités 0306
- Anatomie 0287
- Biologie (Statistiques) 0308
- Biologie moléculaire 0307
- Botanique 0309
- Cellule 0379
- Écologie 0329
- Entomologie 0353
- Génétique 0369
- Limnologie 0793
- Microbiologie 0410
- Neurologie 0317
- Océanographie 0416
- Physiologie 0433
- Radiation 0821
- Science vétérinaire 0778
- Zoologie 0472

Biophysique
- Généralités 0786
- Medicale 0760

SCIENCES DE LA TERRE
Biogéochimie 0425
Géochimie 0996
Géodésie 0370
Géographie physique 0368
Géologie 0372
Géophysique 0373
Hydrologie 0388
Minéralogie 0411
Océanographie physique 0415
Paléobotanique 0345
Paléoécologie 0426
Paléontologie 0418
Paléozoologie 0985
Palynologie 0427

SCIENCES DE LA SANTÉ ET DE L'ENVIRONNEMENT
Économie domestique 0386
Sciences de l'environnement 0768
Sciences de la santé
- Généralités 0566
- Administration des hôpitaux 0769
- Alimentation et nutrition 0570
- Audiologie 0300
- Chimiothérapie 0992
- Dentisterie 0567
- Développement humain 0758
- Enseignement 0350
- Immunologie 0982
- Loisirs 0575
- Médecine du travail et thérapie 0354
- Médecine et chirurgie 0564
- Obstétrique et gynécologie 0380
- Ophtalmologie 0381
- Orthophonie 0460
- Pathologie 0571
- Pharmacie 0572
- Pharmacologie 0419
- Physiothérapie 0382
- Radiologie 0574
- Santé mentale 0347
- Santé publique 0573
- Soins infirmiers 0569
- Toxicologie 0383

SCIENCES PHYSIQUES
Sciences Pures
Chimie
- Généralités 0485
- Biochimie 487
- Chimie agricole 0749
- Chimie analytique 0486
- Chimie minérale 0488
- Chimie nucléaire 0738
- Chimie organique 0490
- Chimie pharmaceutique 0491
- Physique 0494
- PolymÇres 0495
- Radiation 0754

Mathématiques 0405
Physique
- Généralités 0605
- Acoustique 0986
- Astronomie et astrophysique 0606
- Électronique et électricité 0607
- Fluides et plasma 0759
- Météorologie 0608
- Optique 0752
- Particules (Physique nucléaire) 0798
- Physique atomique 0748
- Physique de l'état solide 0611
- Physique moléculaire 0609
- Physique nucléaire 0610
- Radiation 0756

Statistiques 0463

Sciences Appliqués Et Technologie
Informatique 0984
Ingénierie
- Généralités 0537
- Agricole 0539
- Automobile 0540
- Biomédicale 0541
- Chaleur et thermodynamique 0348
- Conditionnement (Emballage) 0549
- Génie aérospatial 0538
- Génie chimique 0542
- Génie civil 0543
- Génie électronique et électrique 0544
- Génie industriel 0546
- Génie mécanique 0548
- Génie nucléaire 0552
- Ingénierie des systèmes 0790
- Mécanique navale 0547
- Métallurgie 0743
- Science des matériaux 0794
- Technique du pétrole 0765
- Technique minière 0551
- Techniques sanitaires et municipales 0554
- Technologie hydraulique 0545

Mécanique appliquée 0346
Géotechnologie 0428
Matières plastiques (Technologie) 0795
Recherche opérationnelle 0796
Textiles et tissus (Technologie) 0794

PSYCHOLOGIE
Généralités 0621
Personnalité 0625
Psychobiologie 0349
Psychologie clinique 0622
Psychologie du comportement 0384
Psychologie du développement 0620
Psychologie expérimentale 0623
Psychologie industrielle 0624
Psychologie physiologique 0989
Psychologie sociale 0451
Psychométrie 0632

OPTIMAL ANALYSIS OF A SUBSURFACE BARRIER FOR SALTWATER INTRUSION CONTROL

BY

MUNDZIR HASAN BASRI

A Thesis submitted to the Faculty of Graduate Studies of the University of Manitoba in partial fulfillment of the requirements for the degree of

MASTER OF SCIENCE

Abstract

Saltwater intrusion is a major groundwater quality problem due to excessive freshwater abstraction from coastal aquifers at many locations of the world. Artificial recharge has been widely used to limit the expansion of intruded areas. However, at some locations such as in densely populated areas and metropolitan cities, artificial recharge is neither a feasible nor practical solution. Furthermore, even where it is feasible clogging problems may still exist. This study attempts to assess whether a subsurface barrier can be used to prevent or stop further seawater intrusion. A subsurface barrier is an underground structure which rests on an impervious layer. This structure is made from semi-impervious material, such as puddled clay, silica gel or grouting cement. Because of the difference in permeability between the aquifer and the subsurface barrier, it can lower the fresh-saltwater interface line to the contact point between the subsurface barrier and aquifer in the freshwater region. To simulate the fresh-saltwater interface, the Navier-Stokes, Continuity and Energy equations were solved using the finite element technique. The FLOTRAN computer program (Compuflo, 1992) has been used to investigate the interface encroachment phenomenon. The ANSYS computer package (Swanson, 1992) which uses the Sequential Unconstrained Minimization Technique was employed to optimize the design characteristics and location of the barrier. The results obtained from the numerical calculations were compared with observed values of a laboratory sand-box model conducted by

Sugio et al. (1987). Good agreement was found between calculated and observed values. It is concluded that a subsurface barrier is one alternative that should be seriously considered for saltwater intrusion control in coastal aquifers.

ACKNOWLEDGMENTS

I would like to express my gratitude to the members of my thesis committee. Special appreciation and gratitude are expressed to Professor Slobodan P. Simonovic for his advice and suggestions which have greatly contributed to the progress of this research. His charming personality and continuous encouragement have made the thesis possible.

Sincere thanks are offered to Professor Caspar C. Booy for his help in providing new ideas and in discussing materials, Kathy Norman and Budi Rahardjo for their assistance in arranging the use of ANSYS and FLOTRAN, and James Hildebrandt P.Eng. (WARDROP Inc.) for his patience to guide me in using ANSYS and FLOTRAN in the initial stages of this study. I would also like to thank Roberta Mitchell for her patience and careful attention to detail during the writing of this thesis.

The financial support of the Canadian International Development Agency (CIDA), Canada has made the current study possible and is gratefully acknowledged.

Loving appreciation is expressed to my wife and my family in Indonesia for their love, sacrifice and encouragement which has made this study possible.

CONTENTS

LIST OF FIGURES

LIST OF TABLES

Chapter 1

Introduction

1.1 Saltwater Intrusion Phenomena

In recent years saltwater intrusion, which has been threatening many coastal aquifers, has become one of the major groundwater quality issues in the world. The invasion of seawater into aquifers begins when the amount of abstracted water from aquifers increases without being able to control. This is a common consequence resulting from a dramatically increased demand for water. This increase is due to a vast growth in population and rapid expansion in economy. Moreover, conflicts among users as well as droughts exacerbate the situation. Therefore, efficient planning and proper management of a coastal aquifer, are needed to avoid suffering from a chronic shortage of freshwater in the future.

One of the most important tasks in managing coastal aquifers is the prediction of the shape of the freshwater-saltwater interface and the location of the interface toe. By being able to analyze the shape of the interface and the location of its toe over time, managing coastal aquifers becomes much more reliable.

Saltwater intrusion phenomena have been investigated by a number of authors. Many mathematical simulations of the freshwater-saltwater interface

have been reported. These reports can be classified into two groups: an abrupt interface approach and a transition zone approach.

The first approach assumes that the thickness of a transition zone is much smaller compared to the aquifer thickness. A freshwater-saltwater system has a very narrow contact zone. Jacobs and Schmorak (1960) and Schmorak (1964) investigated the contact zone in coastal areas of Israel and proved that the sharp interface could be justified. Another investigation done by Contractor and Srivastava (1990) indicated that a sharp interface model fits the measured data in most regions of the Northern Guam Lens. Several other authors, Bear and Dagan (1964), Strack (1976), Liu and Cheng (1981), Wilson and Costa (1982), have used this approach in their analyses.

The second approach refers to the existence of a mixing zone between fresh and saltwater. This zone is fairly wide compared to the aquifer thickness. Therefore, the sharp interface is no longer valid. Some researchers have ascertained that consideration of the transition zone is a very important factor in order to perform hydrologic analysis and water supply prediction. In the case of a groundwater basin where pumping rates, natural and artificial recharges, and tidal stresses are the main components, the transition zone approach is the only one which fits the situation. The extracted water, natural replenishment and artificial recharge in the freshwater region and the variation in sea water level in the saltwater region can affect the width of the transition zone simultaneously. Most investigators do believe that the transition zone approach most closely models the saltwater intrusion phenomena. This approach is supported by the fact that freshwater and saltwater are miscible fluids. The investigators who studied the problem using this assumption are Lee and Cheng (1974), Segol and Pinder (1976), Volker and Rusthon (1982), Frind (1982b), and as well as several others.

Although these two approaches have been widely adopted, several investigators have introduced a new classification, namely the multiphase flow approach. In this approach a different immiscible fluid occupies each of several regions of the density-stratified aquifers. The mixing zone between the two regions does not contain an abrupt interface. They suggested that this approach should only be used when the first two approaches fail to provide an acceptable solution.

After developing a better understanding of the saltwater intrusion phenomena, the research continued to study various methods of saltwater intrusion control. There are five known methods for seawater intrusion control (Todd, 1980); (1) modification of pumping pattern; (2) artificial recharge; (3) extraction barrier; (4) injection barrier; and (5) subsurface barrier. The first two methods are widely accepted and commonly implemented. The three other methods are not so common. The idea behind modification of the pumping rate is to reestablish the seaward hydraulic gradient back to the natural condition gradient. To reach such a gradient in the areas where pumping rates are very high, the number of production wells must be reduced. As a compensation, the areas with less abstraction may have more pumping wells. This may change the pattern of the hydraulic gradient. In brief, this method implies relocation of pumping wells.

Artificial recharge is a more popular method than the modification of pumping patterns. The purpose of this method is to recharge freshwater into the water bearing formations where the water table, or the piezometric level, is lowered because of heavy pumping rates. After recharging water into an aquifer with or without pressure, the water table or piezometric level will be raised and the seaward gradient reestablished.

The third method used to control seawater intrusion is installation of a line of wells along the sea coast. Wells that are used to pump seawater flowing from

the sea inland are called trough wells. In addition to removing saltwater, trough wells can lower the water table in the vicinity of the wells. The water table is maintained so that a flow pattern to the sea is formed. If the trough wells work properly, they can act as an extraction barrier to stop the invasion of seawater landward.

A method similar to artificial recharge is the injection barrier method. High pressure injection wells are used to force seawater and freshwater to undisturbed positions. The injection well method involves building a ridge line of wells along the sea coast. They are located in front of the seawater wedge. Injecting water into the aquifers also causes an increase in the water table. This increase in the vicinity of the injection wells, again, creates a seaward gradient flow. If such a flow can be maintained, saltwater intrusion can be controlled.

The least explored method for saltwater intrusion control is a subsurface barrier. A subsurface barrier is an underground structure made from puddled clay, emulsified asphalt, cement grout, bentonite, silica gel, calcium acrylate or plastics. The use of such materials creates a less pervious layer in the subsurface barrier. This layer works as a stopper for the movement of seawater intrusion. It also works as a dam to increase groundwater storage. Despite some advantages, Todd (1980) reported that this method has many problems related to construction cost, resistance to earthquakes, and chemical erosion.

Literature published on controlling saltwater intrusion using subsurface barriers is very limited: Aiba (1983), Sugio et. al. (1987), and several publications in Japanese. Aiba reported the results of experimenting with one subsurface barrier at Miyako Jima Island, Japan and a plan for constructing five other barriers on the same island. Sugio presented the simulation of a moving interface which involves subsurface barrier analysis under transient conditions. Both reported studies have not yet included the optimization approach in their analyses. The

optimization of some design parameters in analyzing subsurface barriers may be beneficial. The parameters to be included in the optimization are the barrier width, the construction material and the location of the subsurface barrier. Without using the optimization approach, the implementation of a subsurface barrier method leads to high construction costs. This is because these costs are dependent upon the width and construction material of the barrier. The location of the subsurface barrier is another important factor because if built at an optimum site the barrier will maximize the freshwater region to be protected. The location of the subsurface barrier is an important factor in maximizing the freshwater region to be protected.

It is clear that saltwater intrusion control using the subsurface barrier method has not been extensively discussed. Therefore, this thesis explores this method and its advantages in order for it to be applied in the future. Also, the author is motivated by the saltwater intrusion problem in Jakarta, the capital city of Indonesia. The author originally comes from that city. In the Jakarta Groundwater Basin, saltwater intrusion is a major groundwater quality problem and tends to be very serious. Seawater continues to advance inland. This is because no action has yet been taken. A very rapid increase in demand for water from industrial, domestic and agricultural sectors aggravates the situation.

A number of studies have been conducted concerning the problem in Jakarta. Most of these studies conclude with suggestions to reduce the pumping rate, to modify the pumping pattern and to implement artificial recharge. These recommendations, to date have been difficult to implement. The author suggests an alternative method - that of a subsurface barrier which should be considered in order to halt or to lessen the acute intrusion problem in the Jakarta Groundwater Basin. The subsurface barrier method may provide a better solution to this

serious problem. Therefore, the author has chosen to explore this method and its advantages for future application in Indonesia.

A review of the literature indicates that only two studies have resulted in shapes of fresh-saltwater interfaces which can be closely compared with those in laboratory tests. The rest of the studies have shown unmatched calculated and observed values. The two successful approaches have been developed using the finite difference method (Sugio et al., 1987) and the boundary integral element method (Liu et al., 1990). As a matter of fact, these two methods are not as widely used as the finite element method. Therefore, an analysis of a moving fresh-saltwater interface using the finite element method is presented in this work.

The objective of the present research is to examine the use of the FLOTRAN computer program, for predicting the location of a fresh-saltwater moving interface with or without a subsurface barrier in an unconfined aquifer. The second objective is to optimize the design of the subsurface barrier and its location subject to a number of constraints using the Sequential Unconstrained Minimization Technique.

1.2 The Objectives of the Study

Groundwater constitutes an important freshwater source which is used to fulfill a basic human need. In recent years the demand for freshwater has increased dramatically. Therefore, more and more people are using groundwater. A rapid increase in population, aggressive industrial growth and a steady rise in the standard of living, together with a diminishing quality of surface water, are reasons for an increase in the use of groundwater. In most cases, the groundwater flow is bordered by the sea. This situation may create problems. Once the

pumping rate exceeds the natural replenishment, flow from the sea starts advancing inland. As a result, saltwater intrusion in coastal aquifers can hardly be avoided.

As mentioned previously, the discussion of saltwater intrusion in coastal aquifers has been motivated by the problems in the Jakarta Groundwater Basin. Knowing that some methods for stopping the invasion of seawater intrusion in the basin have failed to be implemented, the author does believe that the subsurface barrier method is an alternative way to limit the intrusion.

A review of the literature indicates that the investigation of subsurface barriers for saltwater intrusion control is very limited. No approach has been reported which discusses the effort to minimize the construction costs. To date, this cost is still a major constraint in implementing the subsurface barrier method. Thus, research of the subsurface barrier which includes the optimization approach to reduce its contribution cost becomes very important in groundwater management of coastal aquifers.

The literature on the fresh-saltwater interface has been investigated as well. It was found that the shape of the fresh-saltwater interface does not closely compare with the result achieved in laboratory tests. Therefore, a study which examines another model to obtain a better shape of the interface is valuable. One objective of the study is to examine the heat transfer analogy model which may provide acceptable solution. Another objective is to simulate the moving fresh-saltwater interface in response to the existence of a subsurface barrier at some locations in the freshwater region. At the same time, the design parameters and location of the barrier are optimized to create the largest possible freshwater region or the smallest possible intruded area.

To achieve this, the following steps are completed in the research presented in this thesis:

1. Development of a thermal analogy model derived from the Navier-Stokes, continuity, and energy equations for modeling seawater intrusion in coastal aquifers.
2. A numerical simulation of the fresh-saltwater interface in a steady state using the finite element method. A sharp interface model and a transition zone model, which are commonly accepted, are investigated using a simulation approach.
3. Comparison of the numerical results obtained using the FLOTRAN computer program with the laboratory results of Sugio et al. (1987) obtained by the Sand-Box model .
4. Analysis of previous studies that fail to obtain the expected shape of the fresh-saltwater interface, and conducting further simulations in order to improve the solution.
5. Investigating the movement of the fresh-saltwater interface when a subsurface barrier is constructed.
6. Optimization of the design and location of a subsurface barrier in order to maximize benefits from constructing a barrier for seawater intrusion control.

1.3 Outline of the Thesis

This thesis consists of seven chapters. The method of controlling seawater intrusion discussed in this study is one alternative among four other methods. These methods are presented in Chapter 2. Chapter 3 is devoted to an extensive review of the literature on the topics relevant to the present study. This chapter is

divided into three sections. The first section deals with the transition zone approach in simulating seawater intrusion. The second section covers the abrupt interface model. The last section presents the literature on subsurface barriers in more detail.

Mathematical modeling issues involved in groundwater flow calculations are given in Chapter 4. Background on the Sequential Unconstrained Minimization Technique is described in the same chapter.

Chapter 5 presents the solution procedure for the saltwater intrusion problem using the subsurface barrier. A description of the simulation model used in this study, the mesh generation applied and boundary conditions, numerical calculation, data requirement, and primary difficulties constitute this chapter. The optimization procedure, optimization problem formulation and input/output data requirements are also covered in Chapter 5.

Chapter 6 records the results and presents a detailed discussion regarding the findings of this study.

Finally, conclusions derived from the present research as well as recommendations for possible future work are presented in Chapter 7.

Chapter 2

Methods of Controlling Saltwater Intrusion

Under natural undisturbed conditions, a state of equilibrium at the fresh-saltwater interface in a coastal aquifer is maintained. It has a stationary seawater wedge and a freshwater flow to the sea above it. This condition tends to form a hydraulic gradient toward the sea.

By pumping water from a coastal aquifer in excess of natural replenishment, the water table in the freshwater region is lowered to the extent that the piezometric head becomes lower than in the vicinity of the seawater wedge. Under these conditions, the interface starts to advance landward. Once it moves inland, it will reach a new equilibrium. This phenomenon is called seawater intrusion.

Coastal aquifers constitute important sources of water. Many coastal aquifers are intensively exploited. The exploited water may exceed the storage capacity of the aquifer. Consequently, a new equilibrium may not be reached. The lack of equilibrium causes the encroachment of seawater and is a crucial problem. To prevent further intrusion inland, several methods for controlling saltwater intrusion may be applied. A description of the methods for controlling seawater intrusion follows.

2.1 Altering existing pumping schedules.

The method of altering the existing pumping schedule is often called modification of the pumping pattern. This method is widely used for limiting seawater intrusion. It involves changing the location of production wells. Spreading the wells throughout inland areas may reduce the accumulated drawdown.

The main objective of this measure is to reestablish the lowest groundwater level required to form the seaward hydraulic gradient. Usually, the relocation of wells is followed up by altering the pumping schedule. Although the ideas of relocating and scheduling have been widely used, sometimes they are not sufficient to reestablish the water table. The additional action of reducing pumping rates is then required. If the reduction of the amount of groundwater extracted becomes more important than the need for relocation and scheduling changes, the method is no longer called altering the existing pumping schedule but instead, reduction of groundwater extraction.

This situation is shown in Figure 2.1. The figure illustrates the effect of the concentration of pumping wells on the drawdown of the water table. High concentration tends to create groundwater overdraft. Lowering of the water table due to an individual pumping is much less than that due to group pumping.

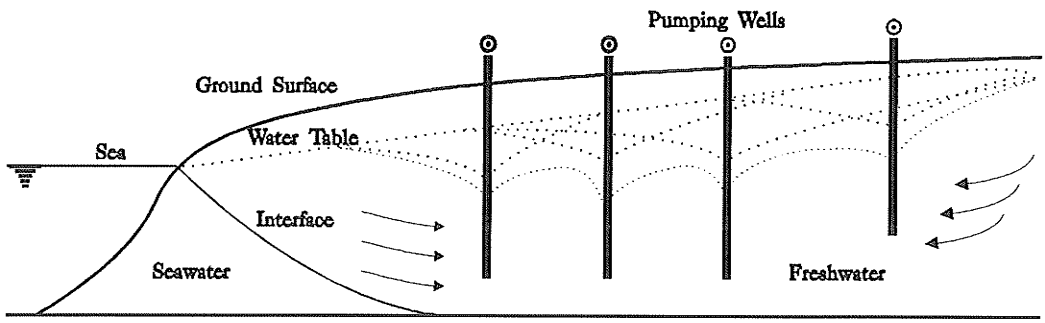

Figure 2.1 Schematic cross section showing individual and composite drawdowns.

Determination of how much water is to be pumped, the schedule of pumping over the entire basin, and the relocation of production wells are essential factors in the implementation of this approach. Hence, this method requires special tools to make the system working properly. A groundwater management model can be used to manage these factors. The model is not a simple system. It involves the recharge system as well. The model becomes more complicated when the source of water is not only from groundwater but also from surface water or even imported water.

Groundwater management, without considering the water surface distribution system as an integral part, simply simulates the rate of withdrawal and the pumping schedule. Then the response can be seen in the observation wells. The level in the observation wells should not be lower than the acceptable level. This level indicates the safe yield of the aquifer. When integrating the surface and groundwater systems, it is necessary to deal with not only the capacity of each, but both. In this case the problem becomes a dual capacity problem. The system, which depends upon the availability of surface water, must consider the quality of water as well as the storage. Modeling a coupled surface-groundwater system is more difficult to handle.

The cost of production is also an important factor to be considered. In most cases, pricing of surface and groundwater supplies is quite different. Based on the quality, accessibility, and exploitation cost considerations, the use of surface water is not more attractive than the use of groundwater. In reality it is quite the opposite. The groundwater source is much more attractive than the surface water source in many cases. It is important to note that the choice exists and is very subjective. People who have been served by fairly reliable piped water consider exploitation of groundwater as the second alternative.

Another important point is that in recent years, economic growth is a main concern in developing countries. A result of this is the growing need for water. Accordingly, the application of this method is not appropriate. It is viable theoretically, but not feasible practically. For instance, pumpers tend to discourage the policy of reduction of pumping rates, the schedule of pumping time or any type of control.

2.2 Artificial Recharge.

Todd (1980) has defined artificial recharge as augmenting the natural movement of surface water into underground formations by some method of construction. The objective of an artificial recharge project may be increased water supply, groundwater quality improvement or low flow augmentation. One of the primary purposes for using artificial recharges in coastal areas is to prevent seawater intrusion. The method of construction depends on several factors, such as topography, geology, soil conditions and, of course, the availability of water surrounding the area of interest. The artificial recharge methods that have been developed include: water spreading, recharge wells and induced recharge wells.

The water spreading method is a method whereby groundwater is recharged by infiltration into unsaturated media and percolates to the water table. Structures like stream channels, ditches and furrows, as well as flooding and irrigation are often used in the water spreading method of artificial recharge. This surface spreading method works very well if there is no impervious layer between the water table to be raised and the bottom layer of flooded areas. It suits only unconfined aquifers. In the case of confined aquifers, an impervious layer is too

difficult to percolate without additional effort. Therefore, recharging water into a confined aquifer, by means of recharge wells is more effective.

Whether or not to choose the surface spreading technique is dependent on several factors. The first is cost and availability of land. The availability of land to be occupied as a flooded area is a necessary condition to be met. The cost of land is an important factor when considering an area of land to be used. The type of soil is the second factor to be taken into account. Gravel, or gravel and sand are strongly recommended. One basic concern is the infiltration rate, which may become the bottleneck in the application of this technique over time. The third factor that should be considered is evaporation. The loss of water by evaporation is a major constraint in areas where the evaporation rate is very high.

After assessing the three main factors above, additional consideration should be given to the following factors: benefit from recreation, the environmental impact , and in some cases, the distance between the recharge areas and the exploited areas.

The effectiveness of this technique is questioned when it faces clogging problems. The surface water spreading method relies on the rate of infiltration to transfer water from the surface into porous formations. The rate of infiltration is high only at the beginning of the operation and it decreases considerably after reaching the peak. This is due to saturation of the soil. The saturated soil causes the swelling of soil particles. At the same time, the soil dispersion phenomenon takes place. Both soil responses due to saturated conditions may reduce the pore space for water infiltration. Furthermore, Bear (1979) points out a number of causes of clogging after the soil saturation is reached. They are: the retention of the suspended solids; growth of algae and bacteria; entrained or dissolved gases released from water; and chemical reactions between dissolved solids and the soil particles and/or the native water present in the void space. As a result, the

spreading operation method works very well only at the outset. After working a relatively short period of time, in most cases the bottom of the infiltration basin is clogged.

Another type of artificial recharge method is the recharge well method. A well is utilized to recharge water from the surface into the aquifer. The well used may be an ordinary pumping well or one specially designed for this purpose. A multi-purpose well that has two functions, to discharge and recharge water from/to aquifer, is a very attractive mechanism. Use of a multi-purpose well is more economical than the construction of a special recharge well. The purpose of this method is indeed to overcome the high cost of the water spreading method in urban areas.

The design of the recharge well makes it appear as if it reverses the function of a pumping well. Unfortunately, this is not the case. The design of a recharge well involves many complicated tasks and solves several problems. It has been acknowledged that pumping water from an aquifer withdraws not only freshwater, but also fine material. This material can go through the pores of water-bearing formations and then approach the well. This may cause clogging of the well screen. Conversely, recharging water from the surface quite often carries fine material such as silt. Again, clogging of the screen and the aquifer itself may occur.

In addition to clogging problems, there are several other difficulties related to the recharge well method. For instance, a large amount of dissolved air is carried together with recharge water. The existence of dissolved air in aquifers may lessen their permeability. Research on water quality indicates that different bacteria can also be found in recharge water. Under certain circumstances, bacteria can grow quickly and eventually reduce the opening space of the well screen. It has also been found that recharge water contains chemical constituents

which in turn lead to flocculation. This is described as a reaction between high sodium water content and soil particles.

Despite the several mentioned disadvantages, this method remains as the primary option to combat seawater intrusion.

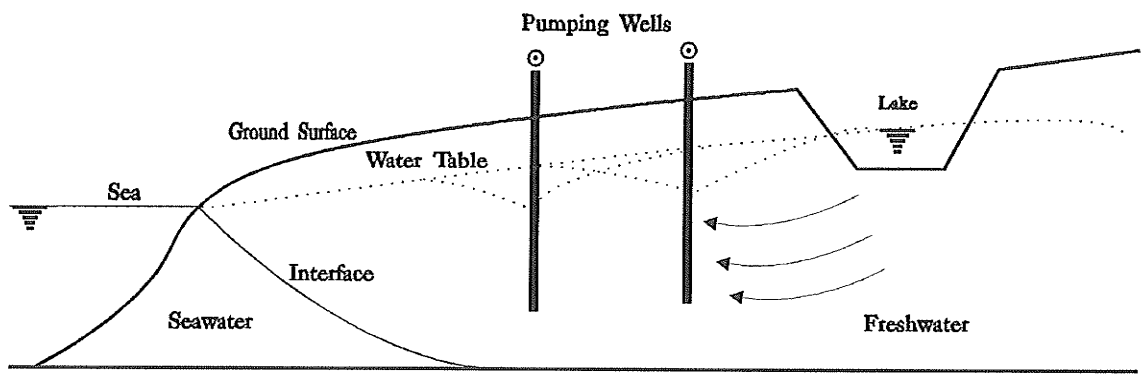

Figure 2.2 Diagram showing the method of induced recharge from the lake.

The third type of artificial recharge method is induced recharge. The induced recharge method is an indirect way of recharging water into the aquifer. The water recharged into the aquifers is supplied by lakes, ponds or rivers. By pumping groundwater surrounding the lakes, ponds or lakes, the water table in the vicinity of the source is decreased. The water table must be lower than the water level of the lake, pond, or river. In this case, the water flows from the lake, pond, or river to the areas where the water table needs to be raised. Therefore, these wells induce water to flow to the aquifer. Figure 2.2 illustrates the way an induced well works.

The effectiveness of this method in terms of the amount of water to be recharged depends upon several factors. The most important factor is the permeability of the aquifer and areas adjacent to the lake, pond or river. Higher permeability allows more induced water to enter the aquifers. The second factor is the pumping rate which affects the hydraulic gradient. Clearly, flow rate from

the lake to the aquifer is a function of the hydraulic gradient. Other factors such as type of soil, distance from the stream surface and natural groundwater movement also contribute to the increase in the amount of water to be stored in the aquifer. By analyzing the factors above, one can ascertain that this method is similar to the water spreading method.

2.3 Hydraulic Ridge (Injection Barrier)

The purpose of this method is to recharge freshwater into the aquifer by injection. It requires a line of recharge wells. These wells are usually located upstream from the toe of the interface or seawater wedge. The wells must be located far enough from the interface toe to provide enough space for seaward flow. Thus, the pressure of recharged water can push the interface seaward. By injecting freshwater with pressure, it is hoped that a pressure ridge can be maintained (see Figure 2.3).

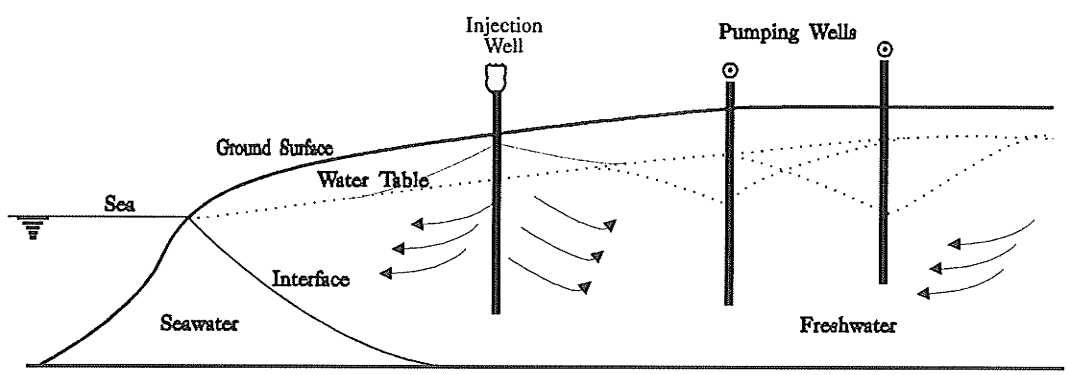

Figure 2.3 Diagram showing injection well increasing water table and forming seaward gradient.

The advantages and disadvantages of this method are quite similar to those of the artificial recharge method. In addition to the information discussed in the

two previous sections, it is important to mention that the freshwater to be recharged must be cleaner than the water used in the artificial recharge methods.

2.4 Pumping Trough (Extraction Barrier).

In contrast to the injection wells method, the pumping trough or extraction barrier method requires a line of pumping wells. They control how much water will be pumped along the fresh-saltwater interface region. These pumping wells should be located between the interface toe and the coast line. The exact location should be determined based on the shape of the interface (see Figure 2.4). Pumping wells are used to withdraw intruded saline water and to drain it to the sea. Pumping wells work if the seaward hydraulic gradient is not large enough to push the freshwater-seawater interface. In addition to withdrawing seawater through trough wells, the groundwater level along the line of trough wells will be lowered. This will cause a seaward flow of freshwater. After a period of time a new equilibrium may eventually be reached. Conversely, if the water table in the freshwater zones decreases, a landward hydraulic gradient is formed.

A major disadvantage of this method is that the amount of freshwater that can be pumped must be reduced. Without reducing the pumping rate, it is impossible to let the system reach equilibrium. Reducing the demand for water is not a popular solution. Other difficulties in implementing this method are related to monitoring the water table and determining the amount of water pumped. Monitoring of the water table over the entire groundwater basin is needed. This will indirectly provide information on the location of the interface toe. Water table data can be used to predict the time when a new equilibrium will be reached. To ensure the shape of saline wedge and the location of the interface toe, there must

be additional monitoring of groundwater quality (for example, monitoring the concentration of Cl^- or salinity). Using a concentration of chlor is more accurate in providing the position of the saline wedge. However, it is an expensive monitoring system.

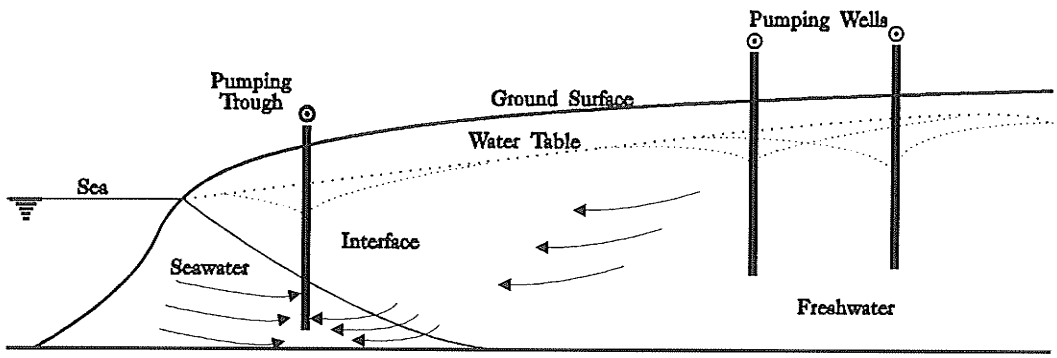

Figure 2.4 Example of pumping trough withdrawing seawater.

After gathering the interface information, determining the amount of water to be pumped is the next task. Pumping less water than is actually needed will lead to the following problems: (a) leaving some saline water in the freshwater region which in turn moves inland; and (b) a seaward hydraulic gradient may not be formed. Conversely, if more water is pumped than what is actually needed, not only saline water but also some freshwater will be withdrawn from the aquifer. Although the amount of freshwater pumped is not very large, it may still cause problem in areas where there is a lack of freshwater sources. Ideally, the amount of water to be pumped should be slightly more than the rate at which seawater is intruding.

2.5 Subsurface barrier.

In the past, constructing a subsurface barrier for controlling saltwater intrusion was not really popular. This is because the construction costs of a physical barrier were very high and the technology was not available. This method was ranked last as a measure of controlling seawater intrusion. A subsurface barrier can be defined as an underground semi-impervious structure in an unconfined coastal aquifer. It is used to delay the movement of seawater inland, and at the same time to increase the groundwater storage capacity.

This idea is illustrated in Figure 2.5a-d. In the first case (Figure 2.5a), the groundwater flow runs off to the sea because of a considerable difference in the water table relative to sea level. Thus, a large amount of potential groundwater can not be used. To avoid groundwater flow toward the sea, it is possible to construct a barrier at an appropriate location. The function of the barrier is to increase the groundwater storage capacity (see Figure 2.5b). In other words, the barrier can raise the water table close to the ground surface. In the second case, the slight difference between the water table and sea level may cause seawater intrusion (Figure 2.5c). As illustrated in Figure 2.5d, the barrier can effectively stop the movement of seawater. As a consequence, it would be possible to maintain a stable water table, or an even higher level, than without the barrier.

The structure is placed between the sea water and the production wells and constructed parallel to the coast. It works in the same fashion as a dam across a river, thus the name of "underground dam" given to it by engineers. In the same way as a dam, the barrier should rest on an impervious layer. The method of construction for such a substructure might be an excavated trench backfilled with bentonite clay, or a closely spaced line of wells through which impermeable grout is injected. It is likely that such a barrier could be effective only in relatively

shallow formations. It is also important to monitor the effectiveness of the barrier to determine the magnitude of the leakage of sea water.

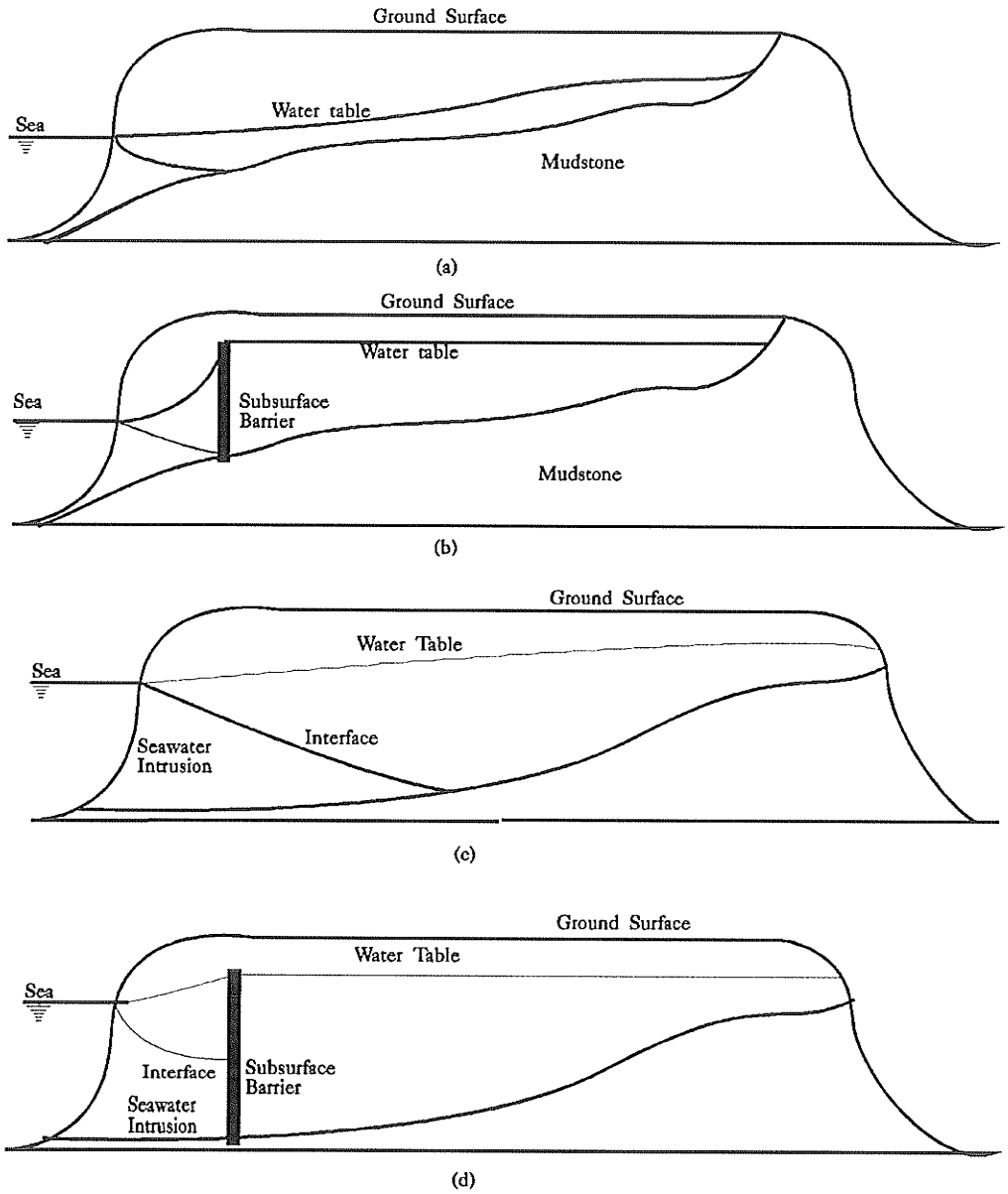

Figure 2.5 An illustration of subsurface barrier.
(a) Minimum groundwater storage out of the barrier; (b) Groundwater table increase with the barrier; (c) Seawater intrusion advancing inland; (d) Seawater intrusion delayed by the subsurface barrier.

The material used for the subsurface barrier is one of the most important factors in its construction. This is not only due to the fact that the material will be used as underground structure, but also because it must solve three major problems explained in the next paragraph. A material which has the properties needed to fulfill all requirements is very rare. However, sheet piling, puddled clay, emulsified asphalt, silica gel, calcium acrylate, and plastics may be used.

Monitoring seawater leakage is an important aspect to be taken into account. Leakage is often used as the measure of whether a barrier works effectively or not. Leakage from the bottom part of the barrier is allowed to release undesirable substances, such as fertilizers, pesticides, or other chemical waste from agricultural and industrial uses. It is important to note that this leakage flow should have a seaward gradient. In coastal aquifers where such dangerous materials can be negligible in the sense of their quantity, there is no need to consider leakage flow through the barrier.

Todd (1980) reported that there are three major obstacles in implementing this method of controlling seawater intrusion: construction cost, resistance to earthquakes, and chemical erosion. Since constructing a physical barrier involves underground work, the cost of construction becomes fairly high compared to other methods. Although many groundwater engineers believe that construction cost is a major constraint in building a barrier, Japanese engineers have succeeded in reducing the cost by utilizing a cement grouting technique. The effect of earthquakes on the barrier has not been intensively investigated. Chemical erosion is related to the aforementioned leakage problem. Subsurface outflow from the basin is difficult to control in order to achieve a balance of salinity.

If the subsurface barrier is effective, the system has the advantage of not allowing significant drawdowns of water levels, which might permit the use of large amounts of stored fresh water. The steepening of the seaward gradient can

be achieved as well. Basically, this method provides a delay, or halts saltwater intrusion into the freshwater zones and therefore enhances the groundwater storage capacity of the aquifer.

Chapter 3

Subsurface Barrier: Literature Review

Literature on groundwater flow and related fields discussing the saltwater intrusion problem and methods of making predictions on the interface encroachment over time, falls into two categories. The first category includes methods that acknowledge the existence of a transition zone between freshwater and saltwater. Investigators using the transition zone assumption are Lee and Cheng (1974), Segol et al. (1975), Liu et al. (1981), Volker and Rushton (1982), Frind (1982b), Rubin (1983), Huyakorn et al. (1986), Huyakorn et al. (1987), Voss and Souza (1987), and Herbert et al. (1988). The second category concentrates on numerical modeling with an abrupt interface in the contact zone. The sharp interface assumption is used by Bear and Dagan (1964), Shamir and Dagan (1971), Volker and Rushton (1982), Taigbenu et al. (1984), Sugio et al. (1987), Contractor and Srivastava (1990), Calvache and Pulido-Bosch (1991), Sugio and Mohamed (1992), and Sugio and Nakada (1992).

3.1 Transition Zone Models

A very common approach dealing with saltwater intrusion is modeling coupled groundwater flow and solute transport with varied density. Fluid density in this approach is a function of solute concentration in the groundwater. Although the density of the groundwater, generally, is nearly constant, it can vary considerably near the coast. This is because seawater near the coast contains much stronger saline solutions than freshwater. The difference in concentration between seawater and freshwater can be modeled using density variations which are a function of solute concentration.

A number of authors have discussed variable density flow and solute transport to analyze and to simulate the fresh-saltwater interface. Henry (1959) developed the first analytical solution for the simulation of saltwater intrusion. This solution is based on the assumption that there is transport of salt in density-dependent fluid flow and a transition zone between the freshwater and saltwater. The transition zone formed is due to hydrodynamic dispersion which in turn varies the density from freshwater to saltwater. Henry's model which is valid only for steady state conditions and confined aquifers was then developed and referred to by many investigators as a basis for their model verification. The shape and position of the interface in Henry's solution are shown in Figure 3.1. The figure does not only present the result of Henry's work but also that of Pinder and Cooper (1970) and Segol et al. (1975). As shown, the interface can be divided into two parts: one being convex, the other concave. The convex part is close to the interface toe. It forms wide angle to the impervious boundary. The concave part is close to the upper interface toe. It is important to note that the starting point of the upper interface toe is at the top boundary.

Using the method of characteristics, Pinder and Cooper (1970) attempted to solve the problem initiated by Henry for unsteady state conditions. The model, known as a particle tracking model, provides results nearly identical to Henry's work but uses reversed initial conditions. Usually, non-zero velocity as an initial value is given to the freshwater side at time $t = 0$. The velocity is then decreased instantly to zero velocity at time $t \neq 0$. In their simulation, zero velocity is the initial value and is increased suddenly. The shape and the location of the interface obtained from this model match Henry's steady state result. Voss and Souza (1987) indicated that porosity included in solute mass balance in Pinder and Cooper's model results in a different shape of the interface. In Henry's original work, it does not. Although Pinder & Cooper and Henry worked with different assumption, their results are almost identical (see Figure 3.1). The only difference is the location of the interface toe. Henry's interface toe is a little further left than Pinder & Cooper's interface.

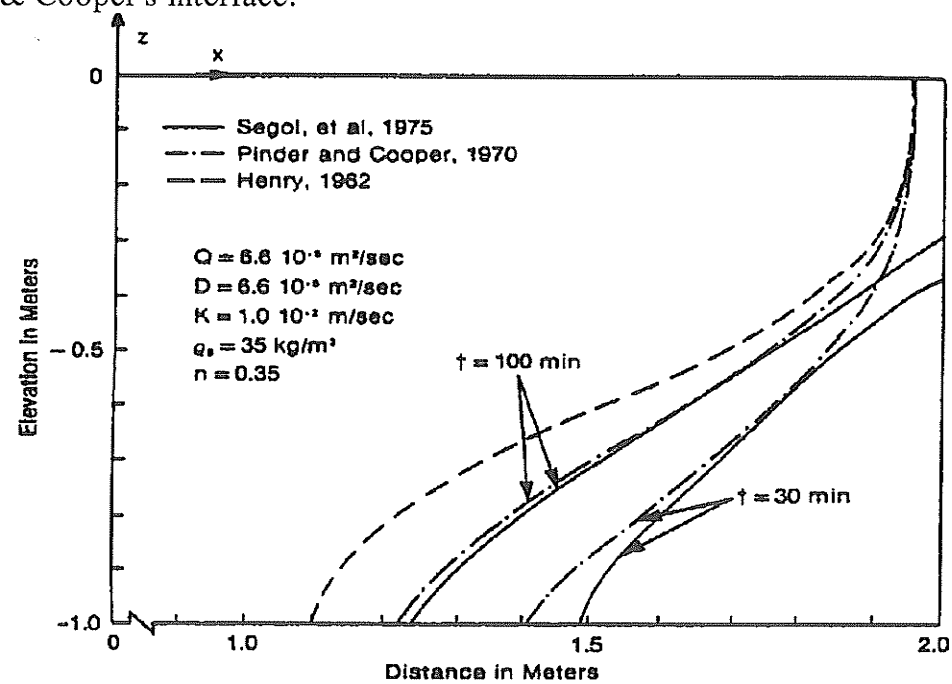

Figure 3.1 Comparison of freshwater-saltwater interface results obtained by Segol et al., Pinder & Cooper and Henry's analytical solution. (After Willis & Yeh, 1987).

The diffused interface model simulation was analyzed by Lee and Cheng (1974). The approach used in their model is similar to Henry's work so that the results are almost identical. Both solutions have the same interface shape, even though they differ in the location of the interface toe. They also have a different upper interface toe, located at the top boundary of the model. Other studies resulted in the upper interface toe being located at the seaside boundary. There are two reasons why this can happen. First, Lee and Cheng specified different transport boundary conditions. Second, they used different numerical techniques (Huyakorn et al., 1987). The numerical technique used in Lee and Cheng's study is the stream function finite element method. This work can be distinguished from previous methods because it treats solute concentration as a dependent variable. Figure 3.2 depicts the results of Lee and Cheng's work. Again, it closely resembles Henry's interface. There are two other interfaces which provide a more reliable solution than those given by Lee & Cheng and Henry. They are those given by Frind (1982b) and Huyakorn et al. (1987) in Figure 3.2 and are represented by solid and dashed lines. They will also be described later.

Another important research document in this group is a study done by Segol et al. (1975) and Segol and Pinder (1976). The model was developed based on the assumption that solute concentration is a dependent variable. They introduced the use of fluid pressure and a velocity component in the formulation of their finite element model. This approach results in the shape of the interface approximating the real one, where the upper interface toe is in the seaside boundary. Although the lower interface toe (this point on called the interface) has a less sharp angle than that obtained under laboratory conditions, results are much improved over those achieved in the two previous studies done by Henry and Lee & Cheng (see Figure 3.1). The location of the upper interface toe is at the saltwater boundary. This indicates outflow above the interface line to the sea.

The outflow above the interface can be used to explain the mass balance over the entire domain. There is outflow to the sea to balance the inflow from the freshwater boundary. The real phenomenon proves this outflow.

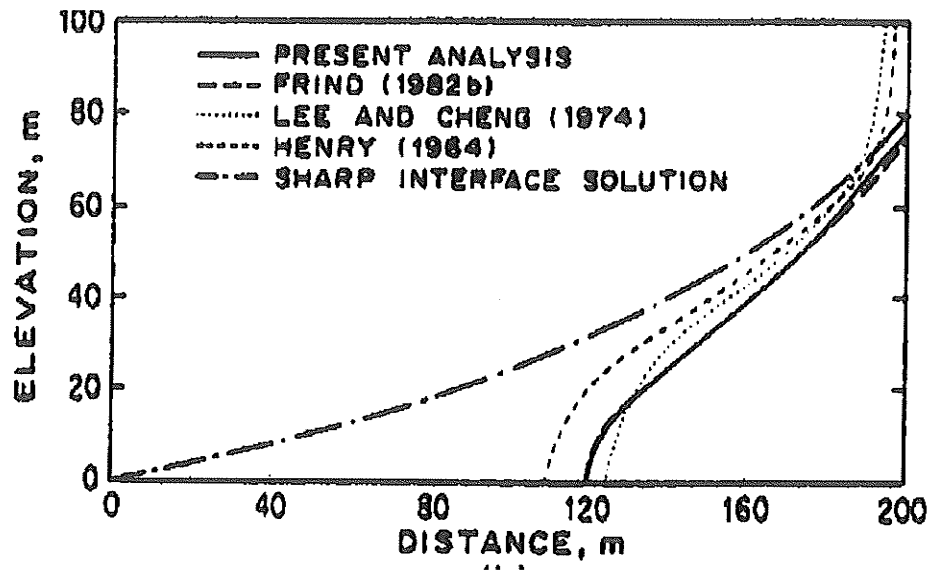

Figure 3.2 Comparison of the result obtained by Huyakorn et al. (1987) for the constant dispersion and several other interfaces (From Huyakorn, 1987).

Frind (1982b) proposed the use of a consistent method to deal with the difficulty in numerical calculations. Using the Galerkin finite element approximation with a consistent method implies the use of one velocity per element. This single value is calculated at the element centroid. Another implication is that the calculation of density is based on the average value. Also, other variables in the mass balance must use an average concentration for each element. Except for these numerical differences, specifying the boundary conditions is practically the same as in the Huyakorn's case. The results of this model were in agreement with the results of the model developed by Huyakorn (see Figure 3.2 and Figure 3.3). One aspect to be noted is that all interfaces in both figures are almost perpendicular to the impervious layer (compared to the sharp interface solution). These results will be improved in this research.

An attempt to complete the consistent approximation developed firstly by Frind was carried out by Voss and Souza (1987). The authors pointed out that inaccuracies in numerical modeling lead to unsuccessful results in solving variable density flow and solute transport problems. To overcome this numerical problem, they proposed three steps toward improved accuracy. The use of a consistent approach in fluid velocity is the first step to be performed. Similar to the approach used in Frind's model, velocities must be evaluated within each finite element. Consequently, the standard Galerkin finite element should be modified in order to have consistent velocities. The second remedy is to have sufficient verification in order to obtain an accurate and stable model. It is simply not enough to verify the model comparing it with Henry's solution. The third aspect to be considered is to use finer spatial and temporal discretization. The size of an element and time step remain major factors in numerical analysis to simulate a narrow transition zone.

The investigation of coupled groundwater flow and solute transport was followed by Huyakorn et al. (1987). As previously described, most investigations dealt with a coupled problem for a confined single layer aquifer. This research was carried out to elaborate more complicated situations, such as multi-aquifer systems and phreatic aquifers. The model was developed not only for the simulation of many types of aquifers, but also for a three dimensional regional coastal aquifer. A Picard sequential solution algorithm with special provisions is used to converge to the Frind and Segol et al. solutions. It can be concluded that these three solutions result in exactly the same interface (see Figure 3.4).

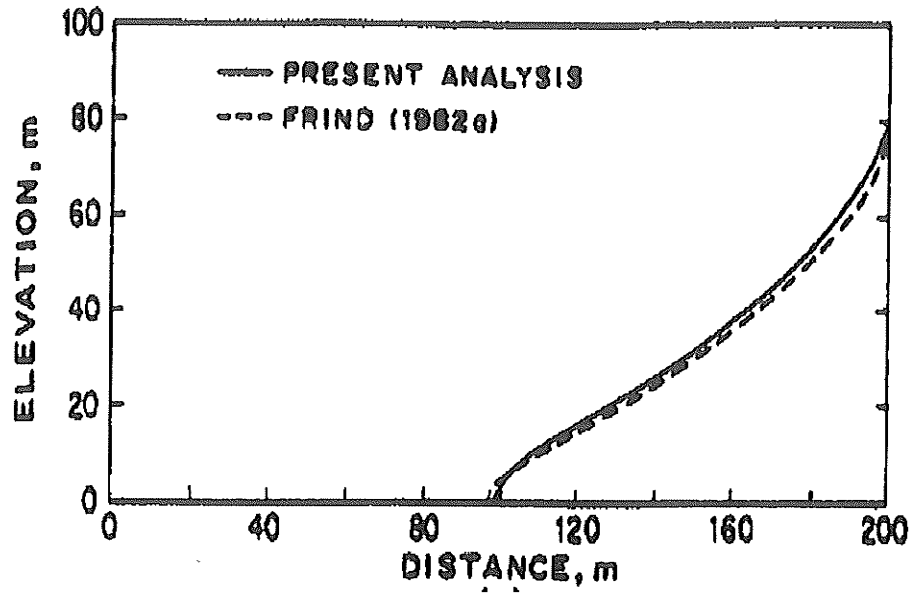

Figure 3.3 Comparison of the 0.5 isochlor for the variable dispersion at steady state obtained by Huyakorn et al. (1987) and freshwater-saltwater interface given by Frind (1982a). (From Huyakorn, 1987).

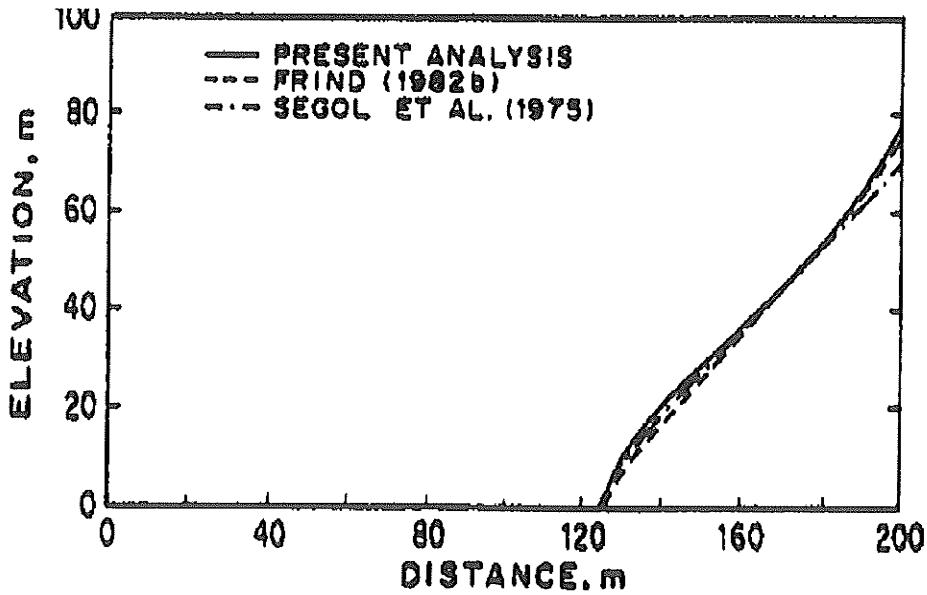

Figure 3.4 Comparison of the 0.5 isochlor for Huyakorn et al. (1987) under transient solution and the results given by Frind (1982b) and Segol et al. (1975). (From Huyakorn et al., 1987).

Figure 3.3 and Figure 3.4 show the difficulty in solving fresh-saltwater interface problems. Although three different research studies substantiate each other, the intersection to the bottom boundary still forms a wide angle.

Another coupled groundwater flow and solute transport model is a model developed by Herbert et al. (1988). Contrary to many solute transport models which assume that the density of the fluid can not be affected by the presence of the solute or tracer, these authors believe that the solute may weaken the density. In the case of density which is strongly dependent upon the concentration of the tracer, applying the mass fraction weighted average velocity, the mass fraction of concentrated salt solution and underlying approximations on the formulation of conservation equations are suggested. The three equations of mass, salt and momentum conservation, should be modified. Since this model was not verified by comparing it with Henry's solution or with other previously mentioned work, the results can not be commented on. The most important contribution of Herbert's work is that it offers an approach which avoids the need for a very fine grid.

3.2 Sharp Interface Models

After discussing the first approach for the simulation of saltwater intrusion, this section deals with the second approach, namely the sharp interface approach. Many researchers believe that a coupled groundwater flow and solute transport approach is more logical to the phenomenon of saltwater intrusion. On the other hand, many others proved that a sharp interface assumption is more often found in the contact zone between freshwater and saltwater. Investigations by Jacobs and Schmorak (1960) and Schmorak (1967) along a coastal aquifer in Israel showed that the shape and the position of the interface approaches an abrupt front. Since the width of the contact zone between freshwater and saltwater is too small compared to the aquifer thickness, the sharp interface is a valid concept used to

explain the intrusion problem. The results of this investigation are used as a basis for later analysis.

An analytical solution for the movement of the fresh-saltwater interface in a confined coastal aquifer was derived by Bear and Dagan (1964). There are several assumptions used in deriving this solution. There are three assumptions used in deriving this solution. They are that the Dupuit approximation must be applied, that the aquifer is homogeneous and isotropic and that there is no hydrodynamic dispersion and compressibility. A rectangular Hele-Shaw cell with an impervious layer on both horizontal boundaries, top and bottom, is used to observe the moving interface over a period of time when a sudden reduction of the discharge from the freshwater side boundary is applied. The observed interfaces from this experiment are compared with the analytical solution. Both solutions, in general, indicate good agreement.

The moving interface under several conditions using the sharp interface assumption was discussed by Strack (1976). The conditions which are valid for steady state flow with homogeneous isotropic permeability are applied to confined and unconfined aquifers. The three dimensional moving interface model is developed to complete the single potential theory of previous studies. For the sake of simplicity, this three dimensional model is treated as two dimensional by discarding the velocity in the y direction. The use of a single potential technique can solve the problem of the discontinuity of velocity gradients and potential at the boundaries. The author suggested that this analytical solution may be used as a part of the numerical solutions. Using the results of this study, it is possible to locate pumping wells properly in the freshwater zone in order to prevent the seawater from advancing toward the inland areas.

One of the authors who used the boundary integral equation method (BIEM) for solving the moving interface in coastal aquifers is Liu et al. (1981).

The BIEM code was developed to simulate the movement of a sharp interface. This numerical solution is verified by comparing the results with the Hele-Shaw experimental model. The comparison shows good agreement. The results were also compared to the experimental results reached by Bear and Dagan (1964) and the finite element model developed by Costa and Wilson (1979) under transient conditions (see Figure 3.5 and Figure 3.6). They are very similar. The observed values obtained by Bear and Dagan show a concave interface at higher time steps. There is a strong indication that an error in performing the Bear & Dagan's experiment causes the results to be different from the numerical calculations. The authors claimed that the difficulty in predicting the shape and location of the interface with any method can be resolved by using the BIEM.

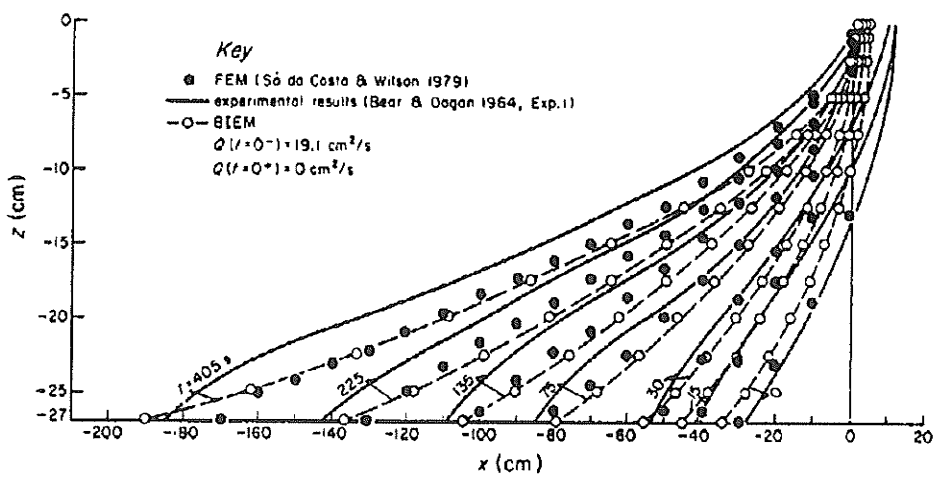

Figure 3.5 Comparison of numerical results obtained by Costa & Wilson (Finite Element) and Liu et al. (Boundary Element) with experimental result observed by Bear & Dagan. Sudden decrease of freshwater level is applied. (After Liu et al., 1981)

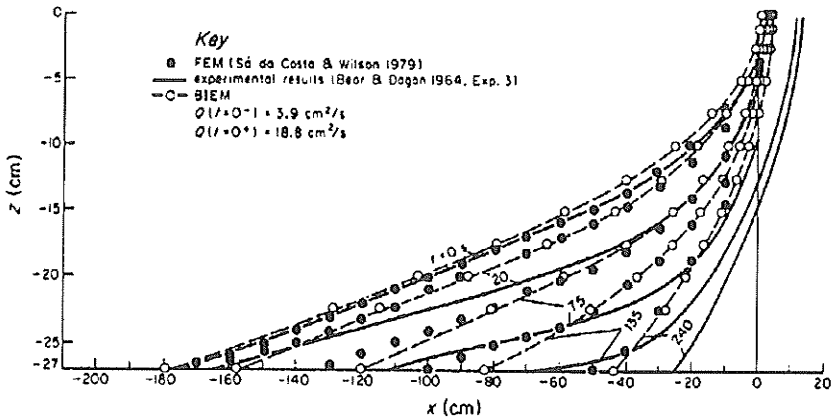

Figure 3.6 Comparison of numerical results obtained by Costa & Wilson (Finite Element) and Liu et al. (Boundary Element) with experimental result observed by Bear & Dagan. Sudden increase of freshwater level is applied (After Liu et al., 1981)

All interfaces in Figure 3.5 are different from those in Figure 3.6. The differences occur because of the use of different experimental procedures. Interfaces in Figure 3.5 are obtained from the experiment with a decrease in discharge flow. In contrast, interfaces in Figure 3.6 are obtained from the experiment with an increase in discharge flow. A sudden decrease of inflow is more meaningful than a sudden increase. Most research on this topic does use the former procedure. However, the interfaces tend to form a convex curve over a longer time. To obtain a concave interface, the procedure is reversed.

The use of a microcomputer to simulate saltwater intrusion was introduced by Contractor and Srivastava (1990). They modified a two-dimensional finite element model developed by Contractor (1983). The reduction in bandwidth size and the manipulation in the stiffness matrix are carried out to obtain an efficient code. This reduces the need for computer memory considerably so that a microcomputer can be used. The modified model applied to the Northern Guam aquifer, indicates that most sub-aquifers match the assumption of the sharp interface. Another conclusion is that verification using the Ghyben-Herzberg approximation does not provide good parameters for aquifers affected by sea level fluctuation. This can be explained by looking at the assumption used in the

Ghyben-Herzberg investigation. They assumed static equilibrium with a hydrodinamic pressure distribution in the freshwater region and with stationary seawater. Obviously, Contractor and Srivastava's model use a dynamic equilibrium. Therefore, the use of the Ghyben-Herzberg approximation is not advocated.

Calvache and Pulido-Bosch (1991) also used the sharp interface approach in analyzing saltwater intrusion in Southern Spain. The finite element model (MODEN2) developed by Verruijt (1987) and the finite difference model (MOCDENSE) by Konikow and Bredehoeft (1984) were applied for the analysis. The finite element model is used to analyze the geometry of the interface and its movement over the time. The groundwater flow equation with the Ghyben-Herzberg relation is used to derive the finite element formulation (Bear and Verruijt, 1987). Unfortunately, due to lack of available data, the results of this simulation can not be verified.

3.3 Subsurface Barrier

A number of research projects have evaluated the success of both approaches, the transition zone and sharp interface, for the analysis of the saltwater intrusion phenomena. Many papers have been published about methods for controlling saltwater intrusion . However, very limited literature is available about saltwater intrusion control using the subsurface barrier method.

Aiba (1980) reported the plan for using a subsurface barrier in several groundwater basins in the South of Japan. The groundwater basins with high permeability and favorable geological structure as well as with the problem of raising groundwater levels are considered to be the best candidates for

construction of subsurface barriers. To examine the ability of a barrier to store groundwater, an experimental subsurface barrier in a small valley of Miyako Island was built. By using the cement grouting method on coral reef limestone it was proved that the barrier can increase the groundwater level even before the construction has been completed.

After the experience with the first subsurface barrier, it was also reported that the design and planning of a subsurface barrier for the National Irrigation Project in Miyako Island was being prepared. A complete plan for five subsurface barriers is still being discussed. In the meantime, the study on the subsurface barrier for coral reef limestone is still continuing. Other geologic conditions, such as alluvial fans, river valleys with gravel and the piedmonts of volcanoes are being extensively investigated as well.

Another research study which focuses on subsurface barriers is the finite difference model developed by Sugio et al. (1987). This study also included an experiment in the laboratory with a physical sand-box model. Sugio's numerical model assumes that there is no transition zone. In other words, it is classified as the sharp interface model. The investigation concentrates on an unconfined aquifer or phreatic aquifer. Test results obtained from the physical sand-box model were used to validate the numerical model. The sand-box apparatus is 1.2 meters long, 0.10 meters wide, and 0.45 meters high. The hydraulic conductivity and porosity of sand material as an aquifer are 0.0038 m/sec. and 0.34 respectively. The freshwater enters the aquifer at the left hand side at the level of 0.403 meters and the saltwater at the right hand side at the level of 0.381 meters. The freshwater and saltwater have densities of 1002 kg/m3 and 1025 kg/m3, respectively. The steady state flow is observed. After reaching an equilibrium, the water level at the left side is lowered instantly. The unsteady state flow is

then observed during a period of 210 minutes using time step of 30 minutes. All these parameters will then be used in this study.

The determination of the location of the interface toe and its shape is the most difficult problem in the simulation of the fresh-saltwater interface. Most of the research indicates that the interface line is perpendicular to the bottom of the impervious layer or that it approaches the bottom at a wide angle. On the other hand, results of laboratory tests show a sharp angle. To solve such a problem, there are a number of techniques that can be employed. A moving grid proposed by Shamir & Dagan (1971) and Bear & Kapuler (1981) and a pseudo interface used by Wilson and Costa (1982) are the most commonly applied. Sugio et al. used the latter method to form a better shape of the interface line. The result proves that the calculated values are exactly the same as the observed values from the sand-box model (see Figure 3.7).

After successfully predicting the fresh-saltwater interface under transient conditions, the next step consists of the simulation of a moving interface with a subsurface barrier. The exact location of the barrier is 0.40 m from the saltwater side. The barrier has a permeability of 0.00005 m/sec. which is a lower permeability than that of the aquifer. The width of the barrier is 0.05 m. At the second stage of the experiment, the density of saltwater and the water level at both sides are changed. The density of saltwater is 1030 kg/m3 and the water levels at the freshwater and saltwater sides are 0.381 m and 0.311 m, respectively. Then, the level at the freshwater side is decreased to 0.312 m. The location of the interface and its movement are observed during a period of 150 minutes (see Figure 3.8). Although calculated and observed values are a poor match, the shape and position of the interface are similar to the expected results.

From the results it can be inferred that the subsurface barrier can stop the movement effectively even though the agreement between the calculated and

observed values is not as good as in the case without the barrier. The authors claim that, even in the worst case scenario, the barrier is able to delay seawater intrusion and to increase the water table.

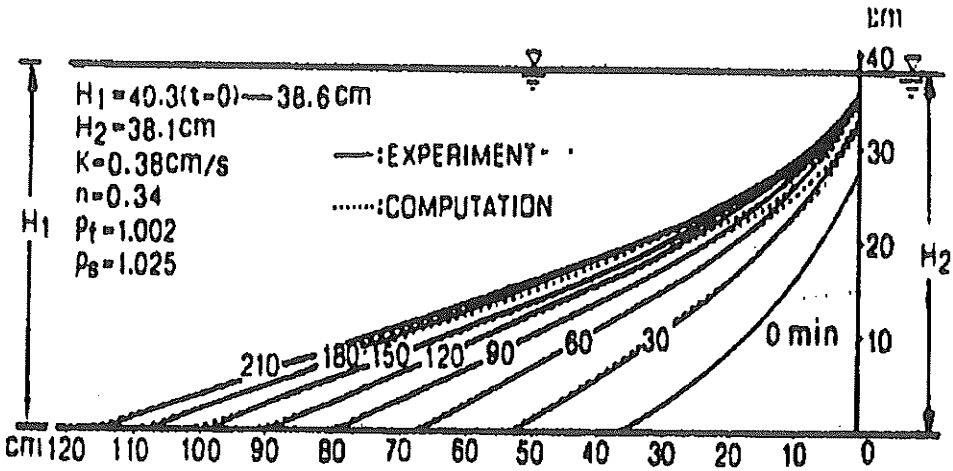

Figure 3.7 Comparison of the finite difference method and observed experimental values (without a subsurface barrier) given by Sugio et al. (After Sugio et al., 1987).

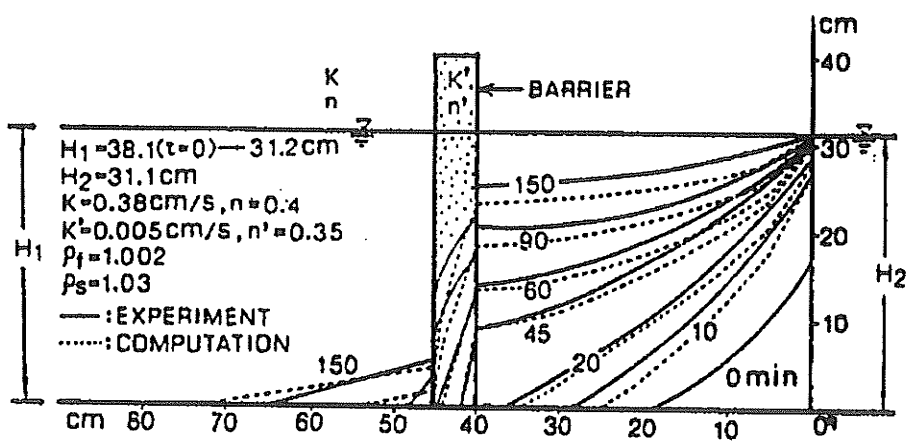

Figure 3.8 Comparison of the finite difference method and observed experimental values (with a subsurface barrier) given by Sugio et al. (After Sugio et al., 1987).

Chapter 4

Subsurface Barrier: Theoretical Background

4.1 Modeling Saltwater Intrusion Using The Heat-Transfer Analogy

A variety of methods have been developed, from physical to complex mathematical models, to simulate saltwater intrusion in coastal aquifers. The thermal analogy model is considered in this thesis. It has not been used for analysis of the seawater intrusion phenomena. The flow of heat can be modeled using the same governing equations are used for groundwater flow. Therefore, the heat-transfer problem is analogous to groundwater flow problems. The analogy as presented by (Todd, 1980) is in Table 4.1.

Table 4.1 Seawater Intrusion Analogy

GROUNDWATER MODEL	THERMAL MODEL
Hydraulic conductivity	Permeability factor
Diffusion coefficient	Fluid conductivity
Storage coefficient	Model thickness*density*specific heat
Flow rate	Heat Flow
Solute concentration	Temperature

The model used in this present study is developed based on the analogy shown in Table 4.1.

4.1.1 Governing Equations

The mathematical model describing incompressible laminar fluid flow with density variations consists of three partial differential equations: the continuity equation, the Navier-Stokes equation and the energy transport equation.

The continuity equation derived from mass conservation in a two-dimensional Cartesian coordinate system may be expressed as:

$$\frac{\partial \rho}{\partial t}+\frac{\partial}{\partial x}(\rho u)+\frac{\partial}{\partial y}(\rho v)=0 \tag{4.1}$$

where ρ is fluid density, u and v are velocities and t is time.

The set of Navier-Stokes equations is used to describe the motion of fluid flow through porous media and may be written as:

$$\begin{aligned}
&\frac{\partial(\rho u)}{\partial t}+\frac{\partial(\rho uu)}{\partial x}+\frac{\partial(\rho vu)}{\partial y}=\rho g_x-\frac{\partial p}{\partial x}+\frac{\partial}{\partial x}\left(\mu\frac{\partial u}{\partial x}\right)+\frac{\partial}{\partial y}\left(\mu\frac{\partial u}{\partial y}\right)+f_x+R_x \\
&\frac{\partial(\rho v)}{\partial t}+\frac{\partial(\rho uv)}{\partial x}+\frac{\partial(\rho vv)}{\partial y}=\rho g_y-\frac{\partial p}{\partial y}+\frac{\partial}{\partial x}\left(\mu\frac{\partial v}{\partial x}\right)+\frac{\partial}{\partial y}\left(\mu\frac{\partial v}{\partial y}\right)+f_y+R_y
\end{aligned} \tag{4.2}$$

where μ is the dynamic viscosity of fluid, g_x and g_y are the gravitational acceleration, p is the fluid static pressure, R_x and R_y are distributed resistance terms. For the sake of simplicity, R_x and R_y are replaced by R_i. R_i is a distributed resistance term for enforcing the barriers that are distributed uniformly over the cross section of porous media. These barriers create uniform resistance

to flow. Therefore, R_i may be characterized as the loss due to the flow through porous media and is then written as:

$$R_i = C\mu V_i \tag{4.3}$$

where C is the permeability factor, and V_i is velocity. The permeability factor in the flow through porous media was discussed by Idelchik (1986). From Equation (4.2) it can be derived that the permeability factor has units [1/length^2] because of the following relationship:

$$R = \frac{\Delta P}{l_0} = C\mu V \tag{4.4}$$

where ΔP is a difference in pressure and l_o is a specified length.

To relate the permeability factor to characteristics of an aquifer, the intrinsic permeability term which depends solely on properties of the solid matrix is used. Combining the permeability factor and the intrinsic permeability leads to:

$$C = \frac{1}{k} \tag{4.5}$$

where k is intrinsic permeability.

Nutting (as quoted by Bear, 1979) developed the relationship between hydraulic conductivity and intrinsic permeability. The relationship is given by:

$$K = \frac{k\rho g}{\mu} \tag{4.6}$$

where K is hydraulic conductivity, ρ is fluid density, g is gravitational acceleration, and μ is the dynamic viscosity. Inserting Equation (4.6) in the Equation (4.5) yields:

$$K = \frac{\rho g}{C\mu} \tag{4.7}$$

Using Equation (4.7), hydraulic conductivity can be replaced by the permeability factor.

For incompressible fluid flow the energy transport equation can be expressed in the following form:

$$\frac{\partial(\rho T)}{\partial t} + \frac{\partial(\rho u C_p T)}{\partial x} + \frac{\partial(\rho v C_p T)}{\partial y} = \frac{\partial}{\partial x}\left(K\frac{\partial T}{\partial x}\right) + \frac{\partial}{\partial y}\left(K\frac{\partial T}{\partial y}\right) + Q_V \tag{4.8}$$

where T is static temperature, C_p is specific heat, Q_V is an unspecified volumetric energy source. Several assumptions are made regarding a number of values in the incompressible energy equation above. First, dynamic temperature is much smaller than static temperature. Therefore, the kinetic energy term can be ignored. Second, the extra viscous term is much smaller than the advection, diffusion, and volumetric heat source terms and therefore, is neglected. Third, the pressure work term is not taken into account in the energy equation.

Equation (4.8) comprises two major terms: (a) the advection term which is described by the two non-linear terms on the left hand side and (b) the diffusion term which is represented by the first two terms on the right hand side. The first term on the right hand side is the transient fluctuation of scalar quantity in an infinite control volume and the last term is a generalized source term.

A summary of the governing equations for laminar incompressible flow in porous media is:

(1) Continuity Equation.

$$\frac{\partial \rho}{\partial t}+\frac{\partial}{\partial x}(\rho u)+\frac{\partial}{\partial y}(\rho v)=0$$

(2) Navier-Stokes Equations.

$$\frac{\partial(\rho u)}{\partial t}+\frac{\partial(\rho uu)}{\partial x}+\frac{\partial(\rho vu)}{\partial y}=\rho g_x-\frac{\partial p}{\partial x}+\frac{\partial}{\partial x}\left(\mu\frac{\partial u}{\partial x}\right)+\frac{\partial}{\partial y}\left(\mu\frac{\partial u}{\partial y}\right)+f_x+R_x$$

$$\frac{\partial(\rho v)}{\partial t}+\frac{\partial(\rho uv)}{\partial x}+\frac{\partial(\rho vv)}{\partial y}=\rho g_y-\frac{\partial p}{\partial y}+\frac{\partial}{\partial x}\left(\mu\frac{\partial v}{\partial x}\right)+\frac{\partial}{\partial y}\left(\mu\frac{\partial v}{\partial y}\right)+f_y+R_y$$

(3) Energy Transport Equation.

$$\frac{\partial(\rho T)}{\partial t}+\frac{\partial(\rho uC_pT)}{\partial x}+\frac{\partial(\rho vC_pT)}{\partial y}=\frac{\partial}{\partial x}\left(K\frac{\partial T}{\partial x}\right)+\frac{\partial}{\partial y}\left(K\frac{\partial T}{\partial y}\right)+Q_V$$

The following three dependent variables should be solved from these three equations:

(1) Velocities in x and y directions;

(2) Static pressure; and

(3) Static temperature.

The variable required in saltwater intrusion problems is the density which varies from freshwater to saltwater. The density is then related to the static temperature. The linear relationship between density and temperature is used:

$$\rho = 1025 - 2.3\ (T - 288) \tag{4.9}$$

4.1.2 Finite Element Method

The finite element method is a numerical technique for solving partial differential equations using an integral equation. This method is more powerful in comparison to the finite difference method developed earlier. It has been applied to numerous problems of flow through porous media, groundwater flow and any other fluid flow. In other disciplines, the use of the finite element method is more advanced than in water resources engineering. The major advantage of the finite element method is that it can accommodate any form of boundary conditions and any combination of them.

The basic partial differential equation describing the advection term for steady state conditions in porous media is:

$$\frac{\partial}{\partial x}\left(\Gamma_\phi \frac{\partial \phi}{\partial x}\right) + \frac{\partial}{\partial y}\left(\Gamma_\phi \frac{\partial \phi}{\partial y}\right) + S_\phi = 0 \tag{4.10}$$

in which ϕ is the general term used to express temperature in Equation (4.8). Equation (4.9) is based on the assumption that for steady state conditions, the flow is dominated by diffusion. Compared to diffusion, advection is much smaller so that it can be neglected. Hence, the second term in the energy equation is

eliminated. Due to no variation in temperature over time, the transient term is also ignored.

To discretize the entire domain in the finite element scheme, the Galerkin method of weighted residuals is used. This method requires the integration of the main governing equation:

$$\int W\left[\frac{\partial}{\partial x}\left(\Gamma_\phi \frac{\partial \phi}{\partial x}\right)+\frac{\partial}{\partial y}\left(\Gamma_\phi \frac{\partial \phi}{\partial y}\right)+S_\phi\right]d\forall^e = 0 \tag{4.11}$$

where W is the weighting factor which has the same meaning as the element interpolation function in the Galerkin weighted residual finite element method.

The integration as described above is performed over elements independently, and summed to provide the total contribution. Because the weighting function is made equal to the shape function defining the approximation, there is a requirement of a higher order of continuity in the shape function. To obtain the first order derivative term, an integration by parts is used to transform the second order derivative term, then:

$$\int \Gamma_\phi\left[\frac{\partial W}{\partial x}\frac{\partial \phi}{\partial y}+\frac{\partial W}{\partial y}\frac{\partial \phi}{\partial y}\right]d\forall^e - \int W\Gamma_\phi\left[\frac{\partial \phi}{\partial x}+\frac{\partial \phi}{\partial y}\right]dS^e - \int WS_\phi dV^e = 0 \tag{4.12}$$

One way to solve Equation (4.12) is to assume a trial solution of the form:

$$\phi = \sum_{i=1}^{N^n} W_i \phi_i \tag{4.13}$$

$$S_\phi = \sum_{i=1}^{N^n} W_i S_{\phi_i} \tag{4.14}$$

$$\Gamma_\phi = \sum_{i=1}^{N^n} W_i \Gamma_{\phi_i} \tag{4.15}$$

where N_n is the number of nodes in the element, W_i are interpolation or shape functions satisfying the boundary conditions imposed on (4.10) and ϕ_i, S_i, and Γ_i are, respectively, the nodal values of variables at N_n discrete node points of the finite element grid.

Substituting these three equations above into Equation (4.12) yields:

$$\int \sum_{i,j,k=1}^{N^n} W_i \Gamma_{\phi_i} \left[\frac{\partial W_j}{\partial x} \frac{\partial W_k}{\partial x} \phi_k + \frac{\partial W_j}{\partial y} \frac{\partial W_k}{\partial y} \phi_k \right] d\forall^e$$

$$-\int \sum_{i,j,k=1}^{N^n} W_i W_j \Gamma_{\phi_j} \left[\frac{\partial W_k}{\partial x} \phi_k + \frac{\partial W_k}{\partial x} \phi_k \right] dS^e - \int \sum_{i,j=1}^{N^n} W_i W_j S_{\phi_j} d\forall^e = 0 \tag{4.16}$$

Let:

$$K_{ij}^e = \int \sum_{i,j,k=1}^{N^n} W_i \Gamma_{\phi_i} \left[\frac{\partial W_j}{\partial x} \frac{\partial W_k}{\partial x} \phi_k + \frac{\partial W_j}{\partial y} \frac{\partial W_k}{\partial y} \phi_k \right] d\forall^e$$

$$-\int \sum_{i,j,k=1}^{N^n} W_i W_j \Gamma_{\phi_j} \left[\frac{\partial W_k}{\partial x} \phi_k + \frac{\partial W_k}{\partial x} \phi_k \right] dS^e \tag{4.17}$$

and:

$$F_i^e = \int \sum_{i,j=1}^{N^n} W_i W_j S_{\phi_j} d\forall^e \tag{4.18}$$

then, Equation (4.15) becomes:

$$\sum_{j=1}^{N^n} K_{ij}^e \phi_j^e = F_i^e \ldots\ldots\ldots j = 1,2,3,,,N^n \tag{4.19}$$

In matrix form (4.18) can be expressed as:

$$[K]\{X\} = \{F\} \tag{4.20}$$

The discretization of Equation (4.18) is done on an element basis and assembled into the global system in which coefficient matrix K_{ij} and source vector are defined as:

$$K_{ij} = \sum_{e=1}^{N^n} K_{ij}^e \ldots\ldots\ldots\ldots F_i = \sum_{e=1}^{N^n} F_j^e \ldots \tag{4.21}$$

where N_e is the number of elements in the solution domain.

The element used is the bilinear quadrilateral. The weighting or interpolation function have the following form for each element:

$$W_i = a_i + b_i x + c_i y + d_i xy \tag{4.22}$$

where the constants a, b, c, and d are expressed in terms of the four grid-point values of ϕ.

4.1.3 Advection Term

The use of Galerkin's method for solving the advection terms numerically causes a dispersion error (Patankar, 1980). The dispersion error describes a spatial oscillation in the solution field of ϕ. This is due to a central difference approximation for any first order derivative term not including ϕ_i for calculating any variable at node i. To resolve this problem, the upwind discretization scheme is used. This scheme uses the value of ϕ at the grid point on the upwind side of the face to the value of ϕ at an interface. The monotone streamline upwind method which can minimize 'crosswind' numerical diffusion considers upwinding occurring along the streamline.

Consider the advection term without the source term in the general form:

$$\frac{\partial(\rho u\phi)}{\partial x}+\frac{\partial(\rho v\phi)}{\partial y}=0 \tag{4.23}$$

This expression can be rewritten in term of the stream wise coordinate system as:

$$\frac{\partial(\rho u_s\phi)}{\partial s}=0 \tag{4.24}$$

where $(\rho u_s\phi)$ is constant along a streamline. It implies that the change of $(\rho u_s \phi)$ in the element basis is also constant as:

$$\left[\frac{\partial(\rho u_s\phi)}{\partial s}\right]^e = const \tag{4.25}$$

Consequently, the discretization of the advective term leads to:

$$A^e = \int W\left[\frac{\partial(\rho u\phi)}{\partial x} + \frac{\partial(\rho v\phi)}{\partial y}\right]^e d\forall^e = \int W\left[\frac{\partial(\rho u_s\phi)}{\partial s}\right]^e d\forall^e = \left[\frac{\partial(\rho u_s\phi)}{\partial s}\right]^e \int W d\forall^e \tag{4.26}$$

To start discretizing the advective term, the downwind node is first defined. A downwind node is a node which has the velocity vector originated from the element itself. This node is at the opposite side from the outflow. The outflow side or face is determined based on the mass flow through each of the element faces. The next step is to calculate the weighting factors for the nodes on the opposite sides using a ratio of mass flows. For instance, in Figure 4.1 N1 is the downwind node. The weighting factors for N2, N3, and N4 would be:

$$WF_{N2} = \frac{\dot{m}_{F2}}{\dot{m}_{F1}} \ldots\ldots WF_{N3} = \frac{\dot{m}_{F3}}{\dot{m}_{F1}} \ldots\ldots WF_{N4} = \frac{\dot{m}_{F4}}{\dot{m}_{F1}} \tag{4.27}$$

where m is mass flow and F denotes a face opposed from the downwind node.

The calculation is followed by the determination of the intersection point between the upstream face and the streamline that coincides with the downstream node. The same figure indicates that the point having the coordinates of X_{us}, Y_{us} and Z_{us} is the intersection point and is defined as:

$$X_{u_s} = \sum_{j=N2,N4} WF_j X_j \qquad Y_{u_s} = \sum_{j=N2,N4} WF_j Y_j \qquad Z_{u_s} = \sum_{j=N2,N4} WF_j Z_j \tag{4.28}$$

The following equation is used to calculate the distance from the downwind node to the intersection point:

$$ds = \sqrt{\left(X_{N1} - X_{u_s}\right)^2 + \left(Y_{N1} - Y_{u_s}\right)^2} \tag{4.29}$$

Therefore, the gradient in Equation (4.24) is formed as:

$$\left[\frac{\partial(\rho u_s \phi)}{\partial s}\right]^e = \frac{(\rho u_s \phi)_{N1} - (\rho u_s \phi)_{u_s}}{ds} \tag{4.30}$$

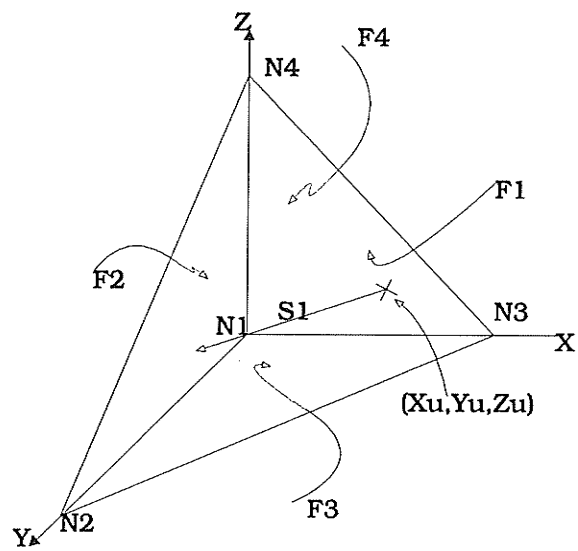

Figure 4.1 Example of a 3-D tetrahedron element in streamline upwind.

Then the influence of the other nodes on the downwind node is calculated and assigned to the off-diagonal terms of the element matrix E_{ij} as the negative of sum of the off-diagonal terms.

$$E_{N1j} = \frac{-\rho_j \sqrt{u_j^2 + v_j^2}}{ds} WF_j \tag{4.31}$$

When all element matrices have been computed, they are assembled into the global coefficient matrix.

4.1.4 Velocity-Pressure Solution

The discretized energy equation is solved for static temperature and the Navier-Stokes equations are solved for the velocity components. Therefore, the continuity equation is needed to relate the velocity components to static temperature. As usual, this relationship can be solved using the velocity-pressure coupling manipulation. Velocity-pressure coupling is performed in two stages. The first stage consists of relating velocity to pressure. This can be done by rearrangement of the partially discretized momentum equations:

$$a_{ii}^{u} u_i = -\sum_{j}^{j\neq 1} a_{ij}^{u} u_j + f_i^{u} - \int W \left[\frac{\partial p}{\partial x}\right]^e d\forall^e$$

$$a_{ii}^{v} v_i = -\sum_{j}^{j\neq 1} a_{ij}^{v} v_j + f_i^{v} - \int W \left[\frac{\partial p}{\partial y}\right]^e d\forall^e \tag{4.32}$$

where a's are coefficients that contribute to the element matrix from the streamline upwind advection terms and the diffusion terms, and f's represent the buoyancy terms, natural boundary condition terms and any other source terms. Equations (4.32) can be rewritten in the form of:

$$u_i = \hat{u}_i - \frac{1}{a_{ii}^{u}} \int W \left[\frac{\partial p}{\partial x}\right]^e d\forall^e \qquad v_i = \hat{v}_i - \frac{1}{a_{ii}^{v}} \int W \left[\frac{\partial p}{\partial y}\right]^e d\forall^e \tag{4.33}$$

where:

$$\hat{u}_i = -\frac{\sum_{j}^{j\neq 1} a_{ij}^u u_j + f_i^u}{a_{ii}^u} \qquad \hat{v}_i = -\frac{\sum_{j}^{j\neq 1} a_{ij}^v v_j + f_i^v}{a_{ii}^v} \tag{4.34}$$

Assuming that the pressure gradient is constant over the elements, Equations (4.33) can be reformulated as:

$$u_i = \hat{u}_i - K_i^u \frac{\partial p}{\partial x} \qquad v_i = \hat{v}_i - K_i^v \frac{\partial p}{\partial y} \tag{4.35}$$

where:

$$K_i^u = \frac{\int W d\forall^e}{a_{ii}^u} \qquad K_i^v = \frac{\int W d\forall^e}{a_{ii}^v} \tag{4.36}$$

Equations (4.35) are then called coupled velocity-pressure equations. These equations are used to update the velocities after achieving the pressure solution.

At the second stage the continuity equation is discretized using Galerkin's weighted residual finite element method. This method implies that the velocity-pressure coupling equations are substituted into the discretized continuity equation. This can lead to the flow pressure equation expressed for the case of incompressible flow in the following form:

$$\int\left[\frac{\partial W}{\partial x}\rho K^{u}\frac{\partial p}{\partial x}+\frac{\partial W}{\partial y}\rho K^{v}\frac{\partial p}{\partial y}\right]d\forall^{e}=\int\left[\frac{\partial W}{\partial x}\rho\hat{u}+\frac{\partial W}{\partial y}\rho\hat{v}\right]d\forall^{e}$$

$$-\int W[\rho u]^{s}dA^{s}-\int W[\rho v]^{s}dA^{s} \tag{4.37}$$

where the integral on the left hand side denotes the pressure diffusion term. The first integral on the right hand side represents known values, and the second integral includes the pressure boundary conditions at the inlet and outlet.

4.2 Optimization

Saltwater intrusion control using a subsurface barrier is optimized by considering two objectives: (a) minimizing the intruded areas; and (b) minimizing subsurface barrier parameters. The optimization scheme is developed based on fresh and saltwater densities. The state variable is the saltwater density at a certain node, and the decision variables are the design parameters (width and construction material) and location of the subsurface barrier.

In general, the optimization problem involves minimization of the nonlinear objective function:

$$Min\ F=F(X_1,X_2,\ldots,X_n) \tag{4.38}$$

subject to

$$\underline{X}_i \le X_i \le \overline{X}_i \cdots (i=1,N) \tag{4.39}$$

$$\underline{g}_j \le G_j(X_1,X_2,\cdots X_N) \le \overline{g}_j \cdots\cdots\cdots\cdots (j=1,M) \tag{4.40}$$

where F is the objective function, X_i is a decision variable, N is the number of decision variables, G_i is a state variable, and M is the number of state variables. $\underline{X}_i$ and $\overline{X}_i$ are the lower and upper bounds of the decision variables and $\underline{g}_j$ and $\overline{g}_j$ are the lower and upper values of the state variables, respectively.

A number of nonlinear solution methods and algorithms can be employed to deal with the above formulation. They include: primary methods, penalty and barrier methods, dual methods and quasi-linearization. The primal solution methods can be divided into four groups in terms of algorithms used: (a) feasible direction; (b) gradient projection; (c) reduced gradient; and (d) projected Lagrangian methods. In the group of penalty and barrier solution methods, the Sequential Unconstrained Minimization Technique (SUMT) is one of the most known algorithms. Dual methods of nonlinear programming include the gradient and cutting plane algorithms. Algorithms of linear and quadratic programming are commonly employed for the quasi-linearization of nonlinear problems.

In this study, the ANSYS computer package is used to optimize a number of parameters. In the ANSYS package, the SUMT optimization algorithm (Fiacco and McCormick, 1968) is applied .

In the ANSYS computer package, F is not a real function of the decision variables, but an approximation. Therefore, F is formulated as the approximation of f. Also, an approximation is introduced for state variables so that G_j is the approximation of g_j. The following equations are the approximations for both the objective function and state variables.

$$F = f + error \tag{4.41}$$

$$G_j = g_j + error \ldots\ldots (j = 1, M) \tag{4.42}$$

The normalized decision variables X_i of the least square regression are used to derive the approximations of F and G_j where X_i is given by:

$$X_i = \frac{x_i - \underline{x}_i}{\overline{x}_i - \underline{x}_i} \ldots\ldots (i = 1, N) \tag{4.43}$$

If the approximations of F and G are replaced by H, the form of the approximation for H is:

$$H = a_0 + \sum_{i=1}^{N} a_i X_i + \sum_{i=1}^{N} b_i X_i^2 + \sum_{i=1}^{N-1} \sum_{j=i+1}^{N} c_{ij} X_i X_j \tag{4.44}$$

where the coefficients a_o, a_i , b_i, c_{ij} are determined by the least square regression. Assuming that $h(k)$ is the k-th function value for design set $x_{i(k)}$, the weighted least square error is:

$$E_k^2 = W^k (h^{(k)} - H^{(k)})^2 \tag{4.45}$$

where $K(k)$ is the weight for design set k. For the design set the total least square error is:

$$E^2 = \sum_{k=1}^{K} E_k^2 = \sum_{k=1}^{K} W^{(k)} (h^{(k)} - H^{(k)})^2 \tag{4.46}$$

where K is the total number of design sets.

To obtain the best approximation, the total least square error must be at the minimum. It reaches the minimum value if the first derivative in respect to each coefficient is equal to zero:

$$\frac{\partial E^2}{\partial a_0} = 0, \ldots \frac{\partial E^2}{\partial a_1} = 0, \ldots \frac{\partial E^2}{\partial b_1} = 0, \ldots \frac{\partial E^2}{\partial c_1} = 0 \tag{4.47}$$

Then a set of linear simultaneous equations is formed.

The criteria used to obtain the best curve fitting is the weighted multiple regression coefficient:

$$R^2 = 1 - \frac{(K-1)\sum_{k=1}^{K} W^{(k)}\left(h^{(k)} - H^{(k)}\right)^2}{(K-Q)\sum_{k=1}^{K} W^{(k)}\left(h^{(k)} - \bar{h}\right)^2} \tag{4.48}$$

where $Q = 2N+1$ for the quadratic curve fit, K is the total number of design sets and h is the weighted mean value of h given by:

$$\bar{h} = \frac{1}{K}\sum_{k=1}^{K} W^{(k)} h^{(k)} \tag{4.49}$$

The curve fitting is finished if:

$$\begin{aligned} &K > 2N+1 \\ &K > \tfrac{1}{2}(N+3)N+1 \end{aligned} \tag{4.50}$$

During the process of determining the best curve fit, the initial fit value is obtained as:

$$H = a_0 + a_1 x_1 + b_1 X_1^2 \tag{4.51}$$

The weight to be used in Equation (4.49) is:

$$W^{(k)} = \left(W_2^{(k)} W_3^{(k)} W_4^{(k)}\right)^q \tag{4.52}$$

where q is an aging exponent defined by:

$$q = \frac{K - M_r}{M_r} \ldots (1 \le q \le 5) \tag{4.53}$$

in which M_r is the number of required design sets to be run. While each weight may be defined as:

$$W_2^{(k)} = 1 - \left[\frac{1}{N}\sum_{i=1}^{N}\left(X_i^* - X_i^{(k)}\right)^2\right]^{1/2} \tag{4.54}$$

$$W_3^{(k)} = 1 - \frac{\left|f^* - f^{(k)}\right|}{f_r} \tag{4.55}$$

where:

$$f_r = \max_k \left|f^* - f^{(k)}\right| \tag{4.56}$$

and:

$$W_4^{(k)} = \begin{cases} 1.0 \\ 0.001 \\ \dfrac{1}{M}\sum_{j=1}^{M}\left(9I_j + 1\right)^{-1} \end{cases} \tag{4.57}$$

The value of I_j is formed using the following relationship

$$I_j = \begin{cases} \dfrac{-g_j^{(k)} + \underline{g}_j - \tau_j}{\overline{g}_j - \underline{g}_j + 2\tau_j} & if \quad g_j^{(k)} < (\underline{g}_j - \tau_j) \\ 0 \quad if \quad (\underline{g}_j - \tau_j) \le g_j^{(k)} \le (\overline{g}_j + \tau_j) \\ \dfrac{g_j^{(k)} - \overline{g}_j - \tau_j}{\overline{g}_j - \underline{g}_j + 2\tau_j} & if \quad g_j^{(k)} > (\overline{g}_j + \tau_j) \end{cases} \tag{4.58}$$

where τ_j is the tolerance level for state variable j.

To enforce the decision and state variables to stay within the prespecified constraints, the penalty functions are employed within the optimization formulation. The penalty function for state variables, is illustrated in Figure 4.2.

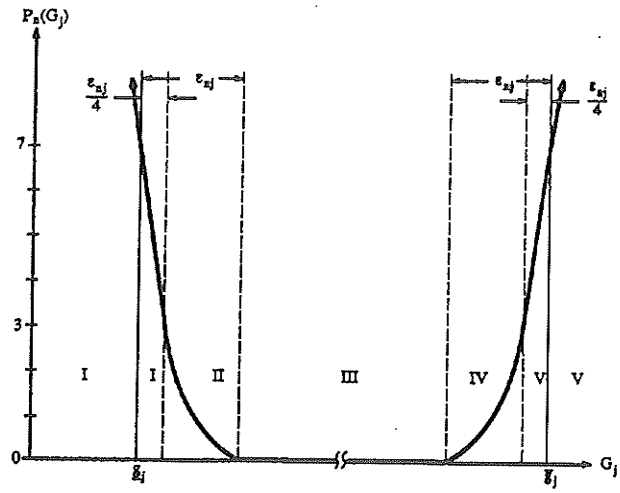

Figure 4.2 Example of Penalty Function for State Variable

The mathematical form of penalty functions for the decision variables is presented in Table 4.2 and for state variables in Table 4.3.

Table 4.2 Penalty function for decision variables.

Region	Limits	Penalty Function Pn(Gj)
I	$x_i \le \left(\underline{x}_i + \frac{\varepsilon_i}{4}\right)$	$10^3\left[7 - 16\frac{(x_i - \underline{x}_i)}{\varepsilon_i}\right]$
II	$\left(\underline{x}_i + \frac{\varepsilon_i}{4}\right) \le x_i \le (\underline{x}_i + \varepsilon_i)$	$10^3\left[\frac{\varepsilon_i}{(x_i - \underline{x}_i)} - 1\right]$
III	$(\underline{x}_i + \varepsilon_i) \le x_i \le (\overline{x}_i - \varepsilon_i)$	0
IV	$(\overline{x}_i - \varepsilon_i) \le x_i \le \left(\overline{x}_i - \frac{\varepsilon_i}{4}\right)$	$10^3\left[\frac{\varepsilon_i}{(\overline{x}_i - x_i)} - 1\right]$
V	$\left(\overline{x}_i - \frac{\varepsilon_i}{4}\right) \le x_i$	$10^3\left[7 - 16\frac{(\overline{x}_i - x_i)}{\varepsilon_i}\right]$

Table 4.3 Penalty function for state variables

Region	Limits	Penalty Function Pn(Gj)
I	$G_j \le \left(\underline{g}_j + \frac{\varepsilon_{nj}}{4}\right)$	$7 - 16\frac{\left(G_j - \underline{g}_j\right)}{\varepsilon_{nj}}$
II	$\left(\underline{g}_j + \frac{\varepsilon_{nj}}{4}\right) \le G_j \le \left(\underline{g}_j + \varepsilon_{nj}\right)$	$\frac{\varepsilon_{nj}}{\left(G_j - \underline{g}_j\right)} - 1$
III	$\left(\underline{g}_j + \varepsilon_{nj}\right) \le G_j \le \left(\overline{g}_j - \varepsilon_{nj}\right)$	0
IV	$\left(\overline{g}_j - \varepsilon_{nj}\right) \le G_j \le \left(\overline{g}_j - \frac{\varepsilon_{nj}}{4}\right)$	$\frac{\varepsilon_{nj}}{\left(\overline{g}_j - G_j\right)} - 1$
V	$\left(\overline{g}_j - \frac{\varepsilon_{nj}}{4}\right) \le G_j$	$7 - 16\frac{\left(\overline{g}_j - G_j\right)}{\varepsilon_{nj}}$

In Tables 4.2 and 4.3, ε_{nj} is a tolerance factor that can be calculated from:

$$\varepsilon_{nj} = (0.002)3^{(3-n)}(\overline{g}_j - \underline{g}_j) \tag{4.59}$$

in which n is the response surface number that varies from 1 to 5.

Adding the penalty function from Table 4.2 and Table 4.3 to the approximated objective function, the unconstrained function or response surface is formed as follows:

$$\phi_n^{(l)} = F^{(l)} + 3^{(n-3)} F^{(l)} \left[\sum_{i=1}^{N} P\left(x_i^{(l)}\right) + \sum_{j=1}^{M} P_n\left(G_j^{(l)}\right) \right] \tag{4.60}$$

where $\phi_n^{(l)}$ is the n-th response surface of the design loop l, $F^{(l)}$ is the least square fit objective function for the design loop l, $P\left(x_i^{(l)}\right)$ and $P\left(G_j^{(l)}\right)$ are penalty functions for the decision and state variables, respectively.

The idea behind the SUMT algorithm is to search for the minimum value of Equation (4.60). This is done using the result from one response surface for the search in the next iteration. This statement can be expressed as:

$$x_i^{(l)} \rightarrow \hat{x}_i \qquad (i = 1, N) \tag{4.61}$$

or:

$$\phi_n^{(l)} \rightarrow a \min \textit{ with respect to } x_i^{(l)} \tag{4.62}$$

For the next loop, a new trial combination is defined as:

$$x_i^{(l+1)} = x_i^* + A(\hat{x}_i - x_i^*) \ldots i = 1, N \tag{4.63}$$

where x_i^* is the current best combination set, $\hat{x}_i$ is the minimum solution from the updated response surface, and $x_i^{(l+1)}$ is a new trial combination which is used to calculate the next objective function. The constant A is calculated using the following expression:

$$A = 1.0 - C_0 - C_r C_i^* \tag{4.64}$$

with the constants C_0, C_i, and C_j :

$$C_0^{'} = C_0 \tag{4.65}$$

$$C_r^{'} = \min \begin{cases} \max \begin{cases} 0.25 \\ C_r \end{cases} \\ 1.0 - C_0^{'} \end{cases} \tag{4.66}$$

$$C_0^{''} = \max \begin{cases} 0.75 \\ C_0 \end{cases} \tag{4.67}$$

and

$$C_r^{''} = 1.0 - C_0^{''} \tag{4.68}$$

Finally, to reach the convergence the following criteria must be met.

$$\left| f^{(l)} - f^{*} \right| < \tau \tag{4.69}$$

$$\left| f^{(l)} - f^{(l-1)} \right| < \tau \tag{4.70}$$

$$\left| f_i^{(l)} - f_i^{*} \right| < \tau_i \quad for\, all\, i = 1, N \tag{4.71}$$

$$\left| f_i^{(l)} - f_i^{(l-1)} \right| < \tau_i \quad for\, all\, i = 1, N \tag{4.72}$$

Using the theoretical background of the optimization approach mentioned above, the optimization procedure, the input/output data and any limitations of the procedure will be presented in Chapter 5.

Chapter 5

Subsurface Barrier: Problem Solution

5.1 Saltwater Intrusion

The analysis of saltwater intrusion presented here can be broken down into six subsections: model description, mesh generation, boundary conditions, numerical calculation, data requirements, and primary difficulties.

5.1.1 Model Description

The problem considered in this study is schematically presented in Figure 5.1. This is an idealization of the laboratory Sand-Box model developed by Sugio et al. (1987). The aquifer thickness 0.45 meters in Sugio's model of will not to be considered in this research. The aquifer thickness is determined on the basis of water tables imposed at both sides. As illustrated, an isotropic phreatic aquifer is subjected to seawater. Freshwater enters the aquifer from the left hand side (or upper side), and seawater from the right hand side. The water table depth at the left hand side and at the right hand side is 0.403 and 0.381 meters, respectively, and it is assigned as the depth of aquifer. The depth of the aquifer between the

sides is assumed to be a straight line. The length of the aquifer is 1.2 meters. Other characteristics of the model are enclosed in the Table 5.1.

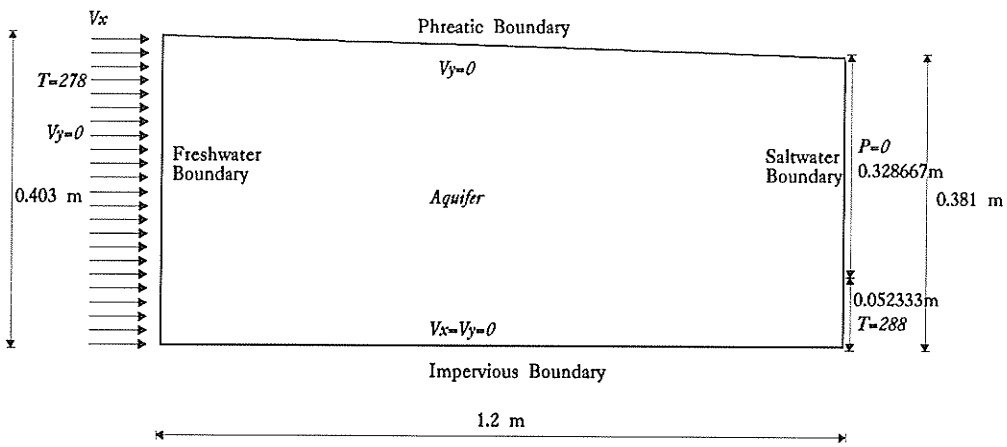

Figure 5.1 Schematic diagram of the model.

Table 5.1 Input data.

Properties of Aquifer and Fluid	Symbols	Values	Units
Permeability factor	C	$7.58e^{+9}$	m^{-2}
Density (freshwater)	ρ_f	1002	kg/m^3
Density (saltwater)	ρ_s	1025	kg/m^3
Temperature (freshwater)	T_f	278	°K
Temperature (saltwater)	T_s	288	°K
Dynamic Viscosity (constant)	μ	$1.518*10^{-3}$	kg/m-sec.
Specific Heat	C_p	4186	J/kg-K
Conductivity	K	$6.11*10^{-4}$	W/m-K

The relationship between density and temperature is given by:

$$\rho = 1025 - 2.3(T - 288) \tag{5.1}$$

where ρ is the fluid density, T is the fluid temperature.

The simulation of fresh-saltwater intrusion uses velocity approximated by Darcy's Law. The hydraulic gradient and the hydraulic conductivity of the aquifer are known, so velocity can be calculated. Velocity and permeability are subjected to change until an acceptable agreement between calculated and observed values (using laboratory tests done by Sugio et al.) is achieved.

5.1.2 Mesh Generation

In solving groundwater flow and solute transport problems, mesh generation plays an important role in obtaining a reliable and reasonable numerical solution. The domain near the bottom of the impervious boundary must be finely discretized. Finer mesh may provide a more accurate representation of the angle between the freshwater-saltwater interface and the impervious boundary. After examining previous work, it became clear that discretization strongly contributed to inaccurate interface estimation. For example, Voss and Souza (1987) concluded that unrealistically fine mesh is required to obtain a reliable shape of the interface. Accordingly, the need for sufficiently fine mesh is an absolute condition to obtain a stable and accurate interface. To obtain such an interface, a higher density of nodes and elements is discretized in the region near the impervious boundary. A coarser grid is placed near the top boundary. Figure 5.2 shows a sufficiently fine grid.

In order to perform the analysis with the subsurface barrier, a similar mesh generation is used to divide the model domain. The subsurface barrier is discretized with finer mesh to allow the smooth interface through the barrier and to fulfill the requirements of the optimization process. In the optimization process, the width of the barrier and its location are decision variables changing

from iteration to iteration. These changes may affect the mesh generation. Each iteration of the optimization process requires the horizontal discretization to be based on the predefined spatial grid, not on the division of lines. The effect of the slope of the top boundary (phreatic surface) on the division of lines close to the top and the bottom boundaries is also considered. The division of lines may result in a different number of lines between the top and the bottom boundaries. This different number of lines can not be discretized. The initial mesh generated for the simulation of fresh-saltwater interface with the subsurface barrier can be seen in Figure 5.3.

ANSYS 5.0
JUL 14 1994
11:31:53
PLOT NO. 1
ELEMENTS
TYPE NUM

ZV =1
DIST=0.968
XF =0.6
YF =0.2015

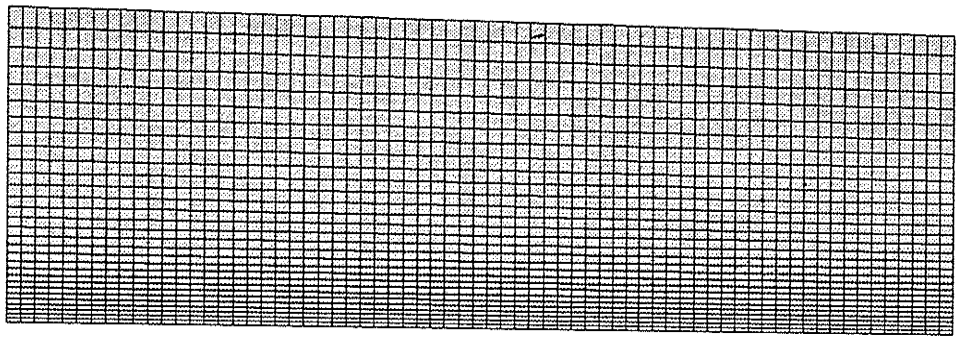

Figure 5.2 Sufficiently fine grid

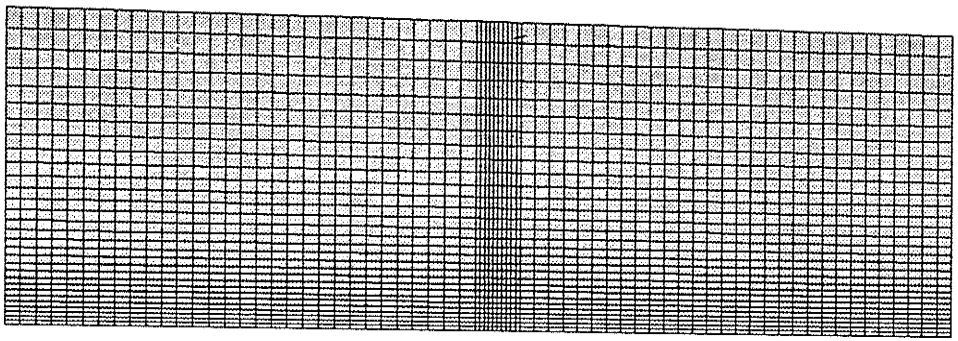

Figure 5.3 Grid for optimization

5.1.3 Boundary Conditions

Boundary conditions employed in this numerical simulation are shown in Figure 5.1. At the left hand side (freshwater boundary) the inlet velocity profile, zero y-direction velocity, and the temperature representing freshwater density are specified. The inlet velocity profile is homogeneous because of the laminar flow assumption. Flow in the y direction is not allowed at the inlet boundary so that zero velocity is specified. Similar to the transition zone approach where zero concentration is specified as representing freshwater, the temperature (278°K) is specified to represent the density of freshwater in this model. At the saltwater front, the temperature of 288°K at the lower portion is specified to simulate saltwater density. Water is allowed to flow out of the system over the top portion of the saltwater boundary. Therefore, zero pressure is specified at that boundary.

Boundary conditions for flow variables at the impervious layer are specified as no flow in all directions. Therefore, the velocity components in x- and y-directions are equal to zero.

Finally, the phreatic surface boundary which has no flow out of the system is considered. Due to the fact that the drawdown of the water table is too small compared to the aquifer thickness, the phreatic surface is assumed to be constant. Zero vertical velocity is specified at the top boundary.

The trial and error process is used to determine the extent of outflow through the seawater boundary. The outflow is considered adequate if the shape of interface and its toe agree with the laboratory results of Sugio's work.

5.1.4 Numerical Calculation

A numerical solution procedure using the finite element method has been presented in Chapter 4. This section is devoted to the description of numerical calculations. The FLOTRAN computer program is used in solving the governing equations. FLOTRAN solves the Navier-Stokes equations employing the Galerkin weighted integral method. Velocity components are solved. By substituting the momentum equations into the continuity equation, the pressure equation is derived. The pressure equation is then solved for static pressure. Finally, the energy equation is solved for static temperature.

In solving the three governing equations, FLOTRAN uses the iterative procedure. It is intended to reduce the amount of required computing time (CPU) as well as the amount of computer memory (RAM). To do this, FLOTRAN uses three iterative solvers: the Tri-Diagonal Matrix Algorithm (TDMA), the Conjugate Residual (CR) and the Conjugate Gradient (CG). In this thesis, the last iterative method is used. The CG iterative solver is derived for incompressible flow and provides the results faster. This can be done by considering only non-zero elements in the matrices.

In brief, the numerical calculation can be summarized as follows:

1. Generate initial guess for velocity field;
2. Calculate the coefficients for velocity solution;
3. Apply velocity boundary conditions;
4. Solve momentum equations with guessed pressure sequentially;
5. Calculate the coefficients for pressure solution;
6. Apply pressure boundary conditions;
7. Solve the pressure equation;
8. Update velocities;

9. Solve energy equation for static temperature; and

10. Update fluid properties.

5.1.5 Data Requirement

From the above description, solution variables obtained from discretized equations are velocities, static pressure and static temperature. These three dependent variables are the output of the model. However, the main concern of this research is the varied density flow. Therefore, the densities for the entire domain are then calculated using Equation (5.1).

Obtaining the discretized equations does not mean that the solution will be obtained. In order to have a complete model, the boundary conditions are needed. These boundary conditions must be considered as the most important component in the development of the complete model. Also, boundary conditions present the greatest difficulty in obtaining a meaningful solution. Generally, there are three types of boundary conditions: the inflow boundary condition, the wall boundary condition and the outflow boundary condition.

The inflow boundary condition consists of prescribed velocities, pressure or temperature. The dependent variables used are those for which there are known values. In this study, velocity and temperature are specified at the inflow boundary. This means that velocity and temperature at the freshwater boundary (left hand side) must be known in advance.

The wall boundary condition is sometimes referred to as the "no slip" boundary. The impervious layer is one example of this type of boundary condition. In this case, the wall boundary condition is at the bottom layer. As

usual, velocity in all directions must be equal to zero. Therefore, the input data for this type of boundary are zero velocities.

The outflow boundary condition can be specified for all three dependent variables. However, in the case of incompressible flow zero pressure is most commonly specified at the outflow boundary. To determine the size of the outflow boundary in the saltwater front, trial and error procedure is carried out.

In most cases the three boundary conditions discussed above are sufficient in order to obtain a solution. Seawater intrusion, discussed in this thesis, is considered for an unconfined aquifer only. Therefore, the phreatic surface boundary must be known. Clearly, the phreatic surface boundary is at the top boundary. It is assumed that the drawdown of the water table in the freshwater region is relatively constant. Hence, specifying zero velocity in the y-direction is the last input data required.

Besides the input boundary conditions, the properties of fluid and the aquifer characteristics are also required. These data are given in Table 5.1 in section 5.1.1.

5.1.6 Primary Difficulties

It is commonly known that using a computer program developed by others is not an easy task. Although theoretical information and user's manuals are available and read, the program may still not be completely understood. For the purpose of this research it was found that a number of important FLOTRAN commands concerning the flow through porous media, were obsolete. Unfortunately, there is no explanation as to which commands can replace the obsolete commands. One can not reach a developer of FLOTRAN without following the chain of command

- support staff, distributor and finally head office. The distributor and support staff, are also users of FLOTRAN. Dealing with each level takes a certain amount of time. If, at the lower level, no answer is obtained, the question may then be presented at the top level (main office in the US). At this level, the importance of any question asked must be proved. Strong arguments supported by output from FLOTRAN are required to convince the FLOTRAN developers to respond to the questions being asked. This takes even more time. Simply put, the version of FLOTRAN used in this thesis seems to have flaws and trying to find another way required much time and energy.

Another difficulty in using FLOTRAN for the research presented was that of limited computer resources. FLOTRAN has large RAM and CPU time requirements. The University of Manitoba Computer Services have identified that FLOTRAN combined with ANSYS represents the largest burden on their resources. The computer resources at the University of Manitoba are designed for multi-user purposes. When the same machine is used by many users, running FLOTRAN becomes a serious problem. Eventually, one machine was specially assigned for FLOTRAN users. This arrangement worked for approximately one month. Then other University needs took precedence and the machine was removed.

5.2 Subsurface Barrier Optimization

This section includes the description of the optimization procedure, the optimization problem formulation and input/output data requirements.

5.2.1 Optimization Procedure

In order to understand the optimization using the SUMT algorithm, several terms are described. Decision variables are independent variables that are subject to upper and lower bounds. State variables are dependent variables that are the function of the decision variables. Typically, state variables are response quantities that can also be constrained by upper and lower limits. The objective function is also a dependent variable and is the quantity to be minimized. As a dependent quantity, the objective function should be the function of the decision variables. A feasible solution refers to a set of decision variables that satisfy all specified constraints and provide the minimum value of the objective function. An infeasible solution is a set of decision variables that violates at least one of the constraints.

Optimization is carried out once the simulation of a fresh-saltwater interface without a subsurface barrier has been successfully completed. The objective of the optimization procedure is to obtain a subsurface barrier which minimizes construction cost as well as maximizes freshwater storage.

Due to the fact that construction cost data are not available, the width and construction material of the barrier, which affect the construction cost, are used as decision variables.

Before explaining the optimization procedure, the link of the optimization routine with ANSYS and FLOTRAN is presented in Figure 5.4.

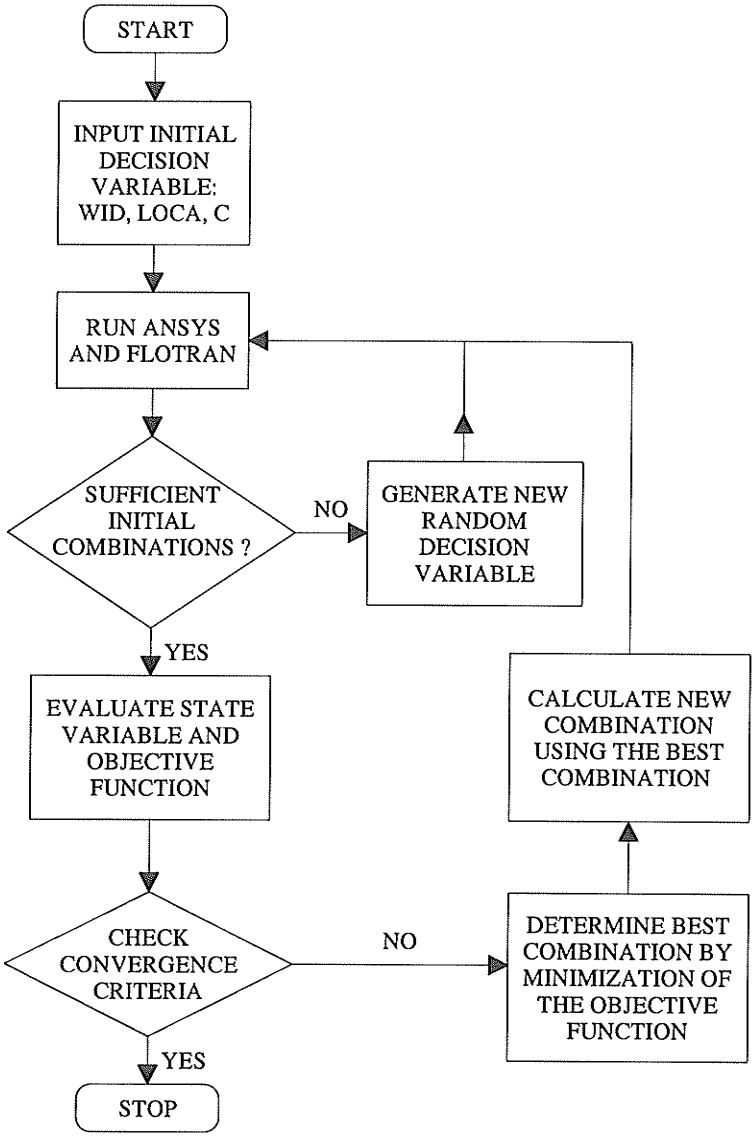

Figure 5.4 Flowchart of integrated process of analysis (optimization, ANSYS and FLOTRAN).
Note: WID is the subsurface barrier, LOCA is the location of the subsurface barrier and C is the construction material of the subsurface barrier.

The optimization procedure is integrated with the analysis of the fresh-saltwater interface.

The procedure includes the following steps:

1. Generation of a set of random decision values (width, material and location of the barrier) in order to obtain a sufficient number of combination sets. More combination sets will increase the chances of obtaining the optimal solution.
2. Calculation of the approximated values for the objective function and state variables. These approximations are calculated using the least square regression on the decision variables. A quadratic plus cross term fit is used to approximate the objective function and a quadratic fit is used to approximate the state variables.
3. Conversion of approximated objective function and approximated state variables to an unconstrained optimization problem. This conversion is performed to achieve a more efficient search for the optimum value. The conversion is performed using penalties for both approximations to take into account constraints on the decision variable and state variables.
4. Optimization of an unconstrained problem. The sequential unconstrained minimization technique (SUMT) is used. The minimum value of decision variables found by SUMT is called the predicted value or the predicted combination.
5. Calculation of the new combination with the best set of decision variables.

To sort a new set of decision variables, the criteria to be used are:

Criterion (a):

$$\left|F_{current} - F_{best}\right| < T_F \tag{5.2}$$

where $F_{current}$ is the objective function value of the current iteration, F_{best} is the objective function value for the best combination of the decision variables, and T_f is the objective function tolerance level.

Criterion (b):

$$\left|F_{current} - F_{current-1}\right| < T_F \tag{5.3}$$

where $F_{current-1}$ is the objective function value from the previous iteration.

Criterion (c):

$$\left|X_{n(current)} - X_{n(best)}\right| < T_n \tag{5.4}$$

where $X_{n(current)}$ is the current value of decision variables, $X_{n(best)}$ is the best value of decision variables, and T_n is the decision variable tolerance level. This is calculated using:

$$T_n = 0.01 * \left(\overline{X}_n - \underline{X}_n\right) \tag{5.5}$$

where $\overline{X}_n$ and $\underline{X}_n$ are the upper and lower bounds of the decision variables.

Criterion (d):

$$\left|X_{n(current)} - X_{n(current-1)}\right| < T_n \tag{5.6}$$

where $X_{n(current-1)}$ is the value of the decision variables from the previous iteration. If one of these conditions is violated, the process continues by returning to step 2 until convergence is achieved.

5.2.2 Optimization Problem Formulation

In most cases concerning the management of groundwater coastal aquifers, modelers tend to use pumping rate as an objective function. When the pumping rate is the single objective function, the maximum extraction is the main goal. In other cases, groundwater level could be used as the objective function . If this the case, then minimum drawdown is the main concern. In this thesis neither pumping rate nor groundwater level is considered. Instead, the freshwater region is used as an objective function. Thus the main goal is to maximize the freshwater region or to minimize the saltwater region. To represent the freshwater region in the optimization formulation, the total density for the entire model is used. For example, if the domain of the model is occupied by saltwater, the total density is equal to 1025 times the number of nodes. Conversely, if the domain is occupied by freshwater, the total density would be 1002 times the number of nodes. In both cases, the number of nodes is constant. The optimum value is somewhere in between what the total density would be with a domain of saltwater and what the total density would be with a domain of freshwater. Therefore, the objective function is to minimize the total density for the whole domain of the model.

In the case of protecting freshwater zones from seawater intrusion using a subsurface barrier, the width of the subsurface barrier (**wid**), the location of the subsurface barrier from the coast line (**loca**), and the construction material of the subsurface barrier (**c**) are chosen as decision variables. Both **wid** and **loca** can not be zero or negative and have the upper and lower limits. Taking **wid** as equal to zero, really means there is no barrier in the fresh-saltwater interface model; in contrast, a very wide barrier results in a very costly solution.

In the same way, taking zero **loca,** or locating the barrier too close to the seawater front allows all the saline water to approach the freshwater area. On the other hand, locating the barrier far away from the saline wedge may decrease the benefits derived from constructing a subsurface barrier.

In the case of the first two decision variable one can see that the ideal solution is not always possible. This is also true for the third decision variable - construction material. The subsurface barrier can not be made of as porous material as the aquifer. This will reduce the main function of the barrier which is to delay saltwater intrusion. However, a fully impervious material for the subsurface barrier will increase the construction cost considerably. A trade-off among the three decision variables is required in order to obtain an optimal solution.

Experience with subsurface barriers using different types of materials is still limited. Consequently, information on construction costs related to various types of material is incomplete. It is believed that the cost of subsurface barriers made of fully impervious material is much higher than those made with less impervious materials. For instance, the cement grouting material and sheet piles that are used to construct fully impervious barriers are costly. Other materials, such as puddle clay and bentonite that can be used to construct less impervious barriers are less expensive. In brief, the cost of constructing the subsurface barrier may vary substantially depending upon the type of construction material used. Therefore, use of the type of material as a decision variable is justifiable.

5.2.3 Input/Output Data Requirements

The most important task in the optimization process within ANSYS is to mesh the domain parametrically. This means that using numbers in generating the mesh becomes invalid in the optimization process. Search for the optimal solution is an iterative process. Each iterative uses different values of decision variables. These different values may provide different grids which can sometimes terminate the calculation. The only way to keep FLOTRAN calculating is to mesh the domain using variables, not numbers. This has been explained in the mesh generation section. The requirements for optimization must be met in developing the grid.

Once the domain is appropriately discretized, input data for optimization are few. The first input is to determine the initial value of decision variables. This starting point is needed in the search for global optimum. The second input is to define decision variables (**loca**, **wid**, and **c**) including the lower and upper bounds on their values. The third input is to define the state variable (**tnode2**) including the lower and upper bounds. The fourth input is to define the objective function (**densum**) without the lower and upper bounds. Finally, the number of iterations needed to reach the expected optimal solution must be specified. Appendix I (Problem Set-up: Optimization) shows the input data required for optimization. Note that the preparation of input data for the optimization is only a small portion of the whole analysis.

The results of the optimization procedure are the output which reports the status of the solution. The solution may be infeasible and/or feasible. If all solutions are infeasible, a new input with a different starting point must be attempted. After obtaining some feasible solutions, the best solution can be identified. Using the best solution, the search can continue. The same procedure can be repeated until the best solution is obtained. Appendix 3 presents an

example of optimization results. All decision variables, state variables and objective function values are reported for every iteration.

Chapter 6

Results and Discussion

6.1 Results

The moving interface phenomena using the heat transfer analogy model has been used. As described in Chapter 5, the simulations have been carried out for unconfined coastal aquifers under steady state conditions. An unconfined aquifer or phreatic aquifer is considered because a subsurface barrier is suitable for this type of aquifer. Technological difficulties have been encountered during construction of the subsurface barrier in deeper aquifers (Todd, 1980). Two main reasons why the simulations were done under steady state conditions are: (a) to provide the expected solution; and (b) to spend less CPU time.

Running the program under transient conditions is more preferable than under steady state conditions. The transient condition is a closer representation of the real problem of seawater intrusion. However, due to the numerical complexity in deriving the discretization equation, the solution can not be obtained by the FLOTRAN program in an efficient manner. Furthermore, limited research has been done regarding the phreatic surface model. Another problem is the seepage face. It is ignored in many studies. Therefore, an approach under steady state conditions is a good approach to model the problem of saltwater

intrusion. Under steady state conditions the FLOTRAN program provides the expected results.

CPU time is also taken into consideration. Running the program under transient conditions, takes much more CPU time than under steady state conditions. With the limited computer resources at the University of Manitoba, the transient condition is not a feasible option.

The problem of saltwater intrusion in an unconfined aquifer has typical difficulties with boundary conditions. The first difficulty is mentioned in the second paragraph of this section - that of the phreatic surface boundary. Because the phreatic boundary changes over time, it becomes a moving boundary. The problem with a moving boundary is still unresolved. The second difficulty is, again, related to a boundary. In the freshwater boundary, the specified load changes because of the fluctuation in the water table over time. Accordingly, the input of the loading system at that boundary must be changed to reflect this. This kind of difficulty has not been resolved by FLOTRAN or by other commercial software. Also, this typical problem has not been solved by most groundwater models. At this point, modeling saltwater intrusion in an unconfined aquifer under steady state conditions is still the best choice. Assuming constant free surface means that the loading system is not necessarily changed.

The simulation begins by matching the fresh-saltwater interface line with observed values of laboratory tests done by Sugio et al. (1987). This matching process, or calibration stage is intended to find approximated values of the aquifer characteristics in terms of the heat transfer analogy scheme. Theoretically, the parameters of Sugio's experimental work can be converted using Equation (4.5), (4.6) or (4.7). However, some required values in those equations are not available. For instance, dynamic viscosity is required but not known. Therefore, the dynamic viscosity was taken by an approximation to obtain a permeability

factor which is a function of dynamic viscosity. This approximation, of course, creates some errors. To avoid unnecessary errors, the calibration was carried out.

The result of the calibration is shown in Figure 6.1. The interface line in this figure was said to match Sugio's observed values, if three criteria were met. The first and second criteria refer to the position of the interface toe and upper interface toe, respectively. They are given by the first line of Table 6.1. These two numerical criteria must be visually matched with the shape of the fresh-saltwater interface line of Sugio's work. Visual calibration as the third criterion for the shape of the interface line was carried out because the numerical results are not available.

The parameters obtained from the calibration were used to determine the shape of the interface line and the position of the interface toe and upper interface toe for the subsequent decrease of a steady state condition. The water table is gradually decreased from 0.403 meters to 0.386 meters. If the three criteria are not met, the parameters may be changed. Then the first run of calibration (water table at 0.403 meters) must be repeated. This trial and error method is repeated until three criteria are matched between calculated and observed values. Appendix 3 presents an example of calculated values for every iteration. This output is taken from the first run in calibration stages and indicates the progress of convergence every ten iterations. All dependent variables for all nodes can be printed. However, in this example, only temperatures are given.

Figures 6.1-6.8 at the end of this section display the results of finite element simulations using the computational fluid dynamic to investigate the shape of the fresh-saltwater interface and the location of its toe. As mentioned, Figure 6.1 depicts the fresh-saltwater interface at the freshwater level of 0.403 meters (see Table 6.1). This is equivalent to the simulation at time t=0 (the number in the brackets in the first column of Table 6.1) of Sugio's experiment. Figure 6.2

presents the interface when the freshwater level drops to 0.3970 meters. It is equivalent to the simulation at time t=30 minutes of Sugio's experiment. Figure 6.3 to Figure 6.8 are the interface lines at the following stages of decreasing freshwater level from 0.3970 meters to 0.3884 meters. These decreases are equivalent to the simulation from t=60 minutes to t=210 minutes of Sugio's experiment.

Table 6.1 Comparison of the location of the freshwater-saltwater interface toe.

	Interface Toe (m)***			Upper Interface Toe (m)****		
Freshwater Level (m)	Present Study	Observed Values*	Numerical Results**	Present Study	Observed Values*	Numerical Results**
0.4030 [0]	0.83478	0.84	0.84	0.26713	0.273	0.273
0.3970 [30]	0.67857	0.68	0.68	0.28745	0.345	0.345
0.3938 [60]	0.53571	0.53	0.53	0.30893	0.352	0.352
0.3916 [90]	0.41071	0.41	0.40	0.30893	0.352	0.352
0.3905 [120]	0.32143	0.32	0.30	0.30893	0.352	0.352
0.3894 [150]	0.21429	0.21	0.19	0.33163	0.352	0.352
0.3887 [180]	0.14286	0.14	0.11	0.33163	0.352	0.352
0.3884 [210]	0.08928	0.07	0.03	0.33163	0.352	0.352

* Sand-Box physical model (Sugio et al., 1987)
** Numerical solution (Sugio et al., 1987)
*** Measured from seawater front (right hand side boundary).
**** Measured from seawater level (downstream top boundary).

It appears that the interface line forms a sharp angle with the bottom impervious boundary. This is valid for all runs at which the velocity of 6.575 m/sec. (freshwater level of 0.403 meters) and less, has been applied. In each step where the water table at the freshwater boundary was lowered from 0.403 meters to 0.386 meters, the shape of the interface did not change considerably. All figures demonstrate a concave interface line. In addition, the location of the upper interface toe is not located at the top of the phreatic surface boundary. Clearly, these findings indicate that there is outflow at the seawater boundary. This may

be used to explain the mass balance included in the formulation of the computational fluid dynamic. These results are nearly identical with those of Sugio et al. (1987). A comparison of results is presented in Table 6.1. This table shows the comparison of the location of the interface toe and the upper interface toe: (a) of this study; (b) observed values from the Sand-Box model (Sugio et al., 1987); and (c) numerical values obtained by Sugio et al.. The values in brackets in the first column indicate time increments in minutes taken by Sugio et al.. They are also a good match with observed values from the Sand-Box model performed by Sugio et al.

Table 6.2 summarizes the optimization results of the subsurface barrier analysis. It seems that the optimum solution has been reached with two combinations of decision variables. The first combination is: the location of the barrier at 0.54 meter from the seawater boundary, width of 0.056 meters; and 9.83 10^{+9} /m^2 permeability factor. This combination results in the total density for all nodes over the entire domain (**densum**) of 2119500 kg/m^3 and the density at node number 2 which is the lowest point of the barrier structure at the freshwater side of 1013 kg/m^3. The second combination is: the location at 0.89 meter; width of 0.042 meter; and permeability factor of 5.99 10^{+9} /m^2. Using this combination, the total density of 211700 kg/m^3 and the density at node number 2 of 1012 kg/m^3 were obtained. It is likely that the global optimum is in the vicinity of the second combination. Simply put, it is the point where total density shows the lowest value. This result provides the optimum solution based on the criteria developed for the optimization of a subsurface barrier.

Table 6.2 Results of Optimization

Simulation Number		Location of Barrier	Width of Barrier	C Values	Total Density	Temp. Node 2
1.	Initial Points	0.50 m	0.060 m	1.0e+10	2119900	280.17
	Feasible Solutions	0.54 m	0.056 m	9.83e+9	2119500	281.29
2.	Initial Points	0.30 m	0.020 m	1.2e+11	2127600	287.98
	Feasible Solutions	all infeasible				
3.	Initial Points	0.55 m	0.035 m	1.9e+10	2118600	278.00
	Feasible Solutions	all infeasible				
4.	Initial Points	0.35 m	0.030 m	3.9e+9	2129000	287.98
	Feasible Solutions	0.87 m	0.040126 m	6.57e+9	2117100	280.14
		0.89 m	0.042134 m	5.99e+9	2117000	280.17
5.	Initial Points	0.60 m	0.045 m	9.0e+9	2119800	287.76
	Feasible Solutions	all infeasible				
6.	Initial Points	0.42 m	0.040 m	9.0e+9	2123400	287.98
	Feasible Solutions	all infeasible				
7.	Initial Points	0.50 m	0.060 m	1.2e+10	2119200	278.00
	Feasible Solutions	0.87 m	0.040 m	6.57e+9	2117200	281.08
		0.89 m	0.040 m	6.00e+9	2117100	282.28
		0.54 m	0.056 m	9.83e+9	2119600	281.75
		0.8967	0.04128	6.03e+9	2117000	280.08
8.	Initial Points	0.35 m	0.064 m	3.2e+10	2119600	278.00
	Feasible Solutions	all infeasible				
Constraints	Upper bounds	0.90 m	0.070 m	9.9e+10		283.00
	Lower bounds	0.30 m	0.015 m	1.0e+09		280.00

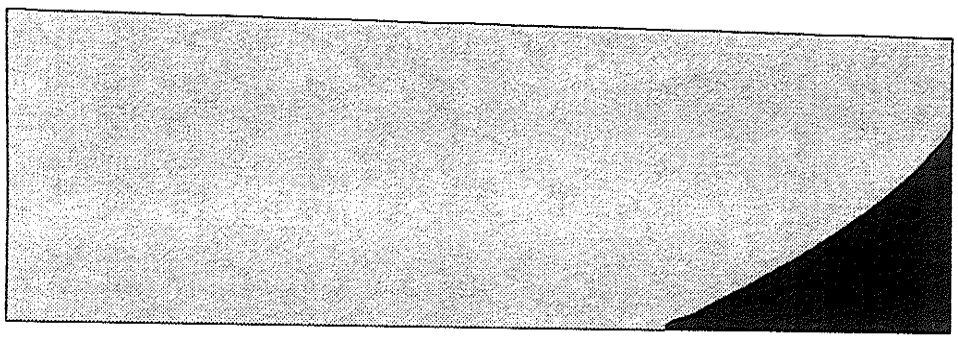

Figure 6.1 Position of the Interface Toe at Hf=0.4030 m.

ANSYS 5.0
JUL 18 1994
11:17:16
PLOT NO. 1
NODAL SOLUTION
NDEN
SMN =1002
SMX =1025

ZV =1
DIST=0.68309
XF =0.6
YF =0.2015
CENTROID HIDDEN
EDGE

1002
1013
1025

ANSYS 5.0 1
JUL 18 1994
09:40:02
PLOT NO. 1
NODAL SOLUTION
NDEN
SMN =1002
SMX =1025

1

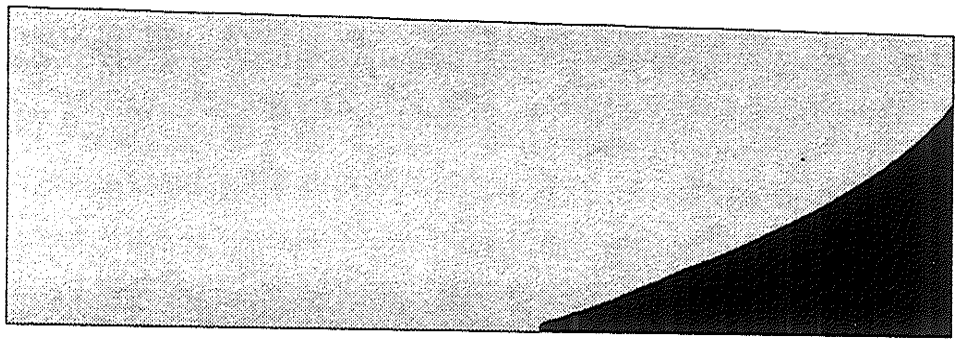

Figure 6.2 Position of the Interface Toe at Hf=0.397 m

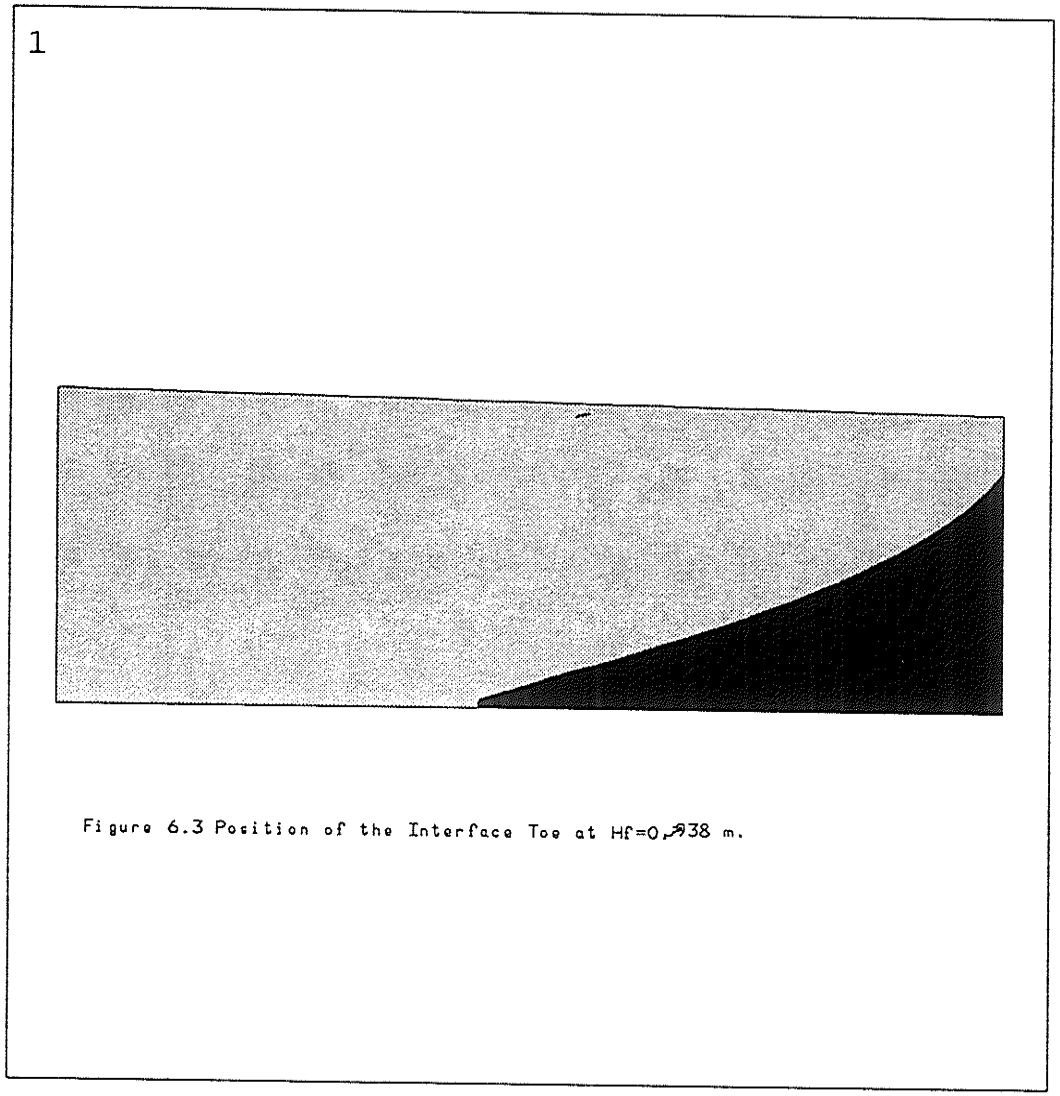

Figure 6.3 Position of the Interface Toe at Hf=0.938 m.

ANSYS 5.0 1
JUL 18 1994
10:35:38
PLOT NO. 1
NODAL SOLUTION
NDEN
SMN =1002
SMX =1025

ZV =1
DIST=0.68309
XF =0.6
YF =0.2015
CENTROID HIDDEN
EDGE
1002
1013
1025

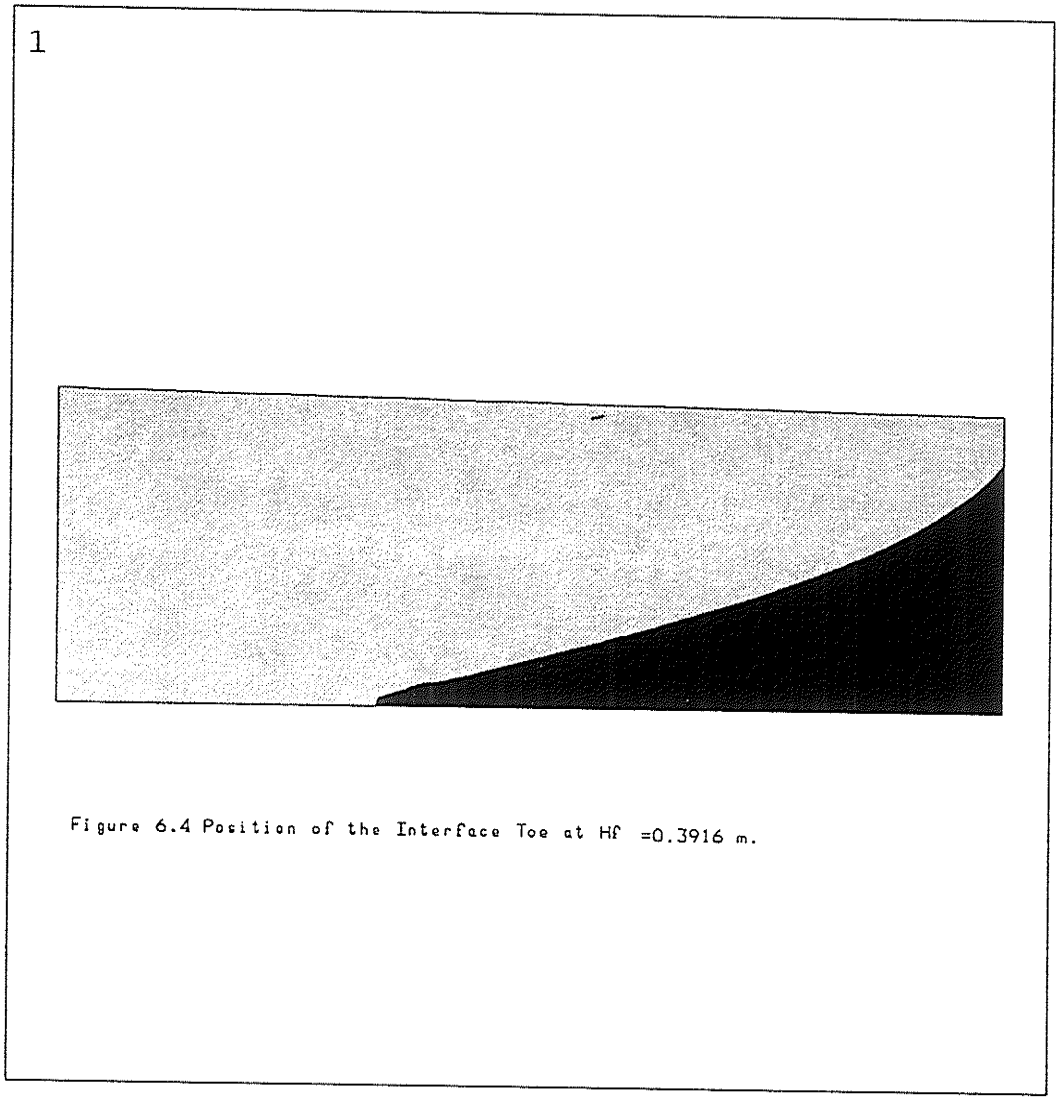

Figure 6.4 Position of the Interface Toe at Hf =0.3916 m.

ANSYS 5.0
JUL 18 1994
11:22:38
PLOT NO. 1
NODAL SOLUTION
NDEN
SMN =1002
SMX =1025

ZV =1
DIST=0.68309
XF =0.6
YF =0.2015
CENTROID HIDDEN
EDGE

1002
1013
1025

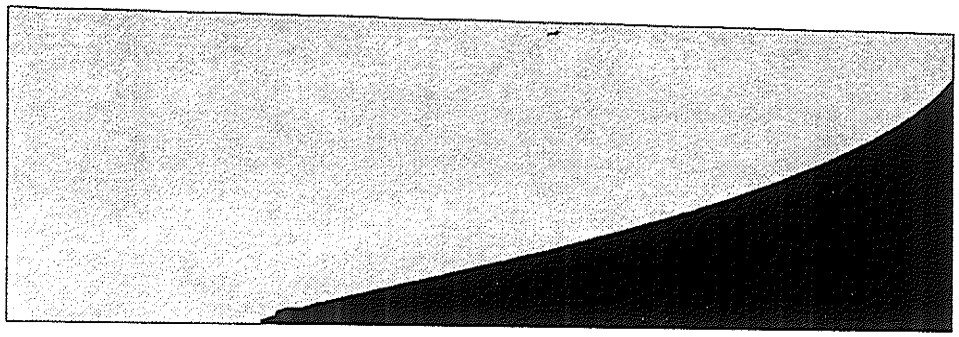

Figure 6.5 Position of the Interface Toe @ Hf=0.3905 m.

ANSYS 5.0
JUL 18 1994
10:47:42
PLOT NO. 1
NODAL SOLUTION
NDEN
SMN =1002
SMX =1025

ZV =1
DIST=0.68309
XF =0.6
YF =0.2015
CENTROID HIDDEN
EDGE

1002
1013
1025

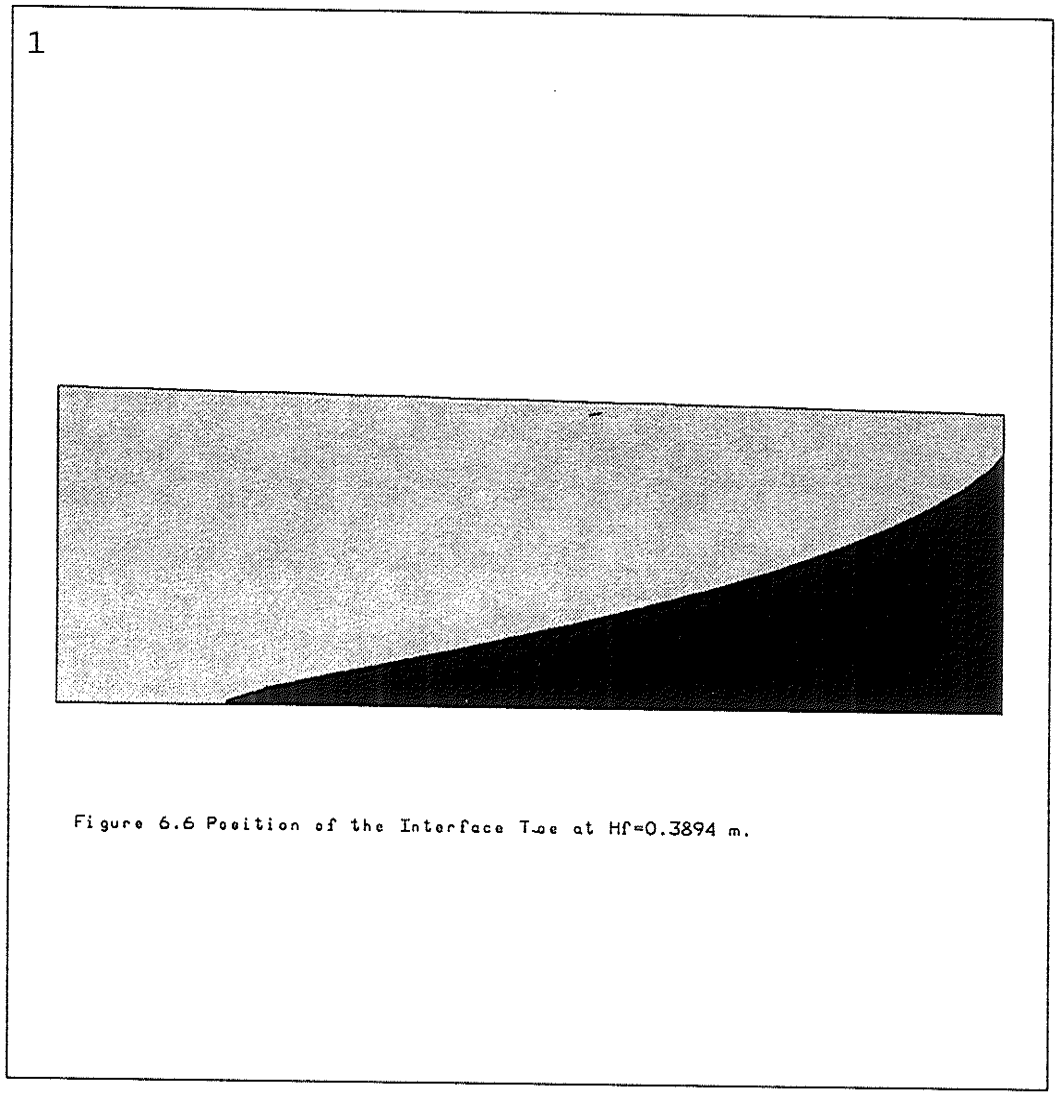

Figure 6.6 Position of the Interface Toe at Hf=0.3894 m.

ANSYS 5.0
JUL 18 1994
10:52:33
PLOT NO. 1
NODAL SOLUTION
NDEN
SMN =1002
SMX =1025

ZV =1
DIST=0.68309
XF =0.6
YF =0.2015
CENTROID HIDDEN
EDGE

1002
1013
1025

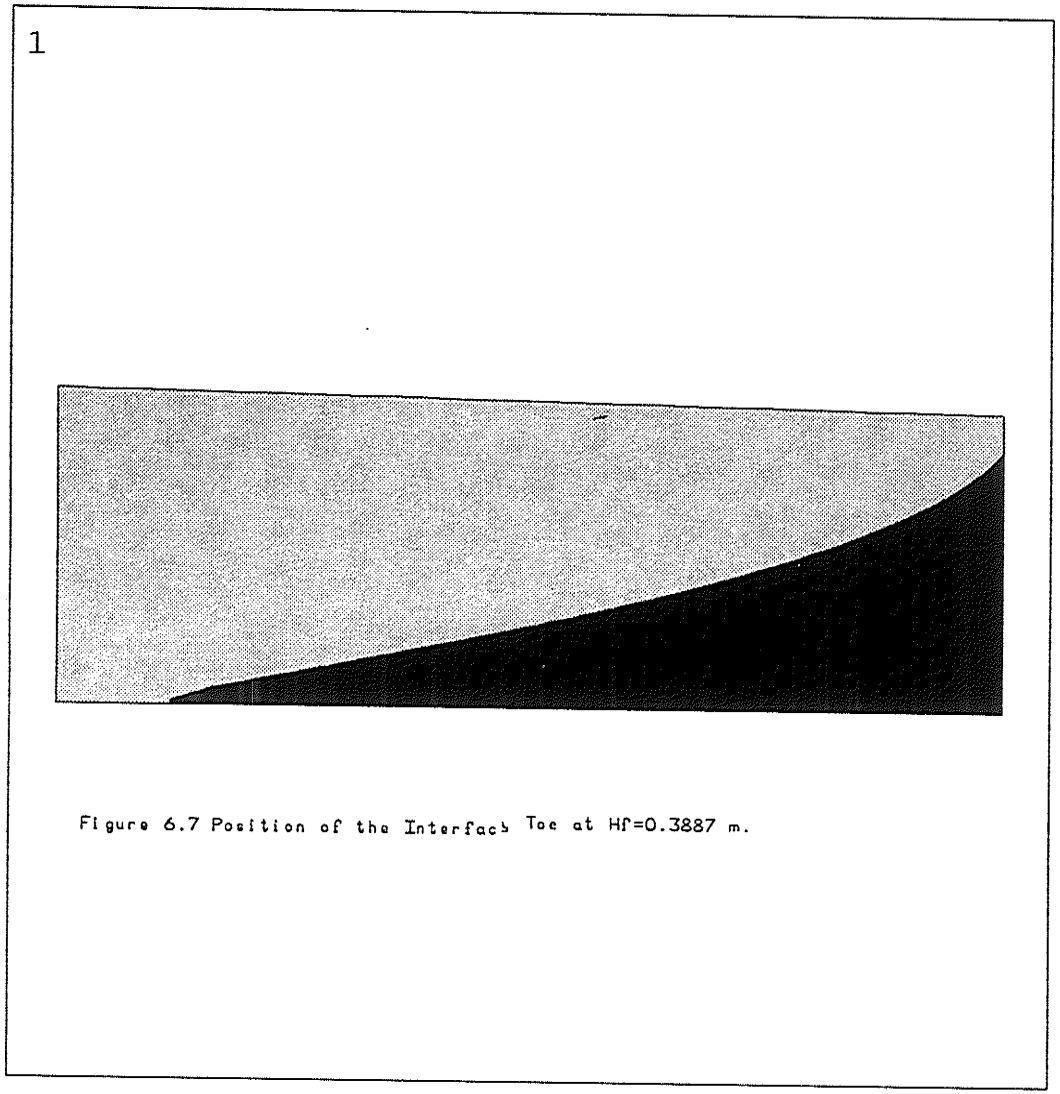

Figure 6.7 Position of the Interface Toe at Hf=0.3887 m.

ANSYS 5.0
JUL 18 1994
10:57:36
PLOT NO. 1
NODAL SOLUTION
NDEN
SMN =1002
SMX =1025

ZV =1
DIST=0.68309
XF =0.6
YF =0.2015
CENTROID HIDDEN
EDGE
1002
1013
1025

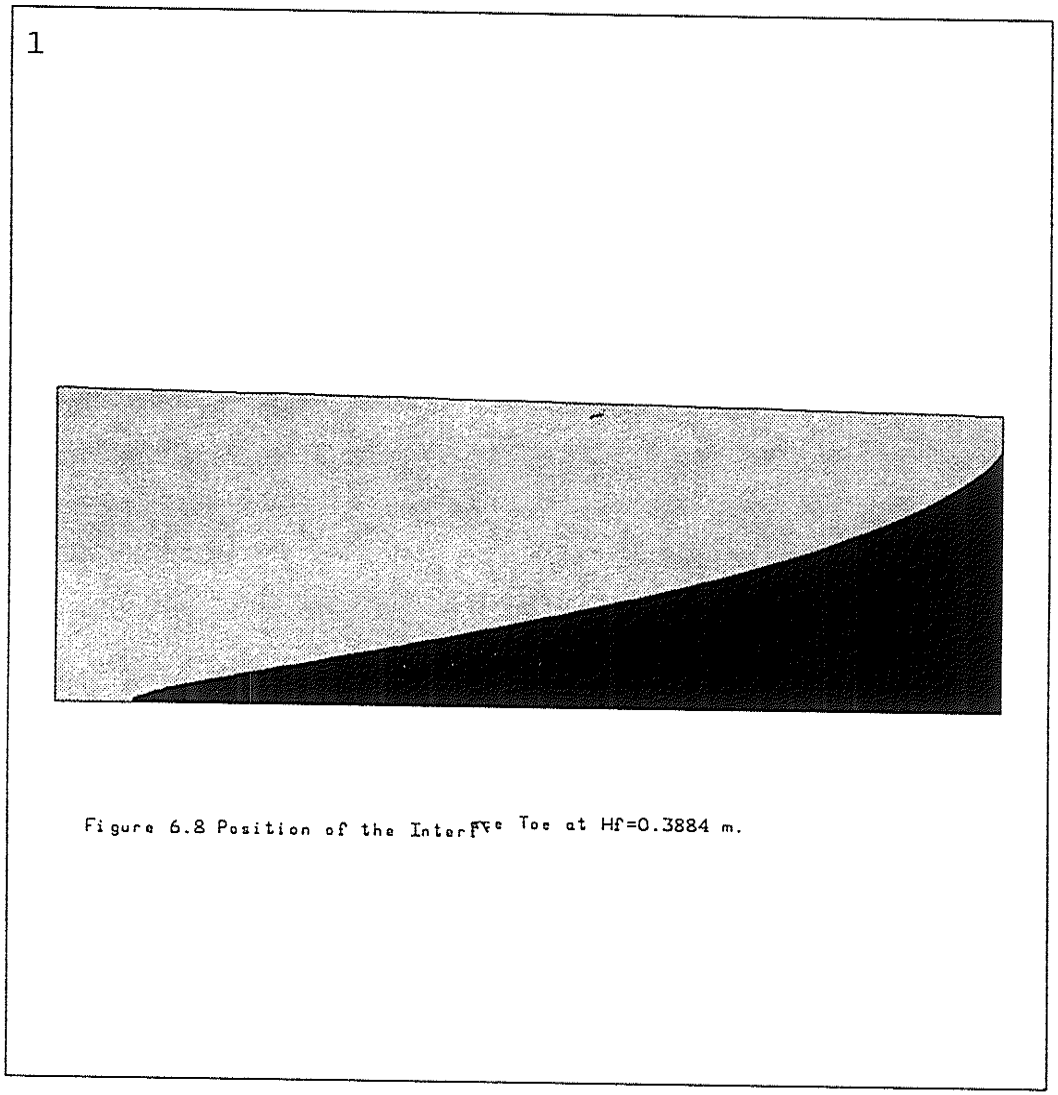

Figure 6.8 Position of the Interface Toe at Hf=0.3884 m.

ANSYS 5.0
JUL 18 1994
11:01:41
PLOT NO. 1
NODAL SOLUTION
NDEN
SMN =1002
SMX =1025

ZV =1
DIST=0.68309
XF =0.6
YF =0.2015
CENTROID HIDDEN
EDGE

1002
1013
1025

6.2 Discussion

The theory governing the sharp fresh-saltwater interface leads us to the conclusion that the shape of the interface curves inwards reaching the interface toe and forms a sharp angle with the impervious boundary (see Figures 3.3, 3.5, 3.6 and 3.7). The experiments conducted by Bear and Dagan (1964) and Sugio et al. (1987) offer clear evidence of the concave shape of the interface and the sharp angle intersecting the bottom of the impervious boundary, supporting the theory. Many studies which use the transition zone model show a convex interface and a wide angle or even perpendicular intersection with the impervious boundary. This research, which also assumes that the transition zone exists in the contact zone, provides a similar shape of the interface to the theory and experimental results. It means that the shape of the interface is concave and the angle with the impervious boundary is sharp.

The results of this research (Figure 6.1- Figure 6.8) can be evaluated by considering at least two points. First, spatial discretization, which is a major component in numerical modeling should be taken into account. It is widely known that adequately fine discretization will result in good calculated values. In contrast, coarse discretization will produce poor results. In the case of saltwater intrusion simulation, Voss and Souza (1987) have addressed the discretization problem when using a transition zone approach. More specifically, the authors have concluded that an unrealistically fine discretization is required to guarantee accuracy and stability for a predominantly horizontal flow. It seems that it is impossible to obtain a successful simulation for this problem. Based on many simulations with several types of discretization, it can be concluded that Voss and Souza's conclusion is correct if the discretization used is homogeneous (i.e. the same density mesh from the bottom of the aquifer to the top, and from the

freshwater to saltwater boundaries). At the beginning of the simulations, a homogeneous grid (2324 nodes and 2100 elements) has been used. The results indicated that the interface shape is not different from previous work, but is, perhaps more convex. Of course, by using a coarser grid, a poorer shape may be obtained. However, the proper grid changes the results significantly. The proper grid is the one with finer mesh in the lower part of the domain and coarser mesh in the upper part. This grid, although having fewer nodes and elements, provides a much better fresh-saltwater interface. The improvement of the shape of the interface and its contact angle to the impervious boundary, is not the only advantage of using the proper grid. The proper grid helps to provide convergence (less iterations). This grid has been suggested by Herbert et al. (1988). In their simulations, three types of grid were used: coarse grid, fine grid and finer grid. All grids had the same pattern; finer at the bottom and coarser at the top of the model domain. Furthermore, they treated the finer grid with higher density mesh in both the freshwater and saltwater boundaries. This indicates that they paid much attention to generating the mesh in order to get better results. A homogeneous grid provides good results if the loads are also homogeneous. Otherwise, another approach must be used.

The application of imaginary nodes in generating the mesh provides good results. This has also been explored in evaluating the effect of discretization on the numerical calculations. The imaginary nodes may eliminate the difficulty of calculating the dependent variable at the nearest boundaries. It is important to note that Sugio et al. (1987) did not use as fine a grid as the one used in the present research. However, the results match the observed values of the Sand-Box model. In other words, the shape of the interface is concave and the angle with the impervious boundary is sharp. One possible explanation for this result is the use of imaginary nodes in their simulation. Additional elements at the impervious

boundary may eliminate the effect of the wide angle on the shape of the interface. Therefore, adding virtual elements at the bottom of the impervious boundary is another way to overcome unrealistically fine discretization problems as suggested by Voss and Souza.

This research has used the proper grid. A gradation of the mesh from the bottom to the top has been made. The ratio of bottom ΔY and top ΔY of 1:7 is sufficient. The ratio of 1:6 will lead to the wide angle of the interface line to the impervious boundary. Using a bigger ratio than 1:7 will result in a coarser grid at the top boundary. It will then provide poor estimation on the upper interface toe. The deviation of the upper interface toe from observed values can be clearly seen after running all simulations. Upper interface toes in several simulations have the same value. This is, of course, due to the coarser grid at the top boundary.

Second, the value of fluid conductivity used can affect how wide the contact zone between freshwater and saltwater is going to be. The basic assumption in that the contact zone can be derived from the fluid conductivity term. This term behaves as a hydrodynamic dispersion in the original formulation of groundwater flow and a solute transport system. Taking a very small value for the fluid conductivity, but non zero, means the hydrodynamic dispersion is neglected. Thus, it leads to the sharp interface model. This research uses the small value of 0.000611 for fluid conductivity. On the other hand, taking a higher value for fluid conductivity provides the transition zone model. This is nicely illustrated in Figure 6.9 which shows the change of density from freshwater (ρ_f=1002 kg/m^3) to saltwater (ρ_s=1025 kg/m^3). The value of fluid conductivity of 0.611 is taken. It can be seen from this figure that a higher value of fluid conductivity will affect the shape of the interface line. The interface is still concave close to the seawater density. However, this shape changes to convex for lower density (close to the freshwater boundary).

1

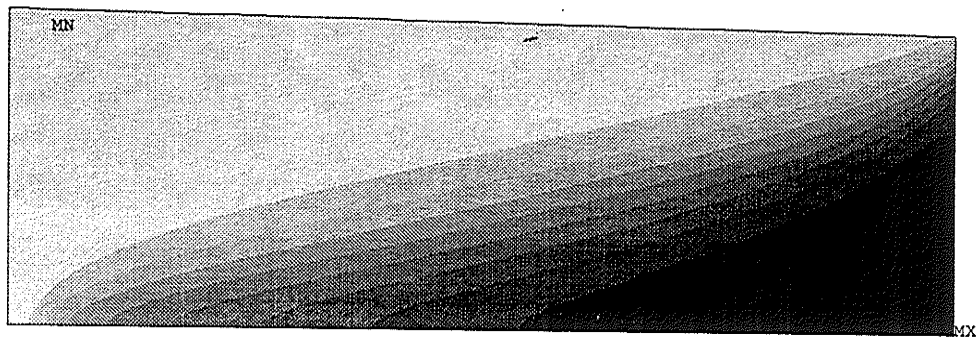

Figure 6.9 Transition zone model

ANSYS 5.0 .4
JUL 13 1994
11:31:06
PLOT NO. 1
NODAL SOLUTION
NDEN
SMN =1002
SMX =1025

ZV =1
DIST=0.68309
XF =0.6
YF =0.2015
CENTROID HIDDEN
EDGE

1002
1005
1007
1010
1012
1015
1017
1020
1022
1025

The implications of these findings are important for groundwater use management policy. The different shape of the interface leads to a different management policy. This is due to the fact that the convex interface tends to come close to the water table at the top of phreatic boundary, while the concave interface is a fair distance away from the water table. For example, in the case of the convex interface, a certain pumping rate may be applied to avoid pumping brackish water. This rate is less than the rate would be if the concave interface were applied. The real interface is indeed a concave curve and is a fair distance from the water table. This concave interface has been proved by several experimental research studies. Therefore, the pumping rate as an output of the management policy is much higher for a concave interface than a convex interface. Eventually, this will affect the overall system of groundwater management.

The implications of these findings become worse over time. Once the convex interface is obtained at time $t=0$ or the initial simulation, a more convex interface will be obtained at time $t \neq 0$ or at later time steps. This research indicates that implication. Before getting concave interfaces, the majority of the results are convex interfaces. The interfaces are more convex when the freshwater level is lowered. When it comes to the lower level (or lower velocity), the whole domain of the model becomes salty water.

The present study has not considered the existence of pumping wells in the freshwater zone. Under real conditions, the reduction of velocity at the freshwater boundary is caused by a gradual drop in the water table. The change in the water table occurs in response to the pumping of water from the aquifers. In addition, this simulation is valid only under steady state conditions. Although the simulations under steady state conditions have shown satisfactory results, it is still important to do similar simulations under transient conditions. These transient conditions are the real phenomena of the movement of seawater in

coastal aquifers. However, running the simulations under transient conditions requires a higher capability of computer resources and presents several difficulties which, at present, remained unsolved.

If the optimization formulation is applied to Sugio's problem, it will lead to: (1) the location of the subsurface barrier at less than 0.4 meters from the seawater front; and (2) the width of the barrier being smaller than 0.05 meters. As a matter of fact, the findings contradict these two conclusions. The location of the barrier is not close to the seawater boundary and the barrier is wider than 0.05 meters (see Table 6.2). Table 6.2 shows that with a number of initial combination points, the feasible solutions seem to approach **loca**=0.89 meters and **wid**=0.065 meters. Using that combination, the total density of the entire domain is minimum density (**densum**=211900 kg/m^3). Several combinations provide the value of total density less than 211900 kg/m^3 but a higher density at node number 2 (above 1012.5 kg/m^3). This means that there is saltwater passing through the subsurface barrier. In this study, such combinations are considered as infeasible solutions.

There are several reasons why the optimal solution falls into an unexpected region. First, considering the properties of the barrier as a decision variable affects the optimal solution. The result will be quite different if only two decision variables (the location and width of the barrier) are considered. Most probably, the optimum solution will be in the expected location. Another possible explanation is that the feasible values for the barrier material vary widely. Consequently, the optimal solution also varies widely. Using the state variable at node number 2 for 1010 - 1012.5 kg/m^3 has a particular consequence too. It means that saltwater with the maximum density of 1012.5 kg/m^3 may not pass through the barrier (see Figure 6.10). The purpose of this state variable is to reduce the effort needed to remove intruded water from behind the barrier. Also, it is used to account for the width of the barrier in the optimization process.

Without setting the state variable at node 2, the impervious barrier would be the optimal solution. The optimal solution tends to go to the minimum total density i.e. no saltwater going through the barrier. For various reasons, letting the saltwater pass through the barrier is not acceptable.

One implication of allowing seawater to pass through the barrier (in this case, the passing node is node number 2) is the necessity of pumping saltwater from behind the barrier. Certainly, this is an additional task to be dealt with in the management of coastal aquifers. If intruding seawater can not be moved back, it may increase further. Eventually, it may threaten the production wells in the freshwater region which are initially to be protected.

It is also important to note that simulations done by Sugio et al. use different values of some variables. In their study, the density of saltwater is 1030 kg/m^3 and the initial water levels at both sides of boundaries are not the same as they would be without a subsurface barrier. This simulation uses the same values of variables for both cases (with and without a subsurface barrier). Therefore, the expected results are not obtained.

Running the model under steady state conditions is the limitation of this research. Under steady state conditions, it is difficult to simulate the moving back of intruded seawater to the initial position. It is possible, of course, to do such simulation under unsteady state or transient conditions. Again, however, simulation under transient condition presents some difficulties which remain unsolved. It is believed that future simulation should employ transient flow including the existence of pumping wells.

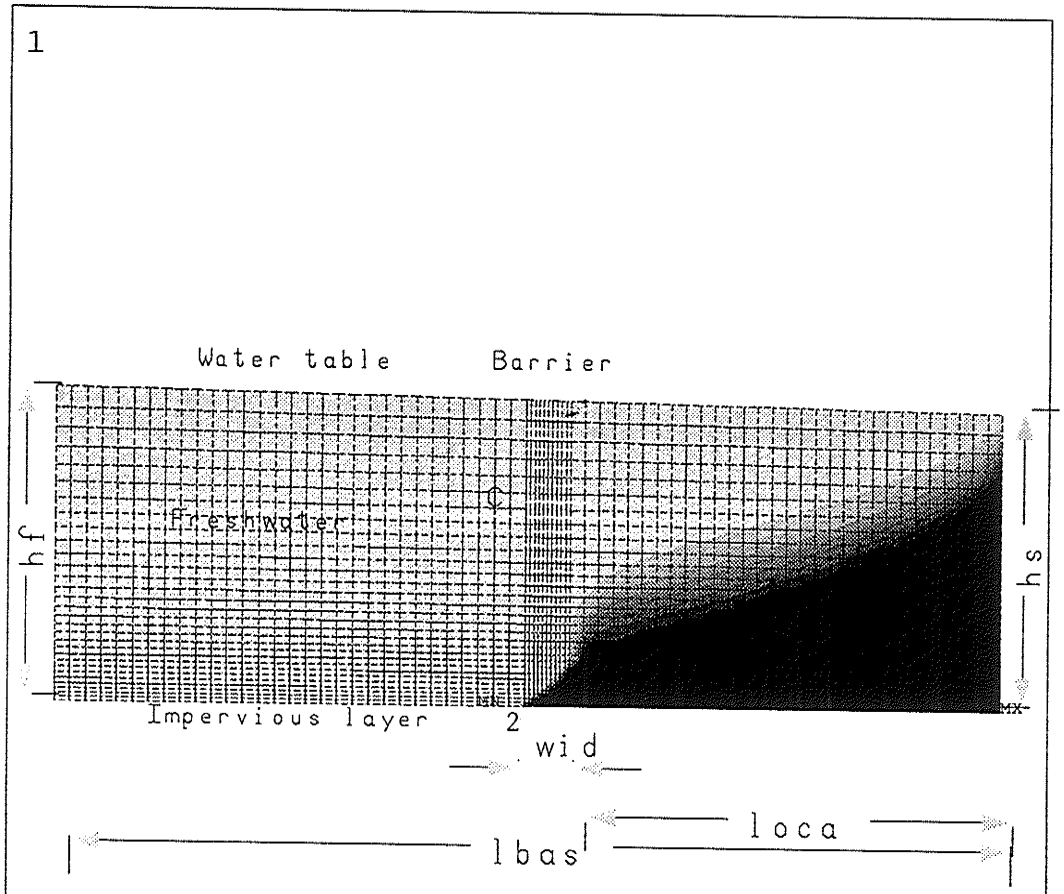

Figure 6.10 Setting state variable at node 2

ANSYS 5.0 4
JUN 15 1994
09:37:33
PLOT NO. 1
NODAL SOLUTION
NDEN
SMN =1002
SMX =1025

1002
1005
1007
1010
1012
1015
1017
1020
1022
1025

Chapter 7

Conclusions and Future Work

This chapter presents the conclusions of this study concerning the optimization of design and location of a subsurface barrier for saltwater intrusion control. Recommendations for future work are also presented.

7.1 Conclusions

The conclusions that can be drawn from this present study are:

1. A system of the Navier-Stokes, continuity, and energy transport equations in the primitive form is more appropriate for modeling the fresh-saltwater interface phenomena than a coupled groundwater flow and solute transport models.
2. For steady state problems, the two-dimensional fresh-saltwater interface model using a computational fluid dynamic yields numerical results that are in good agreement with results obtained from the laboratory Sand-Box model.
3. Generating higher density mesh in the lower portion of model domain leads to reliable and reasonable fresh-saltwater interface estimates. On the other hand, the homogeneous discretization over the domain of the model results in a poor shape of the fresh-saltwater interface.

4. The fluid conductivity in the computational fluid dynamic can be used to examine the sharp interface and the transition zone models.
5. The optimum width, location and material to create a subsurface barrier can be obtained using the Sequential Unconstrained Optimization Technique. Therefore, an effective control of saltwater intrusion problems may be obtained.

7.2 Future Work

This work can be used as an initial step to conduct further studies. A better understanding of the phenomena of aquifer responses to excessive groundwater pumping is hoped to be reached. Eventually, this will lead to efficient and effective control of coastal aquifers.

In future the following three tasks should be addressed:

1. The simulation of the fresh-saltwater interface under a steady state using the computational fluid dynamic model provides good results. This model can be used to assess the intrusion problems facing the exploitation of groundwater resources. The study may be extended to address transient condition to examine the effect of re-establishment of the freshwater level on the seawater wedge behind a subsurface barrier. Such a study would be very useful in developing better criteria for optimization.
2. The relationship between density and temperature has long been accepted. It is known that higher densities correspond to higher temperatures. This relationship is valid only for a single fluid, not for two different fluids. The application of this model to real coastal aquifers will open opportunities to relate density to temperature in two different fluids.

3. The application of the present research for seawater intrusion control is possible in narrow groundwater basins. In the case of alluvial fan basins, the crest length of the subsurface barrier is quite long. It also has no impervious boundary parallel to the flow so that a two-dimensional model can no longer be used. A three-dimensional simulation of the fresh-saltwater intrusion model will be a valuable tool to use in future research.

Bibliography

[1] Aiba, M. 1983. Irrigation Water Resources Development Project by Groundwater Storage Dam. *Civil Engineering in Japan*. 22: 152-163.

[2] American Society of Civil Engineers *Manuals and Reports on Engineering Practice* No. 40. 1987. Ground Water Management.

[3] ANSYS. 1992. *User's Manual*. Revision 5.0. Vol. 1: Procedures. Swanson Analysis Systems, Inc. Houston, PA

[4] ANSYS. 1992. *User's Manual*. Revision 5.0. Vol. 2: Commands. Swanson Analysis Systems, Inc. Houston, PA

[5] ANSYS. 1992. *User's Manual*. Revision 5.0. Vol. 3: Elements . Swanson Analysis Systems, Inc. Houston, PA

[6] ANSYS. 1992. *User's Manual*. Revision 5.0. Vol. 4: Theory. Swanson Analysis Systems, Inc. Houston, PA.

[7] Asano, T. 1985. *Artificial Recharge of Groundwater* , (Butterworth, England).

[8] Bear, J. 1979. *Hydraulics of Groundwater*, (Mc Graw Hill, New York).

[9] Bear, J. & Dagan, G. 1964. Moving Interface in Coastal Aquifers. *J. Hydraulics Division, ASCE* 90: 193-216.

[10] Bearm, J. & Verruijt, A. 1992. *Modeling Groundwater Flow and Pollution: Theory and Application of Transport in Porous Media.* D. Reidel, Dordrecht, Holland.

[11] Calvache, M.L. & Pulido-Bosch, A. 1991. Saltwater Intrusion into A Small Coastal Aquifer (Rio Verde, Almunecar, Southern Spain). *J. Hydrology.* 129: 195-213.

[12] Contractor, D.N. & Srivastava, R. 1990. Simulation of Saltwater Intrusion in the Northern Guam Lens Using A Microcomputer. *J. Hydrology.* 118: 87-106.

[13] Fiacco, A.V. & McCormick, G.P. 1968. *Nonlinear Programming: SequentialUnconstrained Minimization Techniques*, (John Wiley and Sons, New York).

[14] FLOTRAN. 1992. *Release Notes.* Compuflo Inc., Houston, PA

[15] FLOTRAN. 1992. *Theoretical Manual.* Compuflo Inc., Houston, PA.

[16] FLOTRAN. 1992. *User's Manual.* Compuflo Inc., Houoston, PA.

[17] Frind, E.O. 1982a. Seawater Intrusion in Continuous Coastal Aquifer-Aquitard Systems. *Adv. Water Resour.* 5:89-97.

[18] Frind, E. O. 1982b. Simulation of Long-term Transient Density-Dependent Transport in Groundwater. *Adv. Water Resour.* 5: 73-88.

[19] Herbert, A.W., Jackson, C.P. & Lever, D.A. 1988. Coupled Groundwater Flow and Solute Transport With Fluid Density Strongly Dependent Upon Concentration. *J. Water Resource Research.* 24: 1781-1795.

[20] Hoddinghaus, T., Rubin, H., Daniels, H. & Rouve, G. 1992. On the Application of Multiphase Flow Models for the Simulation of Density Stratified Flow in Aquifers. *Groundwater Symposium* 268-274.

[21] Huyakorn, P.S., Andersen, P.F., Mercer, J.W. & White, H.O. 1987. Saltwater Intrusion in Aquifers: Development and Testing of a Three-Dimensional Finite Element Model. *J. Water Resource Research.* 23: 293-312.

[22] Huyakorn, P.S., Thomas, S.D. & Thomson, B.M. 1984. Techniques for Making Finite Elements Competitive in Modeling Flow in Variably Saturated Porous Media. *J. Water Resource Research*, 20: 1099-1115.

[23] Huyakorn, P.S., Springer, E.P., Guvanasen, V. & Wadsworth, T.D. 1986. A Three-Dimensional Finite Element Model for Simulating Water Flow in Variably Saturated Porous Media. *J. Water Resource Research*, 22: 1790-1808.

[24] Idelchik, I.E. 1986. *Handbook of Hydraulic Resistance*, (Hemisphere, New York).

[25] Lee, C.H. & Cheng, R.T. 1974. On Seawater Encroachment in Coastal Aquifers. *J. Water Resource Research*, 10: 1039-1043.

[26] Liu, P.L.-F, Cheng, A.H.-D, Ligget, J.A. & Lee, J.H. 1981. Boundary Integral Equation Solutions at Moving Interface Between Two Fluids in Porous Media. *J. Water Resource Research*, 17: 1445-1452.

[27] Mercer, J.W., Larson, S.P. & Faust, C.R. 1980. Simulation of Salt-Water Interface Motion. *J. Ground Water*, 18: 374-385.

[28] Patankar, S.V. 1980. *Numerical Heat Transfer and Fluid Flow*, (Hemisphere, New York).

[29] Pinder, G.F. & Page, R.H. 1970. A Numerical Technique for Calculating the Transient Position of the Saltwater Front. *J. Water Resource Research*, 6: 875-880.

[30] Rubin, H. 1983. On the Application of the Boundary Layer Approximation for the Simulation of Density Stratified Flows in Aquifers. *Adv. Water Resour.* 6: 96-105.

[31] Rumer, R.R., Drinker, P.A. 1966. Resistance to Laminar Flow Through Porous Media. *J. Hydraulics Division, ASCE*, 92:155-163.

[32] Segol, G., Pinder, G.F. & Gray, W.G. 1975. A Galerkin Finite Element Technique for Calculating the Transient Position of the Saltwater Front. *J. Water Resource Research*, 11: 343-347.

[33] Shamir, V. & Bear, J. 1984. Optimal Annual Operation of a Coastal Aquifer. *J. Water Resource Research*, 20: 435-444.

[34] Shamir, V. & Dagan, G. 1971. Motion of the Seawater Interface in Coastal Aquifers: A Numerical Solution. *J. Water Resource Research*, 7: 644-657.

[35] Sugio, A. & Mohamed, A.R. 1992. Protection of Coastal Aquifer from Saltwater Intrusion by Artificial Recharge. *The 12th Sea Water Intrusion Meeting*.

[36] Sugio, S. & Nakada, K. 1992. Abrupt Interface Model of Seawater in Coastal Aquifer. International Conference on *Interaction of Computational Methods and Measurements in Hydraulics and Hydrology*. Budapest, Hungary.

[37] Sugio, S., Nakada, K. & Urish, D.W. 1987. Subsurface Seawater Intrusion Barrier Analysis. *J. Hydraulic Engineering, ASCE* 113: 767-779.

[38] Taigbenu, A.E., Ligget, J.A. & Cheng, A.H. 1984. Boundary Integral Solution to Seawater Intrusion into Coastal Aquifers. *J. Water Resource Research*, 20: 1150-1158.

[39] Todd, D.K. 1980. *Groundwater Hydrology*, (John Wiley & Sons, New York).

[40] Volker, R.E. & Rushton, K.R. 1982. An Assessment of the Importance of Some Parameters for Seawater Intrusion in Aquifers and a Comparison of Dispersive and Sharp-Interface Modelling Approaches. *J. Hydrology*. 56: 239-250.

[41] Voss, C.I. & Souza, W.R. 1987. Variable Density Flow and Solute Transport Simulation of Regional Aquifers Containing a Narrow Freshwater-Saltwater Transition Zone. *J. Water Resource Research*. 23: 1851-1866.

[42] Willis, R. & Finney, B.A. 1987. Planning Model for Optimal Control of Saltwater Intrusion. *J. Water Resources Planning and Management*. 114: 163-178.

[43] Willis, R. & Yeh, W.G. 1987. *Groundwater Systems Planning and Management*, (Prentice-Hall, New Jersey).

[44] Wilson, J.L. & Costa, A.D. 1982. Finite Element Simulation of a Saltwater/Freshwater Interface With Indirect Toe Tracking. *J. Water Resource Research*. 18: 1069-1080.

APPENDIX 1

PROBLEM SET-UP: Freshwater-saltwater Interface

```
/BATCH
/COM,ANSYS REVISION  5.0          24   09:58:24   11/17/1993
/show,x11
! /menu,on
/FILNAM,velc0
/title,Position of the Interface Toe at Level=0.403 m Without Subsurface Barrier
/UNITS,SI
loc=.4
wid=.05
/PREP7
ETYPE
STAT
ET,  1,55
R,2,1,1,0,.758e+9,0,0
RMORE,1
R,3,1,1,0,.758E+9,0,0
RMORE,1
R,4,1,1,0,.758e+9,0.0
RMORE,1
hf=.403
hs=.381
lbas=1.20
lfre=lbas-(loc+wid)
k,1,0,0
k,2,lfre,0
k,3,(lfre+wid),0
K,4,lbas,0
k,5,lbas,hs
K,6,(lfre+wid),(hs+loc*(hf-hs)/lbas)
k,7,lfre,(hs+(loc+wid)*(hf-hs)/lbas)
k,8,0,hf
l,1,2
l,2,3
l,3,4
l,4,5
l,5,6
l,3,6
l,6,7
l,2,7
l,7,8
l,1,8
nd=30
rd=5
```

```
ld=.018
lz=.018
a,1,2,7,8
a,2,3,6,7
a,3,4,5,6
lesize,1,ld
lesize,8,,,nd,rd
lesize,9,ld
lesize,10,,,nd,rd
lesise,2,lz
lesize,6,,,nd,rd
lesize,7,lz
lesize,3,ld
lesize,4,,,nd,rd
lesize,5,ld
eshape,2
real,2
amesh,1
real,3
amesh,2
real,4
amesh,3
aglue,all
DOF,VX,VY,,PRES,TEMP
nummrg,node
numcmp,node
numcmp,elem
asel,all
lsel,all
ksel,all
esel,all
nsel,all
lsel,s,loc,x,0.0
nsll,s,1
d,all,vx,6.9666e-05
d,all,vy,0.0
d,all,temp,278
nsel,s,loc,x,lbas
nsel,r,loc,y,0.0,(.052333)
d,all,vy,0.0
d,all,temp,288
nall
lsel,s,loc,y,0
nsll,s,1
d,all,vx,0
```

```
d,all,vy,0
nall
nsel,s,loc,x,lbas
nsel,r,loc,y,(.052333),hs
d,all,pres,0
nall
ksel,s,,,5,8,1
lslk,s,1
nsll,s,1
d,all,vy,0.0
nall
FLDA,1S,JB,vel0
FLDA,1S,IT,112
FLDA,1S,OF,10
FLDA,1S,RS,f
FLDA,1S,FL,T
FLDA,1S,TH,T
FLDA,1S,PT,t
FLDA,1s,pv,t
FLDA,1s,pp,t
FLDA,2S,PD,f
FLDA,2S,FL,LIQUID
FLDA,2S,VD,T
FLDA,2S,VV,f
FLDA,2P,D0,1025
FLDA,2P,D1,288
FLDA,2P,D2,2.3
FLDA,2P,C0,.000611
FLDA,2P,V0,1.518e-3
FLDA,2P,CP,4186
FLDA,2P,SR,1.0001
flda,2s,np,101325
FLDA,2S,NT,288
FLDA,2S,at,0
FLDA,2S,AY,-9.8066
FLDA,4S,AV,.001
FLDA,4S,RU,.308
flda,4s,rv,.308
FLDA,4S,RP,.308
flda,5s,cg,t
flda,1s,pu,t
flda,6s,ts,f
flda,6s,dt,10
flda,6s,nt,20
flda,6s,st,200
```

```
flda,6s,to,100
flda,6s,so,10
FLWRITE
FLORUN,vel0
save,vel0,db
finish
/exit
/eof
```

PROBLEM SET-UP: Optimization

```
/COM,ANSYS REVISION  5.0          24   09:58:24   07/17/1994
/show,x11
! /menu,on
/FILNAM,file
/title,Optimization with Subsurface Barrier
/UNITS,SI
loca=.54
wid=.05
/PREP7
ETYPE
STAT
ET,  1,55
R,2,1,1,0,.758e+9,0,0
RMORE,1
R,3,1,1,0,7e+9,0,0
RMORE,1
R,4,1,1,0,.758e+9,0.0
RMORE,1
rmore,loca,wid,c
hf=.403
hs=.381
lbas=1.20
lfre=lbas-(loca+wid)
k,1,0,0
k,2,lfre,0
k,3,(lfre+wid),0
K,4,lbas,0
k,5,lbas,hs
K,6,(lfre+wid),(hs+loca*(hf-hs)/lbas)
k,7,lfre,(hs+(loca+wid)*(hf-hs)/lbas)
k,8,0,hf
l,1,2
l,2,3
l,3,4
l,4,5
l,5,6
l,3,6
l,6,7
l,2,7
l,7,8
l,1,8
nd=30
nz=10
```

```
rd=5
a,1,2,7,8
a,2,3,6,7
a,3,4,5,6
lesize,1,,,nd
lesize,8,,,nd,rd
lesize,9,,,nd
lesize,10,,,nd,rd
lesise,2,,,nz
lesize,6,,,nd,rd
lesize,7,,,nz
lesize,3,,,nd
lesize,4,,,nd,rd
lesize,5,,,nd
eshape,2
real,2
amesh,1
real,3
amesh,2
real,4
amesh,3
aglue,all
DOF,VX,VY,,PRES,TEMP
nummrg,node
numcmp,node
numcmp,elem
asel,all
lsel,all
ksel,all
esel,all
nsel,all
lsel,s,loc,x,0.0
nsll,s,1
d,all,vx,2.3e-05
d,all,vy,0.0
d,all,temp,278
nsel,s,loc,x,lbas
nsel,r,loc,y,0.0,(.052333)
d,all,vy,0.0
d,all,temp,288
nall
lsel,s,loc,y,0
nsll,s,1
d,all,vx,0
d,all,vy,0
```

```
nall
nsel,s,loc,x,lbas
nsel,r,loc,y,(.052333),hs
d,all,pres,0
nall
ksel,s,,,5,8,1
lslk,s,1
nsll,s,1
d,all,vy,0.0
nall
FLDA,1S,JB,optimz
FLDA,1S,IT,141
FLDA,1S,OF,10
FLDA,1S,RS,f
FLDA,1S,FL,T
FLDA,1S,TH,T
FLDA,1S,PT,f
FLDA,1s,pv,f
FLDA,1s,pp,f
FLDA,2S,PD,f
FLDA,2S,FL,LIQUID
FLDA,2S,VD,T
FLDA,2S,VV,f
FLDA,2P,D0,1025
FLDA,2P,D1,288
FLDA,2P,D2,2.3
FLDA,2P,C0,.000611
FLDA,2P,V0,1.518e-3
FLDA,2P,CP,4186
FLDA,2P,SR,1.0001
flda,2s,np,101325
FLDA,2S,NT,288
FLDA,2S,at,0
FLDA,2S,AY,-9.8066
FLDA,4S,AV,.001
FLDA,4S,RU,.308
flda,4s,rv,.308
FLDA,4S,RP,.308
flda,5s,cg,t
flda,1s,pu,f
flda,6s,ts,f
flda,6s,dt,10
flda,6s,nt,20
flda,6s,st,200
flda,6s,to,100
```

```
flda,6s,so,10
FLWRITE
FLORUN,optimz
save,optimz,db
finish
/post1
flread
*get,tnode2,node,2,temp
etable,delem,nden
ssum
*get,densum,ssum,,item,delem
finish
/opt
opvar,loca,dv,0.3,.90
opvar,wid,dv,.015,.07
opvar,tnode2,sv,280,283
opvar,densum,obj,,,0.1
opfile
opcopy
run
loca=.54
wid=.035
run
loca=.450
wid=.045
run
loca=.44
wid=.04
run
oprun,40,,,12
finish
/exit
/eof
```

APPENDIX 2

```
                              FLOTRAN
                         Production Dynamic


                    Version 2.1a    SUN 4  6/01/93

                        License No      040000
                        Licensee        WLW-DEMO
                        Expiration        7/31/94
                        Max Nodes         15000

                  Copyright (c) 1987,1988,1989,1990,1992,1993
               Swanson Analysis Systems Inc, All Rights Reserved

    This is the FLOTRAN (R) general purpose finite element computer program
    for fluid flow and heat transfer analysis.  Neither Swanson Analysis
    Systems, Inc. nor any distributor supplying this program assume any
    responsibility for the validity, accuracy, or applicability of any
    results obtained from the FLOTRAN (R) program.  Users must verify
    their own results.

0
0

 vel0.run
 vel0                           06/13/94  22:23:20 ANSYS   5.0  24
 Position of the Interface Toe at t=0 min. Without Subsurface Barrier

 vel.geom
 06/13/94 22:23:23 GEOMETRY 2.0      ANSYS         FLOPRE  2.1a
 Position of the Interface Toe at t=0 min. Without Subsurface Barrier

 vel0.bc
 06/13/94 22:23:23 BOUNDARY-CONDITIONS 2.0    ANSYS      FLOPRE  2.1a
 Position of the Interface Toe at t=0 min. Without Subsurface Barrier

 vel0.res
 RESULTS         0  ANSYS     06/13/94  22:23:23  FLOPRE  2.1a
 Position of the Interface Toe at t=0 min. Without Subsurface Barrier
     0 ITERATIONS       INITIAL DATA
1      Position of the Interface Toe at t=0 min. Without Subsurface Barrier
0FLOTRAN   2.1a                      RUN file                    06/13/94 22:23:


     Problem            vel0                 Restart               F
                                             Batch                 F

0Analysis Options                         Termination Criteria
     Flow Solution         T                 Flow Convergence         0.00E+00
     Turbulent             F                 Energy Convergence       0.00E+00
     Compressible          F                 Maximum Iterations            112
     Thermal               T                 Output Frequency               10
     Swirl                 F
     Transient             F

0Transient Solution Control
     Number of Time Steps     20             Output Time Increment  1.0000E+02
     Time Step Size        1.0000E+01        Output Step Increment     10
     Solution Stop Time    2.0000E+02

0Debug Output
     Print Residuals       F                 Debug Print Level          0
     Solution Error Est.       0

0Semi-direct Solution Control  Iterations  Convergence
     Pressure              T       300     1.00000E-07
     Energy                F       300     1.00000E-05

0Operating Conditions                     Fluid Property Information
     Reference Pressure    1.0132E+05        Fluid                 LIQUID
     Ambient Temperature         0.00        Heat Capacity          4.1860E+03
     Stagnation Temperatur     293.00        Ratio CP/CV            1.0001E+00
                                             Gas Constant           3.4324E-01
```

```
     Nominal Temperature        288.00        Update Frequency          1
     Nominal Density        1.0250E+03        Variable Density          T
     Nominal Viscosity      1.5180E-03        Variable Viscosity        F
     Nominal Conductivity   6.1100E-04        Variable Conductivity     F

0Variable Property Input Coefficients
     Density                1.02500E+03   2.88000E+02   2.30000E+00   0.00000E+00
     Viscosity              1.51800E-03   0.00000E+00   0.00000E+00   0.00000E+00
     Conductivity           6.11000E-04   0.00000E+00   0.00000E+00   0.00000E+00

0Acceleration
     X component            0.0000E+00
     Y component           -9.8066E+00
     Z component            0.0000E+00

1      Position of the Interface Toe at t=0 min. Without Subsurface Barrier
0FLOTRAN   2.1a                        RUN file                    06/13/94 22:23:


                                   Relaxation       Quadrature   TDMA
 Variable            Schmidt #   Under  Inertial   Diff   Src   Sweep   Print
 --------            ---------   ----------------  ----------   -----   -----
 U Velocity            1.00      0.308  1.00E+15    0      0      1      T
 V Velocity            1.00      0.308  1.00E+15    0      0      1      T
 W Velocity            1.00      0.500  1.00E+15    0      0      1      F
 Pressure              0.00      0.308  1.00E+15    1      1    100      T
 Turb. Kin. Enrg.      1.00      0.500  1.00E+15    0      2     10      F
 Turb. Enrg. Diss.     1.30      0.500  1.00E+15    0      2     10      F
 Temperature           1.00      0.500  1.00E+20    0      0     25      T
 Density               0.00      0.500  0.00E+00    0      0      0      F
 Viscosity             0.00      0.500  0.00E+00    0      0      0      F
 Conductivity          0.00      0.500  0.00E+00    0      0      0      F
 Eff. Viscosity        0.00      0.500  0.00E+00    0      0      0      F
 Eff. Conductivity     0.00      0.500  0.00E+00    0      0      0      F
 Total Temperature     1.00      0.500  1.00E+20    0      0     25      T


 Artificial Viscosity    0.1000E-02


0Turbulence Inlet Parameters              Effective Viscosity Initialization
     Turbulence Intensity  1.0000E-02        Ratio to Laminar       1.0000E+03
     Length Scale Factor   1.0000E-02

0Turbulence Constants
     CMu      0.090            C1     1.440              E     9.000
     Kappa    0.400            C2     1.920              A    26.000

0Rotational Terms
     Rotational Speed                          Rotational Axis Offset
        X   0.0000E+00                            X   0.0000E+00
        Y   0.0000E+00                            Y   0.0000E+00
        Z   0.0000E+00                            Z   0.0000E+00

0Property Calculations
                          Form          Coefficients
     Density                1   3.62600E+02  2.30000E+00  0.00000E+00
     Viscosity              1   1.51800E-03
     Conductivity           1   6.11000E-04

0Geometry                  2D Cartesian    (XY)

0Distributed Resistance Parameters
0    Region Type      K            C            Dh           (a)          (b)
       101   1    0.0000E+00   7.5800E+08   1.0000E+00   0.0000E+00   1.0000E+00
       102   1    0.0000E+00   7.5800E+08   1.0000E+00   0.0000E+00   1.0000E+00
       103   1    0.0000E+00   7.5800E+08   1.0000E+00   0.0000E+00   1.0000E+00
1      Position of the Interface Toe at t=0 min. Without Subsurface Barrier
0FLOTRAN   2.1a                  Convergence Monitor                 06/13/94 22:23:
 ITER    U-MOM      V-MOM      W-MOM      PRESS      ENERG       K      EPSILON
    1  0.000E+00 0.000E+00 0.000E+00 1.000E+00 4.965E-04 0.000E+00 0.000E+00
    2  6.190E-02 4.576E-03 0.000E+00 3.688E-01 5.006E-04 0.000E+00 0.000E+00
    3  4.173E-02 7.843E-03 0.000E+00 2.529E-01 5.026E-04 0.000E+00 0.000E+00
    4  2.813E-02 1.079E-02 0.000E+00 1.724E-01 4.964E-04 0.000E+00 0.000E+00
```

```
    5  1.894E-02 1.319E-02 0.000E+00 1.162E-01 4.910E-04 0.000E+00 0.000E+00
    6  1.302E-02 1.506E-02 0.000E+00 7.805E-02 4.843E-04 0.000E+00 0.000E+00
    7  9.330E-03 1.645E-02 0.000E+00 5.416E-02 4.616E-04 0.000E+00 0.000E+00
    8  7.019E-03 1.732E-02 0.000E+00 4.009E-02 4.444E-04 0.000E+00 0.000E+00
    9  5.532E-03 1.774E-02 0.000E+00 3.206E-02 4.336E-04 0.000E+00 0.000E+00
   10  4.540E-03 1.785E-02 0.000E+00 2.766E-02 4.276E-04 0.000E+00 0.000E+00


                         Global Convergence Statistics
          U-MOM     V-MOM     W-MOM     PRESS     ENERG       K     EPSILON
 Err   3.904E+03 3.475E+03 0.000E+00 3.206E+05 3.035E-01 0.000E+00 0.000E+00
 Sig   3.446E+03 2.246E+03 0.000E+00 5.418E+05 2.071E-01 0.000E+00 0.000E+00
               Lumped Convergence Criteria:   0.733E+00
1      Position of the Interface Toe at t=0 min. Without Subsurface Barrier
0FLOTRAN   2.1a                 Summary - Iter   10              06/13/94 22:23:
0     Variable           Average         Minimum     Node       Maximum     Node

 U Velocity             6.3401E-05    -1.6478E-05    348     1.5462E-04    108
 V Velocity             5.1469E-07    -2.8680E-05    542     9.1749E-05    164
 W Velocity             0.0000E+00     0.0000E+00      1     0.0000E+00      1
 Pressure               4.7382E+01     0.0000E+00   1450     1.2113E+02     74
 Turb. Kin. Enrg.       1.0210E-14     0.0000E+00      1     7.2800E-13     74
 Turb. Enrg. Diss.      1.9456E-19     0.0000E+00      1     1.3872E-17     74
 Temperature            2.8652E+02     2.7800E+02      1     2.8800E+02   1577
 Density                1.0219E+03     1.0020E+03      1     1.0250E+03   1577
 Viscosity              1.5180E-03     1.5180E-03      1     1.5180E-03      1
 Conductivity           6.1099E-04     6.1100E-04      1     6.1100E-04      1
 Eff. Viscosity         0.0000E+00     0.0000E+00      1     0.0000E+00      1
 Eff. Conductivity      0.0000E+00     0.0000E+00      1     0.0000E+00      1
 Total Temperature      2.9300E+02     2.9300E+02      1     2.9300E+02      1
0
0INLETS/OUTLETS

 Region Node 1   X          Y          Z        Mass Flow   Pressure     Bulk T
    1     116    0.     0.537E-02    0.      0.2794E-01   96.43       278.00
    2    1458  1.20     0.497E-01    0.     -0.2748E-01  0.2238E-01   288.00

0Total Mass Flow In  =  0.27945E-01
0Total Mass Flow Out = -0.27476E-01

0Total Energy Flow In  =   32520.
0Total Energy Flow Out =  -33124.

1      Position of the Interface Toe at t=0 min. Without Subsurface Barrier
0FLOTRAN   2.1a                 Convergence Monitor              06/13/94 22:23:
 ITER    U-MOM     V-MOM     W-MOM     PRESS     ENERG       K     EPSILON
   11  3.851E-03 1.779E-02 0.000E+00 2.533E-02 4.256E-04 0.000E+00 0.000E+00
   12  3.372E-03 1.766E-02 0.000E+00 2.417E-02 4.241E-04 0.000E+00 0.000E+00
   13  3.042E-03 1.756E-02 0.000E+00 2.370E-02 4.244E-04 0.000E+00 0.000E+00
   14  2.820E-03 1.752E-02 0.000E+00 2.356E-02 4.433E-04 0.000E+00 0.000E+00
   15  2.687E-03 1.760E-02 0.000E+00 2.366E-02 4.550E-04 0.000E+00 0.000E+00
   16  2.624E-03 1.783E-02 0.000E+00 2.385E-02 4.713E-04 0.000E+00 0.000E+00
   17  2.611E-03 1.821E-02 0.000E+00 2.412E-02 4.782E-04 0.000E+00 0.000E+00
   18  2.629E-03 1.866E-02 0.000E+00 2.438E-02 4.970E-04 0.000E+00 0.000E+00
   19  2.668E-03 1.918E-02 0.000E+00 2.466E-02 5.068E-04 0.000E+00 0.000E+00
   20  2.719E-03 1.972E-02 0.000E+00 2.488E-02 5.085E-04 0.000E+00 0.000E+00


                         Global Convergence Statistics
          U-MOM     V-MOM     W-MOM     PRESS     ENERG       K     EPSILON
 Err   6.559E+01 4.443E+02 0.000E+00 1.885E+03 3.666E-01 0.000E+00 0.000E+00
 Sig   7.392E+01 3.921E+02 0.000E+00 2.677E+03 2.253E-01 0.000E+00 0.000E+00
               Lumped Convergence Criteria:   0.449E+00
1      Position of the Interface Toe at t=0 min. Without Subsurface Barrier
0FLOTRAN   2.1a                 Summary - Iter   20              06/13/94 22:23:
0     Variable           Average         Minimum     Node       Maximum     Node

 U Velocity             6.1466E-05     0.0000E+00      1     1.5574E-04     99
 V Velocity             5.0329E-07    -2.5757E-05    862     7.7110E-05   2118
 W Velocity             0.0000E+00     0.0000E+00      1     0.0000E+00      1
 Pressure               4.6527E+01     0.0000E+00   1450     1.3759E+02     74
 Turb. Kin. Enrg.       1.0210E-14     0.0000E+00      1     7.2800E-13     74
 Turb. Enrg. Diss.      1.9456E-19     0.0000E+00      1     1.3872E-17     74
 Temperature            2.8523E+02     2.7800E+02      4     2.8800E+02   1823
 Density                1.0190E+03     1.0020E+03      4     1.0250E+03   1780
```

```
 Viscosity              1.5180E-03     1.5180E-03      1     1.5180E-03      1
 Conductivity           6.1099E-04     6.1100E-04      1     6.1100E-04      1
 Eff. Viscosity         0.0000E+00     0.0000E+00      1     0.0000E+00      1
 Eff. Conductivity      0.0000E+00     0.0000E+00      1     0.0000E+00      1
 Total Temperature      2.9300E+02     2.9300E+02      1     2.9300E+02      1
0
0INLETS/OUTLETS

 Region Node 1   X          Y          Z        Mass Flow   Pressure     Bulk T
    1     116    0.      0.537E-02    0.       0.2794E-01   98.39       278.00
    2    1458  1.20      0.497E-01    0.      -0.2748E-01  0.2234E-01   288.00

0Total Mass Flow In  =  0.27944E-01
0Total Mass Flow Out = -0.27475E-01

0Total Energy Flow In  =   32519.
0Total Energy Flow Out =  -33123.

1      Position of the Interface Toe at t=0 min. Without Subsurface Barrier
0FLOTRAN   2.1a                  Convergence Monitor                 06/13/94 22:23:
 ITER    U-MOM      V-MOM      W-MOM      PRESS      ENERG        K      EPSILON
   21  2.775E-03 2.018E-02 0.000E+00 2.506E-02 5.035E-04 0.000E+00 0.000E+00
   22  2.829E-03 2.052E-02 0.000E+00 2.519E-02 5.004E-04 0.000E+00 0.000E+00
   23  2.879E-03 2.075E-02 0.000E+00 2.527E-02 4.987E-04 0.000E+00 0.000E+00
   24  2.923E-03 2.090E-02 0.000E+00 2.533E-02 4.980E-04 0.000E+00 0.000E+00
   25  2.961E-03 2.100E-02 0.000E+00 2.537E-02 4.979E-04 0.000E+00 0.000E+00
   26  2.993E-03 2.107E-02 0.000E+00 2.539E-02 4.981E-04 0.000E+00 0.000E+00
   27  3.021E-03 2.112E-02 0.000E+00 2.543E-02 4.984E-04 0.000E+00 0.000E+00
   28  3.044E-03 2.115E-02 0.000E+00 2.545E-02 4.989E-04 0.000E+00 0.000E+00
   29  3.063E-03 2.118E-02 0.000E+00 2.546E-02 4.994E-04 0.000E+00 0.000E+00
   30  3.078E-03 2.120E-02 0.000E+00 2.547E-02 4.999E-04 0.000E+00 0.000E+00


                         Global Convergence Statistics
         U-MOM      V-MOM      W-MOM      PRESS      ENERG        K      EPSILON
 Err   1.125E+01 3.732E+02 0.000E+00 1.821E+02 4.538E-02 0.000E+00 0.000E+00
 Sig   4.191E+00 3.618E+02 0.000E+00 1.664E+02 5.068E-02 0.000E+00 0.000E+00
               Lumped Convergence Criteria:   0.351E+00
1      Position of the Interface Toe at t=0 min. Without Subsurface Barrier
0FLOTRAN   2.1a                  Summary - Iter   30                  06/13/94 22:23:
0     Variable            Average          Minimum      Node        Maximum      Node

 U Velocity             6.0995E-05     0.0000E+00      1     1.4683E-04      90
 V Velocity             5.0610E-07    -2.0728E-05   1209     7.5731E-05    2118
 W Velocity             0.0000E+00     0.0000E+00      1     0.0000E+00       1
 Pressure               4.5096E+01     0.0000E+00   1450     1.4264E+02      74
 Turb. Kin. Enrg.       1.0210E-14     0.0000E+00      1     7.2800E-13      74
 Turb. Enrg. Diss.      1.9456E-19     0.0000E+00      1     1.3872E-17      74
 Temperature            2.8381E+02     2.7800E+02    221     2.8800E+02    1427
 Density                1.0157E+03     1.0020E+03      5     1.0250E+03    1478
 Viscosity              1.5180E-03     1.5180E-03      1     1.5180E-03       1
 Conductivity           6.1099E-04     6.1100E-04      1     6.1100E-04       1
 Eff. Viscosity         0.0000E+00     0.0000E+00      1     0.0000E+00       1
 Eff. Conductivity      0.0000E+00     0.0000E+00      1     0.0000E+00       1
 Total Temperature      2.9300E+02     2.9300E+02      1     2.9300E+02       1
0
0INLETS/OUTLETS

 Region Node 1   X          Y          Z        Mass Flow   Pressure     Bulk T
    1     116    0.      0.537E-02    0.       0.2794E-01   99.10       278.00
    2    1458  1.20      0.497E-01    0.      -0.2748E-01  0.2164E-01   288.00

0Total Mass Flow In  =  0.27944E-01
0Total Mass Flow Out = -0.27483E-01

0Total Energy Flow In  =   32519.
0Total Energy Flow Out =  -33132.

1      Position of the Interface Toe at t=0 min. Without Subsurface Barrier
0FLOTRAN   2.1a                  Convergence Monitor                 06/13/94 22:23:
 ITER    U-MOM      V-MOM      W-MOM      PRESS      ENERG        K      EPSILON
   31  3.089E-03 2.122E-02 0.000E+00 2.549E-02 5.003E-04 0.000E+00 0.000E+00
   32  3.096E-03 2.123E-02 0.000E+00 2.551E-02 5.008E-04 0.000E+00 0.000E+00
   33  3.101E-03 2.124E-02 0.000E+00 2.551E-02 5.013E-04 0.000E+00 0.000E+00
   34  3.101E-03 2.125E-02 0.000E+00 2.553E-02 5.017E-04 0.000E+00 0.000E+00
```

```
   35  3.100E-03 2.126E-02 0.000E+00 2.553E-02 5.021E-04 0.000E+00 0.000E+00
   36  3.095E-03 2.126E-02 0.000E+00 2.553E-02 5.024E-04 0.000E+00 0.000E+00
   37  3.087E-03 2.126E-02 0.000E+00 2.553E-02 5.026E-04 0.000E+00 0.000E+00
   38  3.077E-03 2.125E-02 0.000E+00 2.553E-02 5.027E-04 0.000E+00 0.000E+00
   39  3.065E-03 2.124E-02 0.000E+00 2.551E-02 5.028E-04 0.000E+00 0.000E+00
   40  3.049E-03 2.122E-02 0.000E+00 2.547E-02 5.026E-04 0.000E+00 0.000E+00


                         Global Convergence Statistics
         U-MOM     V-MOM     W-MOM     PRESS     ENERG       K     EPSILON
 Err   2.214E+00 2.163E+01 0.000E+00 2.774E+01 1.290E-02 0.000E+00 0.000E+00
 Sig   1.336E+00 1.336E+01 0.000E+00 2.129E+01 6.511E-03 0.000E+00 0.000E+00
               Lumped Convergence Criteria:   0.205E+00
1      Position of the Interface Toe at t=0 min. Without Subsurface Barrier
0FLOTRAN   2.1a                 Summary - Iter   40              06/13/94 22:23:
0     Variable           Average         Minimum     Node       Maximum     Node

 U Velocity             6.1024E-05     0.0000E+00      1     1.4002E-04     80
 V Velocity             7.3103E-07    -1.7354E-05   1581     6.8880E-05   2118
 W Velocity             0.0000E+00     0.0000E+00      1     0.0000E+00      1
 Pressure               4.3741E+01     0.0000E+00   1450     1.4461E+02     74
 Turb. Kin. Enrg.       1.0210E-14     0.0000E+00      1     7.2800E-13     74
 Turb. Enrg. Diss.      1.9456E-19     0.0000E+00      1     1.3872E-17     74
 Temperature            2.8239E+02     2.7800E+02    354     2.8800E+02   1427
 Density                1.0124E+03     1.0020E+03    237     1.0250E+03   1427
 Viscosity              1.5180E-03     1.5180E-03      1     1.5180E-03      1
 Conductivity           6.1099E-04     6.1100E-04      1     6.1100E-04      1
 Eff. Viscosity         0.0000E+00     0.0000E+00      1     0.0000E+00      1
 Eff. Conductivity      0.0000E+00     0.0000E+00      1     0.0000E+00      1
 Total Temperature      2.9300E+02     2.9300E+02      1     2.9300E+02      1
0
0INLETS/OUTLETS

 Region Node 1   X         Y         Z       Mass Flow   Pressure     Bulk T
    1     116    0.     0.537E-02    0.      0.2794E-01   99.74       278.00
    2    1458  1.20     0.497E-01    0.     -0.2752E-01  0.1828E-01   287.97

0Total Mass Flow In  =  0.27944E-01
0Total Mass Flow Out = -0.27524E-01

0Total Energy Flow In  =   32519.
0Total Energy Flow Out =  -33179.

1      Position of the Interface Toe at t=0 min. Without Subsurface Barrier
0FLOTRAN   2.1a                 Convergence Monitor              06/13/94 22:23:
 ITER     U-MOM     V-MOM     W-MOM     PRESS     ENERG       K     EPSILON
   41  3.032E-03 2.119E-02 0.000E+00 2.546E-02 5.023E-04 0.000E+00 0.000E+00
   42  3.013E-03 2.116E-02 0.000E+00 2.540E-02 5.017E-04 0.000E+00 0.000E+00
   43  2.992E-03 2.112E-02 0.000E+00 2.535E-02 5.009E-04 0.000E+00 0.000E+00
   44  2.969E-03 2.107E-02 0.000E+00 2.528E-02 4.997E-04 0.000E+00 0.000E+00
   45  2.944E-03 2.100E-02 0.000E+00 2.521E-02 4.982E-04 0.000E+00 0.000E+00
   46  2.917E-03 2.092E-02 0.000E+00 2.510E-02 4.961E-04 0.000E+00 0.000E+00
   47  2.889E-03 2.083E-02 0.000E+00 2.497E-02 4.935E-04 0.000E+00 0.000E+00
   48  2.860E-03 2.072E-02 0.000E+00 2.481E-02 4.903E-04 0.000E+00 0.000E+00
   49  2.830E-03 2.058E-02 0.000E+00 2.461E-02 4.863E-04 0.000E+00 0.000E+00
   50  2.800E-03 2.042E-02 0.000E+00 2.438E-02 4.816E-04 0.000E+00 0.000E+00


                         Global Convergence Statistics
         U-MOM     V-MOM     W-MOM     PRESS     ENERG       K     EPSILON
 Err   6.555E+00 1.509E+02 0.000E+00 2.486E+02 7.147E-02 0.000E+00 0.000E+00
 Sig   1.324E+00 8.657E+01 0.000E+00 1.581E+02 5.344E-02 0.000E+00 0.000E+00
               Lumped Convergence Criteria:   0.321E+00
1      Position of the Interface Toe at t=0 min. Without Subsurface Barrier
0FLOTRAN   2.1a                 Summary - Iter   50              06/13/94 22:23:
0     Variable           Average         Minimum     Node       Maximum     Node

 U Velocity             6.1296E-05     0.0000E+00      1     1.3666E-04   1501
 V Velocity             1.8073E-06    -1.0930E-05   1814     4.3519E-05   2118
 W Velocity             0.0000E+00     0.0000E+00      1     0.0000E+00      1
 Pressure               4.2410E+01     0.0000E+00   1450     1.4550E+02     74
 Turb. Kin. Enrg.       1.0210E-14     0.0000E+00      1     7.2800E-13     74
 Turb. Enrg. Diss.      1.9456E-19     0.0000E+00      1     1.3872E-17     74
 Temperature            2.8099E+02     2.7800E+02    383     2.8800E+02   1427
 Density                1.0092E+03     1.0020E+03    354     1.0250E+03   1427
```

```
 Viscosity              1.5180E-03     1.5180E-03      1     1.5180E-03      1
 Conductivity           6.1099E-04     6.1100E-04      1     6.1100E-04      1
 Eff. Viscosity         0.0000E+00     0.0000E+00      1     0.0000E+00      1
 Eff. Conductivity      0.0000E+00     0.0000E+00      1     0.0000E+00      1
 Total Temperature      2.9300E+02     2.9300E+02      1     2.9300E+02      1
0
0INLETS/OUTLETS

 Region Node 1   X          Y          Z        Mass Flow   Pressure     Bulk T
    1     116    0.      0.537E-02    0.       0.2794E-01   100.2       278.00
    2    1458  1.20      0.497E-01    0.      -0.2768E-01  0.7580E-02   287.53

0Total Mass Flow In  =  0.27944E-01
0Total Mass Flow Out = -0.27677E-01

0Total Energy Flow In  =   32519.
0Total Energy Flow Out =  -33312.

1      Position of the Interface Toe at t=0 min. Without Subsurface Barrier
0FLOTRAN   2.1a                  Convergence Monitor                 06/13/94 22:23:
 ITER    U-MOM      V-MOM      W-MOM      PRESS      ENERG        K      EPSILON
   51  2.769E-03 2.024E-02 0.000E+00 2.411E-02 4.759E-04 0.000E+00 0.000E+00
   52  2.737E-03 2.002E-02 0.000E+00 2.379E-02 4.693E-04 0.000E+00 0.000E+00
   53  2.703E-03 1.978E-02 0.000E+00 2.343E-02 4.616E-04 0.000E+00 0.000E+00
   54  2.667E-03 1.950E-02 0.000E+00 2.304E-02 4.528E-04 0.000E+00 0.000E+00
   55  2.628E-03 1.918E-02 0.000E+00 2.258E-02 4.428E-04 0.000E+00 0.000E+00
   56  2.587E-03 1.882E-02 0.000E+00 2.210E-02 4.316E-04 0.000E+00 0.000E+00
   57  2.544E-03 1.842E-02 0.000E+00 2.155E-02 4.182E-04 0.000E+00 0.000E+00
   58  2.497E-03 1.797E-02 0.000E+00 2.096E-02 4.025E-04 0.000E+00 0.000E+00
   59  2.447E-03 1.746E-02 0.000E+00 2.030E-02 3.856E-04 0.000E+00 0.000E+00
   60  2.394E-03 1.688E-02 0.000E+00 1.952E-02 3.709E-04 0.000E+00 0.000E+00


                         Global Convergence Statistics
         U-MOM      V-MOM      W-MOM      PRESS      ENERG        K      EPSILON
 Err   9.065E+00 5.699E+02 0.000E+00 9.101E+02 2.865E-01 0.000E+00 0.000E+00
 Sig   1.658E+00 2.102E+02 0.000E+00 2.979E+02 1.088E-01 0.000E+00 0.000E+00
               Lumped Convergence Criteria:   0.382E+00
1      Position of the Interface Toe at t=0 min. Without Subsurface Barrier
0FLOTRAN   2.1a                  Summary - Iter   60                  06/13/94 22:23:
0     Variable            Average          Minimum      Node        Maximum      Node

 U Velocity             6.1769E-05     -1.7351E-05   1459      1.9320E-04   1450
 V Velocity             4.3312E-06     -7.0636E-06   2117      3.1355E-05   1473
 W Velocity             0.0000E+00      0.0000E+00      1      0.0000E+00      1
 Pressure               4.1069E+01     -1.6833E+00   1446      1.4576E+02     74
 Turb. Kin. Enrg.       1.0210E-14      0.0000E+00      1      7.2800E-13     74
 Turb. Enrg. Diss.      1.9456E-19      0.0000E+00      1      1.3872E-17     74
 Temperature            2.7979E+02      2.7800E+02    585      2.8800E+02   1427
 Density                1.0064E+03      1.0020E+03    585      1.0250E+03   1427
 Viscosity              1.5180E-03      1.5180E-03      1      1.5180E-03      1
 Conductivity           6.1099E-04      6.1100E-04      1      6.1100E-04      1
 Eff. Viscosity         0.0000E+00      0.0000E+00      1      0.0000E+00      1
 Eff. Conductivity      0.0000E+00      0.0000E+00      1      0.0000E+00      1
 Total Temperature      2.9300E+02      2.9300E+02      1      2.9300E+02      1
0
0INLETS/OUTLETS

 Region Node 1   X          Y          Z        Mass Flow   Pressure     Bulk T
    1     116    0.      0.537E-02    0.       0.2794E-01   100.3       278.00
    2    1458  1.20      0.497E-01    0.      -0.2799E-01  0.5496E-03   285.64

0Total Mass Flow In  =  0.27944E-01
0Total Mass Flow Out = -0.27993E-01

0Total Energy Flow In  =   32519.
0Total Energy Flow Out =  -33470.

1      Position of the Interface Toe at t=0 min. Without Subsurface Barrier
0FLOTRAN   2.1a                  Convergence Monitor                 06/13/94 22:23:
 ITER    U-MOM      V-MOM      W-MOM      PRESS      ENERG        K      EPSILON
   61  2.339E-03 1.616E-02 0.000E+00 1.856E-02 3.567E-04 0.000E+00 0.000E+00
   62  2.283E-03 1.531E-02 0.000E+00 1.748E-02 3.436E-04 0.000E+00 0.000E+00
   63  2.229E-03 1.439E-02 0.000E+00 1.644E-02 3.301E-04 0.000E+00 0.000E+00
   64  2.172E-03 1.361E-02 0.000E+00 1.541E-02 3.172E-04 0.000E+00 0.000E+00
```

```
   65  2.113E-03 1.292E-02 0.000E+00 1.444E-02 3.036E-04 0.000E+00 0.000E+00
   66  2.049E-03 1.228E-02 0.000E+00 1.345E-02 2.919E-04 0.000E+00 0.000E+00
   67  1.980E-03 1.167E-02 0.000E+00 1.249E-02 2.773E-04 0.000E+00 0.000E+00
   68  1.908E-03 1.110E-02 0.000E+00 1.157E-02 2.627E-04 0.000E+00 0.000E+00
   69  1.837E-03 1.054E-02 0.000E+00 1.067E-02 2.532E-04 0.000E+00 0.000E+00
   70  1.768E-03 9.980E-03 0.000E+00 9.811E-03 2.356E-04 0.000E+00 0.000E+00


                         Global Convergence Statistics
          U-MOM      V-MOM      W-MOM      PRESS      ENERG       K      EPSILON
 Err   1.033E+01 6.924E+02 0.000E+00 9.534E+02 1.816E-01 0.000E+00 0.000E+00
 Sig   1.183E+00 1.175E+02 0.000E+00 6.553E+01 1.030E-02 0.000E+00 0.000E+00
               Lumped Convergence Criteria:   0.377E+00
1      Position of the Interface Toe at t=0 min. Without Subsurface Barrier
0FLOTRAN   2.1a                  Summary - Iter   70              06/13/94 22:23:
0     Variable            Average          Minimum     Node        Maximum     Node

 U Velocity             6.1974E-05    -6.3345E-05   1459     3.0442E-04   1450
 V Velocity             6.8103E-06    -3.4385E-05   2117     8.6118E-05   1476
 W Velocity             0.0000E+00     0.0000E+00      1     0.0000E+00      1
 Pressure               4.0394E+01    -8.3628E+00   1437     1.4601E+02     74
 Turb. Kin. Enrg.       1.0210E-14     0.0000E+00      1     7.2800E-13     74
 Turb. Enrg. Diss.      1.9456E-19     0.0000E+00      1     1.3872E-17     74
 Temperature            2.7923E+02     2.7800E+02    760     2.8800E+02   1427
 Density                1.0049E+03     1.0020E+03    760     1.0250E+03   1427
 Viscosity              1.5180E-03     1.5180E-03      1     1.5180E-03      1
 Conductivity           6.1099E-04     6.1100E-04      1     6.1100E-04      1
 Eff. Viscosity         0.0000E+00     0.0000E+00      1     0.0000E+00      1
 Eff. Conductivity      0.0000E+00     0.0000E+00      1     0.0000E+00      1
 Total Temperature      2.9300E+02     2.9300E+02      1     2.9300E+02      1
0
0INLETS/OUTLETS

 Region Node 1   X          Y          Z        Mass Flow   Pressure     Bulk T
    1     116    0.      0.537E-02    0.       0.2794E-01   100.6       278.00
    2    1458  1.20      0.497E-01    0.      -0.2815E-01  0.5945E-02   282.26

0Total Mass Flow In  =  0.27944E-01
0Total Mass Flow Out = -0.28151E-01

0Total Energy Flow In  =   32519.
0Total Energy Flow Out =  -33262.

1      Position of the Interface Toe at t=0 min. Without Subsurface Barrier
0FLOTRAN   2.1a                  Convergence Monitor              06/13/94 22:23:
 ITER     U-MOM      V-MOM      W-MOM      PRESS      ENERG       K      EPSILON
   71  1.698E-03 9.463E-03 0.000E+00 8.992E-03 2.263E-04 0.000E+00 0.000E+00
   72  1.627E-03 8.937E-03 0.000E+00 8.227E-03 2.100E-04 0.000E+00 0.000E+00
   73  1.556E-03 8.438E-03 0.000E+00 7.505E-03 2.019E-04 0.000E+00 0.000E+00
   74  1.482E-03 7.957E-03 0.000E+00 6.956E-03 1.862E-04 0.000E+00 0.000E+00
   75  1.405E-03 7.488E-03 0.000E+00 6.258E-03 1.787E-04 0.000E+00 0.000E+00
   76  1.329E-03 7.057E-03 0.000E+00 5.640E-03 1.651E-04 0.000E+00 0.000E+00
   77  1.254E-03 6.627E-03 0.000E+00 5.091E-03 1.502E-04 0.000E+00 0.000E+00
   78  1.183E-03 6.225E-03 0.000E+00 4.597E-03 1.495E-04 0.000E+00 0.000E+00
   79  1.116E-03 5.842E-03 0.000E+00 4.348E-03 1.358E-04 0.000E+00 0.000E+00
   80  1.053E-03 5.489E-03 0.000E+00 3.915E-03 1.211E-04 0.000E+00 0.000E+00


                         Global Convergence Statistics
          U-MOM      V-MOM      W-MOM      PRESS      ENERG       K      EPSILON
 Err   6.852E+00 2.495E+02 0.000E+00 2.348E+02 2.446E-02 0.000E+00 0.000E+00
 Sig   3.337E-01 3.141E+01 0.000E+00 6.376E+01 5.172E-03 0.000E+00 0.000E+00
               Lumped Convergence Criteria:   0.309E+00
1      Position of the Interface Toe at t=0 min. Without Subsurface Barrier
0FLOTRAN   2.1a                  Summary - Iter   80              06/13/94 22:23:
0     Variable            Average          Minimum     Node        Maximum     Node

 U Velocity             6.2030E-05    -5.7925E-05   1459     3.8678E-04   1450
 V Velocity             7.6477E-06    -3.0488E-05   2117     1.3519E-04   1477
 W Velocity             0.0000E+00     0.0000E+00      1     0.0000E+00      1
 Pressure               4.0338E+01    -1.1418E+01   1433     1.4628E+02     74
 Turb. Kin. Enrg.       1.0210E-14     0.0000E+00      1     7.2800E-13     74
 Turb. Enrg. Diss.      1.9456E-19     0.0000E+00      1     1.3872E-17     74
 Temperature            2.7920E+02     2.7800E+02    818     2.8800E+02   1427
 Density                1.0047E+03     1.0020E+03    818     1.0250E+03   1427
```

```
 Viscosity              1.5180E-03     1.5180E-03      1     1.5180E-03      1
 Conductivity           6.1099E-04     6.1100E-04      1     6.1100E-04      1
 Eff. Viscosity         0.0000E+00     0.0000E+00      1     0.0000E+00      1
 Eff. Conductivity      0.0000E+00     0.0000E+00      1     0.0000E+00      1
 Total Temperature      2.9300E+02     2.9300E+02      1     2.9300E+02      1
0
0INLETS/OUTLETS

 Region Node 1   X          Y          Z        Mass Flow   Pressure     Bulk T
    1     116    0.      0.537E-02    0.       0.2794E-01   100.8       278.00
    2    1458  1.20      0.497E-01    0.      -0.2814E-01  0.4856E-02   279.62

0Total Mass Flow In  =  0.27944E-01
0Total Mass Flow Out = -0.28144E-01

0Total Energy Flow In  =   32519.
0Total Energy Flow Out =  -32942.

1      Position of the Interface Toe at t=0 min. Without Subsurface Barrier
0FLOTRAN   2.1a                  Convergence Monitor                 06/13/94 22:23:
 ITER    U-MOM      V-MOM      W-MOM      PRESS      ENERG        K      EPSILON
   81  9.929E-04 5.146E-03 0.000E+00 3.584E-03 1.211E-04 0.000E+00 0.000E+00
   82  9.374E-04 4.816E-03 0.000E+00 3.289E-03 1.133E-04 0.000E+00 0.000E+00
   83  8.824E-04 4.525E-03 0.000E+00 3.027E-03 1.009E-04 0.000E+00 0.000E+00
   84  8.320E-04 4.245E-03 0.000E+00 2.796E-03 8.980E-05 0.000E+00 0.000E+00
   85  7.832E-04 3.949E-03 0.000E+00 2.596E-03 9.463E-05 0.000E+00 0.000E+00
   86  7.411E-04 3.710E-03 0.000E+00 2.414E-03 8.729E-05 0.000E+00 0.000E+00
   87  6.994E-04 3.504E-03 0.000E+00 2.254E-03 7.554E-05 0.000E+00 0.000E+00
   88  6.597E-04 3.275E-03 0.000E+00 2.100E-03 6.651E-05 0.000E+00 0.000E+00
   89  6.208E-04 3.034E-03 0.000E+00 1.958E-03 7.430E-05 0.000E+00 0.000E+00
   90  5.835E-04 2.858E-03 0.000E+00 1.878E-03 6.838E-05 0.000E+00 0.000E+00


                          Global Convergence Statistics
          U-MOM      V-MOM      W-MOM      PRESS      ENERG        K      EPSILON
 Err   2.335E+00 7.533E+01 0.000E+00 3.948E+01 0.000E+00 0.000E+00 0.000E+00
 Sig   4.052E-01 1.398E+01 0.000E+00 1.498E+01 0.000E+00 0.000E+00 0.000E+00
                Lumped Convergence Criteria:   0.242E+00
1      Position of the Interface Toe at t=0 min. Without Subsurface Barrier
0FLOTRAN   2.1a                  Summary - Iter   90                  06/13/94 22:23:
0     Variable            Average          Minimum      Node        Maximum      Node

 U Velocity             6.2035E-05     -4.6718E-05   1459      4.2427E-04   1450
 V Velocity             7.7382E-06     -2.4398E-05   2118      1.6176E-04   1477
 W Velocity             0.0000E+00      0.0000E+00      1      0.0000E+00      1
 Pressure               4.0450E+01     -1.0357E+01   1431      1.4641E+02     74
 Turb. Kin. Enrg.       1.0210E-14      0.0000E+00      1      7.2800E-13     74
 Turb. Enrg. Diss.      1.9456E-19      0.0000E+00      1      1.3872E-17     74
 Temperature            2.7930E+02      2.7795E+02   1429      2.8800E+02   1427
 Density                1.0050E+03      1.0020E+03   1429      1.0250E+03   1427
 Viscosity              1.5180E-03      1.5180E-03      1      1.5180E-03      1
 Conductivity           6.1099E-04      6.1100E-04      1      6.1100E-04      1
 Eff. Viscosity         0.0000E+00      0.0000E+00      1      0.0000E+00      1
 Eff. Conductivity      0.0000E+00      0.0000E+00      1      0.0000E+00      1
 Total Temperature      2.9300E+02      2.9300E+02      1      2.9300E+02      1
0
0INLETS/OUTLETS

 Region Node 1   X          Y          Z        Mass Flow   Pressure     Bulk T
    1     116    0.      0.537E-02    0.       0.2794E-01   101.0       278.00
    2    1458  1.20      0.497E-01    0.      -0.2811E-01  0.3135E-02   278.37

0Total Mass Flow In  =  0.27944E-01
0Total Mass Flow Out = -0.28114E-01

0Total Energy Flow In  =   32519.
0Total Energy Flow Out =  -32760.

1      Position of the Interface Toe at t=0 min. Without Subsurface Barrier
0FLOTRAN   2.1a                  Convergence Monitor                 06/13/94 22:23:
 ITER    U-MOM      V-MOM      W-MOM      PRESS      ENERG        K      EPSILON
   91  5.514E-04 2.708E-03 0.000E+00 1.821E-03 6.296E-05 0.000E+00 0.000E+00
   92  5.231E-04 2.532E-03 0.000E+00 1.785E-03 5.724E-05 0.000E+00 0.000E+00
   93  4.965E-04 2.352E-03 0.000E+00 1.681E-03 4.682E-05 0.000E+00 0.000E+00
   94  4.704E-04 2.173E-03 0.000E+00 1.580E-03 5.603E-05 0.000E+00 0.000E+00
```

95	4.448E-04	2.046E-03	0.000E+00	1.531E-03	4.930E-05	0.000E+00	0.000E+00
96	4.203E-04	1.946E-03	0.000E+00	1.389E-03	4.250E-05	0.000E+00	0.000E+00
97	3.973E-04	1.840E-03	0.000E+00	1.300E-03	3.344E-05	0.000E+00	0.000E+00
98	3.737E-04	1.700E-03	0.000E+00	1.214E-03	2.621E-05	0.000E+00	0.000E+00
99	3.475E-04	1.525E-03	0.000E+00	1.078E-03	2.592E-05	0.000E+00	0.000E+00
100	3.176E-04	1.308E-03	0.000E+00	9.774E-04	2.698E-05	0.000E+00	0.000E+00

Global Convergence Statistics

	U-MOM	V-MOM	W-MOM	PRESS	ENERG	K	EPSILON
Err	5.870E-01	1.852E+01	0.000E+00	7.819E+00	0.000E+00	0.000E+00	0.000E+00
Sig	7.444E-02	3.689E+00	0.000E+00	2.086E+00	0.000E+00	0.000E+00	0.000E+00

Lumped Convergence Criteria: 0.166E+00

1 Position of the Interface Toe at t=0 min. Without Subsurface Barrier

0FLOTRAN 2.1a Summary - Iter 100 06/13/94 22:23:

0 Variable	Average	Minimum	Node	Maximum	Node
U Velocity	6.2019E-05	-3.6927E-05	1459	4.3595E-04	1450
V Velocity	7.5990E-06	-1.9348E-05	2118	1.7506E-04	1477
W Velocity	0.0000E+00	0.0000E+00	1	0.0000E+00	1
Pressure	4.0564E+01	-8.6861E+00	1429	1.4648E+02	74
Turb. Kin. Enrg.	1.0210E-14	0.0000E+00	1	7.2800E-13	74
Turb. Enrg. Diss.	1.9456E-19	0.0000E+00	1	1.3872E-17	74
Temperature	2.7938E+02	2.7795E+02	1428	2.8800E+02	1427
Density	1.0052E+03	1.0019E+03	1428	1.0250E+03	1427
Viscosity	1.5180E-03	1.5180E-03	1	1.5180E-03	1
Conductivity	6.1099E-04	6.1100E-04	1	6.1100E-04	1
Eff. Viscosity	0.0000E+00	0.0000E+00	1	0.0000E+00	1
Eff. Conductivity	0.0000E+00	0.0000E+00	1	0.0000E+00	1
Total Temperature	2.9300E+02	2.9300E+02	1	2.9300E+02	1

0

0INLETS/OUTLETS

Region	Node 1	X	Y	Z	Mass Flow	Pressure	Bulk T
1	116	0.	0.537E-02	0.	0.2794E-01	101.0	278.00
2	1458	1.20	0.497E-01	0.	-0.2808E-01	0.1946E-02	278.01

0Total Mass Flow In = 0.27944E-01
0Total Mass Flow Out = -0.28084E-01

0Total Energy Flow In = 32519.
0Total Energy Flow Out = -32683.

1 Position of the Interface Toe at t=0 min. Without Subsurface Barrier

0FLOTRAN 2.1a Convergence Monitor 06/13/94 22:23:

ITER	U-MOM	V-MOM	W-MOM	PRESS	ENERG	K	EPSILON
101	2.825E-04	1.083E-03	0.000E+00	8.418E-04	4.126E-05	0.000E+00	0.000E+00
102	2.441E-04	8.224E-04	0.000E+00	7.082E-04	3.646E-05	0.000E+00	0.000E+00
103	1.959E-04	6.691E-04	0.000E+00	6.771E-04	2.422E-05	0.000E+00	0.000E+00
104	1.611E-04	6.009E-04	0.000E+00	5.885E-04	2.302E-05	0.000E+00	0.000E+00
105	1.450E-04	5.527E-04	0.000E+00	5.597E-04	2.135E-05	0.000E+00	0.000E+00
106	1.308E-04	5.068E-04	0.000E+00	5.234E-04	1.854E-05	0.000E+00	0.000E+00
107	1.183E-04	4.755E-04	0.000E+00	4.706E-04	2.115E-05	0.000E+00	0.000E+00
108	1.060E-04	4.278E-04	0.000E+00	4.470E-04	3.688E-05	0.000E+00	0.000E+00
109	9.612E-05	4.255E-04	0.000E+00	4.489E-04	2.841E-05	0.000E+00	0.000E+00
110	9.300E-05	3.892E-04	0.000E+00	3.883E-04	2.375E-05	0.000E+00	0.000E+00

Global Convergence Statistics

	U-MOM	V-MOM	W-MOM	PRESS	ENERG	K	EPSILON
Err	0.000E+00	2.921E+00	0.000E+00	1.758E+00	0.000E+00	0.000E+00	0.000E+00
Sig	0.000E+00	2.567E+00	0.000E+00	1.150E+00	0.000E+00	0.000E+00	0.000E+00

Lumped Convergence Criteria: 0.857E-01

1 Position of the Interface Toe at t=0 min. Without Subsurface Barrier

0FLOTRAN 2.1a Summary - Iter 110 06/13/94 22:23:

0 Variable	Average	Minimum	Node	Maximum	Node
U Velocity	6.2006E-05	-3.1516E-05	1459	4.3822E-04	1450
V Velocity	7.4754E-06	-1.6860E-05	2118	1.7886E-04	1477
W Velocity	0.0000E+00	0.0000E+00	1	0.0000E+00	1
Pressure	4.0615E+01	-8.2220E+00	1428	1.4651E+02	74
Turb. Kin. Enrg.	1.0210E-14	0.0000E+00	1	7.2800E-13	74
Turb. Enrg. Diss.	1.9456E-19	0.0000E+00	1	1.3872E-17	74
Temperature	2.7940E+02	2.7796E+02	1334	2.8800E+02	1427
Density	1.0052E+03	1.0019E+03	1334	1.0250E+03	1427

```
 Viscosity              1.5180E-03     1.5180E-03      1     1.5180E-03      1
 Conductivity           6.1099E-04     6.1100E-04      1     6.1100E-04      1
 Eff. Viscosity         0.0000E+00     0.0000E+00      1     0.0000E+00      1
 Eff. Conductivity      0.0000E+00     0.0000E+00      1     0.0000E+00      1
 Total Temperature      2.9300E+02     2.9300E+02      1     2.9300E+02      1
0
0INLETS/OUTLETS

 Region Node 1   X          Y          Z        Mass Flow   Pressure     Bulk T
    1     116    0.      0.537E-02    0.      0.2794E-01   101.0       278.00
    2    1458  1.20      0.497E-01    0.     -0.2807E-01  0.1405E-02   278.00

0Total Mass Flow In  =  0.27944E-01
0Total Mass Flow Out = -0.28068E-01

0Total Energy Flow In  =   32519.
0Total Energy Flow Out =  -32662.

1      Position of the Interface Toe at t=0 min. Without Subsurface Barrier
0FLOTRAN   2.1a                  Convergence Monitor                 06/13/94 22:23:
 ITER    U-MOM     V-MOM     W-MOM     PRESS     ENERG       K      EPSILON
  111  8.889E-05 3.717E-04 0.000E+00 4.020E-04 2.062E-05 0.000E+00 0.000E+00
  112  8.280E-05 3.807E-04 0.000E+00 3.966E-04 3.046E-05 0.000E+00 0.000E+00


                          Global Convergence Statistics
         U-MOM     V-MOM     W-MOM     PRESS     ENERG       K      EPSILON
 Err   0.000E+00 4.372E-01 0.000E+00 4.093E-01 0.000E+00 0.000E+00 0.000E+00
 Sig   0.000E+00 4.496E-01 0.000E+00 4.057E-01 0.000E+00 0.000E+00 0.000E+00
              Lumped Convergence Criteria:  -0.139E-01
1      Position of the Interface Toe at t=0 min. Without Subsurface Barrier
0FLOTRAN   2.1a                  Summary - Iter  112                 06/13/94 22:23:
0     Variable            Average          Minimum     Node        Maximum     Node

 U Velocity             6.2005E-05     -3.0746E-05   1459      4.3830E-04   1450
 V Velocity             7.4574E-06     -1.6518E-05   2118      1.7904E-04   1477
 W Velocity             0.0000E+00      0.0000E+00      1      0.0000E+00      1
 Pressure               4.0622E+01     -8.1763E+00   1428      1.4651E+02     74
 Turb. Kin. Enrg.       1.0210E-14      0.0000E+00      1      7.2800E-13     74
 Turb. Enrg. Diss.      1.9456E-19      0.0000E+00      1      1.3872E-17     74
 Temperature            2.7941E+02      2.7794E+02   1334      2.8800E+02   1427
 Density                1.0052E+03      1.0019E+03   1334      1.0250E+03   1427
 Viscosity              1.5180E-03      1.5180E-03      1      1.5180E-03      1
 Conductivity           6.1099E-04      6.1100E-04      1      6.1100E-04      1
 Eff. Viscosity         0.0000E+00      0.0000E+00      1      0.0000E+00      1
 Eff. Conductivity      0.0000E+00      0.0000E+00      1      0.0000E+00      1
 Total Temperature      2.9300E+02      2.9300E+02      1      2.9300E+02      1
0
0INLETS/OUTLETS

 Region Node 1   X          Y          Z        Mass Flow   Pressure     Bulk T
    1     116    0.      0.537E-02    0.      0.2794E-01   101.1       278.00
    2    1458  1.20      0.497E-01    0.     -0.2807E-01  0.1335E-02   278.01

0Total Mass Flow In  =  0.27944E-01
0Total Mass Flow Out = -0.28066E-01

0Total Energy Flow In  =   32519.
0Total Energy Flow Out =  -32661.

0HEAT TRANSFER

 Energy of Fluid Volumetric Heat Sources =       0.
 Energy of Solid Volumetric Heat Sources =       0.

 Positive Heat Transfer to Wall Faces =  0.27334E-04
 Negative Heat Transfer to Wall Faces = -0.28775E-02
 Net Heat Transfer to Wall Faces =      -0.28502E-02

 Net Conduction Across Inlet/Outlet Faces = -0.13258E-01
```

1 Position of the Interface Toe at t=0 min. Without Subsurface Barrier
0FLOTRAN 2.1a Temperature 06/13/94 22:23:

Temperature ITERATION 112

1	2	3	4	5
2.780E+02	2.780E+02	2.780E+02	2.780E+02	2.780E+02
6	7	8	9	10
2.780E+02	2.780E+02	2.780E+02	2.780E+02	2.780E+02
11	12	13	14	15
2.780E+02	2.780E+02	2.780E+02	2.780E+02	2.780E+02
16	17	18	19	20
2.780E+02	2.780E+02	2.780E+02	2.780E+02	2.780E+02
21	22	23	24	25
2.780E+02	2.780E+02	2.780E+02	2.780E+02	2.780E+02
26	27	28	29	30
2.780E+02	2.780E+02	2.780E+02	2.780E+02	2.780E+02
31	32	33	34	35
2.780E+02	2.780E+02	2.780E+02	2.780E+02	2.780E+02
36	37	38	39	40
2.780E+02	2.780E+02	2.780E+02	2.780E+02	2.780E+02
41	42	43	44	45
2.780E+02	2.780E+02	2.780E+02	2.780E+02	2.780E+02
46	47	48	49	50
2.780E+02	2.780E+02	2.780E+02	2.780E+02	2.780E+02
51	52	53	54	55
2.780E+02	2.780E+02	2.780E+02	2.780E+02	2.780E+02
56	57	58	59	60
2.780E+02	2.780E+02	2.780E+02	2.780E+02	2.780E+02
61	62	63	64	65
2.780E+02	2.780E+02	2.780E+02	2.780E+02	2.780E+02
66	67	68	69	70
2.780E+02	2.780E+02	2.780E+02	2.780E+02	2.780E+02
71	72	73	74	75
2.780E+02	2.780E+02	2.780E+02	2.780E+02	2.780E+02
76	77	78	79	80
2.780E+02	2.780E+02	2.780E+02	2.780E+02	2.780E+02
81	82	83	84	85
2.780E+02	2.780E+02	2.780E+02	2.780E+02	2.780E+02
86	87	88	89	90
2.780E+02	2.780E+02	2.780E+02	2.780E+02	2.780E+02
91	92	93	94	95
2.780E+02	2.780E+02	2.780E+02	2.780E+02	2.780E+02
96	97	98	99	100
2.780E+02	2.780E+02	2.780E+02	2.780E+02	2.780E+02
101	102	103	104	105
2.780E+02	2.780E+02	2.780E+02	2.780E+02	2.780E+02
106	107	108	109	110
2.780E+02	2.780E+02	2.780E+02	2.780E+02	2.780E+02
111	112	113	114	115
2.780E+02	2.780E+02	2.780E+02	2.780E+02	2.780E+02
116	117	118	119	120
2.780E+02	2.780E+02	2.780E+02	2.780E+02	2.780E+02
121	122	123	124	125
2.780E+02	2.780E+02	2.780E+02	2.780E+02	2.780E+02
126	127	128	129	130
2.780E+02	2.780E+02	2.780E+02	2.780E+02	2.780E+02
131	132	133	134	135
2.780E+02	2.780E+02	2.780E+02	2.780E+02	2.780E+02
136	137	138	139	140
2.780E+02	2.780E+02	2.780E+02	2.780E+02	2.780E+02
141	142	143	144	145
2.780E+02	2.780E+02	2.780E+02	2.780E+02	2.780E+02
146	147	148	149	150
2.780E+02	2.780E+02	2.780E+02	2.780E+02	2.780E+02
151	152	153	154	155
2.780E+02	2.780E+02	2.780E+02	2.780E+02	2.780E+02
156	157	158	159	160
2.780E+02	2.780E+02	2.780E+02	2.780E+02	2.780E+02
161	162	163	164	165
2.780E+02	2.780E+02	2.780E+02	2.780E+02	2.780E+02
166	167	168	169	170
2.780E+02	2.780E+02	2.780E+02	2.780E+02	2.780E+02
171	172	173	174	175

2.780E+02	2.780E+02	2.780E+02	2.780E+02	2.780E+02
176	177	178	179	180
2.780E+02	2.780E+02	2.780E+02	2.780E+02	2.780E+02
181	182	183	184	185
2.780E+02	2.780E+02	2.780E+02	2.780E+02	2.780E+02
186	187	188	189	190
2.780E+02	2.780E+02	2.780E+02	2.780E+02	2.780E+02
191	192	193	194	195
2.780E+02	2.780E+02	2.780E+02	2.780E+02	2.780E+02
196	197	198	199	200
2.780E+02	2.780E+02	2.780E+02	2.780E+02	2.780E+02
201	202	203	204	205
2.780E+02	2.780E+02	2.780E+02	2.780E+02	2.780E+02
206	207	208	209	210
2.780E+02	2.780E+02	2.780E+02	2.780E+02	2.780E+02
211	212	213	214	215
2.780E+02	2.780E+02	2.780E+02	2.780E+02	2.780E+02
216	217	218	219	220
2.780E+02	2.780E+02	2.780E+02	2.780E+02	2.780E+02
221	222	223	224	225
2.780E+02	2.780E+02	2.780E+02	2.780E+02	2.780E+02
226	227	228	229	230
2.780E+02	2.780E+02	2.780E+02	2.780E+02	2.780E+02
231	232	233	234	235
2.780E+02	2.780E+02	2.780E+02	2.780E+02	2.780E+02
236	237	238	239	240
2.780E+02	2.780E+02	2.780E+02	2.780E+02	2.780E+02
241	242	243	244	245
2.780E+02	2.780E+02	2.780E+02	2.780E+02	2.780E+02
246	247	248	249	250
2.780E+02	2.780E+02	2.780E+02	2.780E+02	2.780E+02
251	252	253	254	255
2.780E+02	2.780E+02	2.780E+02	2.780E+02	2.780E+02
256	257	258	259	260
2.780E+02	2.780E+02	2.780E+02	2.780E+02	2.780E+02
261	262	263	264	265
2.780E+02	2.780E+02	2.780E+02	2.780E+02	2.780E+02
266	267	268	269	270
2.780E+02	2.780E+02	2.780E+02	2.780E+02	2.780E+02
271	272	273	274	275
2.780E+02	2.780E+02	2.780E+02	2.780E+02	2.780E+02
276	277	278	279	280
2.780E+02	2.780E+02	2.780E+02	2.780E+02	2.780E+02
281	282	283	284	285
2.780E+02	2.780E+02	2.780E+02	2.780E+02	2.780E+02
286	287	288	289	290
2.780E+02	2.780E+02	2.780E+02	2.780E+02	2.780E+02
291	292	293	294	295
2.780E+02	2.780E+02	2.780E+02	2.780E+02	2.780E+02
296	297	298	299	300
2.780E+02	2.780E+02	2.780E+02	2.780E+02	2.780E+02
301	302	303	304	305
2.780E+02	2.780E+02	2.780E+02	2.780E+02	2.780E+02
306	307	308	309	310
2.780E+02	2.780E+02	2.780E+02	2.780E+02	2.780E+02
311	312	313	314	315
2.780E+02	2.780E+02	2.780E+02	2.780E+02	2.780E+02
316	317	318	319	320
2.780E+02	2.780E+02	2.780E+02	2.780E+02	2.780E+02
321	322	323	324	325
2.780E+02	2.780E+02	2.780E+02	2.780E+02	2.780E+02
326	327	328	329	330
2.780E+02	2.780E+02	2.780E+02	2.780E+02	2.780E+02
331	332	333	334	335
2.780E+02	2.780E+02	2.780E+02	2.780E+02	2.780E+02
336	337	338	339	340
2.780E+02	2.780E+02	2.780E+02	2.780E+02	2.780E+02
341	342	343	344	345
2.780E+02	2.780E+02	2.780E+02	2.780E+02	2.780E+02
346	347	348	349	350
2.780E+02	2.780E+02	2.780E+02	2.780E+02	2.780E+02
351	352	353	354	355
2.780E+02	2.780E+02	2.780E+02	2.780E+02	2.780E+02
356	357	358	359	360
2.780E+02	2.780E+02	2.780E+02	2.780E+02	2.780E+02

361	362	363	364	365
2.780E+02	2.780E+02	2.780E+02	2.780E+02	2.780E+02
366	367	368	369	370
2.780E+02	2.780E+02	2.780E+02	2.780E+02	2.780E+02
371	372	373	374	375
2.780E+02	2.780E+02	2.780E+02	2.780E+02	2.780E+02
376	377	378	379	380
2.780E+02	2.780E+02	2.780E+02	2.780E+02	2.780E+02
381	382	383	384	385
2.780E+02	2.780E+02	2.780E+02	2.780E+02	2.780E+02
386	387	388	389	390
2.780E+02	2.780E+02	2.780E+02	2.780E+02	2.780E+02
391	392	393	394	395
2.780E+02	2.780E+02	2.780E+02	2.780E+02	2.780E+02
396	397	398	399	400
2.780E+02	2.780E+02	2.780E+02	2.780E+02	2.780E+02
401	402	403	404	405
2.780E+02	2.780E+02	2.780E+02	2.780E+02	2.780E+02
406	407	408	409	410
2.780E+02	2.780E+02	2.780E+02	2.780E+02	2.780E+02
411	412	413	414	415
2.780E+02	2.780E+02	2.780E+02	2.780E+02	2.780E+02
416	417	418	419	420
2.780E+02	2.780E+02	2.780E+02	2.780E+02	2.780E+02
421	422	423	424	425
2.780E+02	2.780E+02	2.780E+02	2.780E+02	2.780E+02
426	427	428	429	430
2.780E+02	2.780E+02	2.780E+02	2.780E+02	2.780E+02
431	432	433	434	435
2.780E+02	2.780E+02	2.780E+02	2.780E+02	2.780E+02
436	437	438	439	440
2.780E+02	2.780E+02	2.780E+02	2.780E+02	2.780E+02
441	442	443	444	445
2.780E+02	2.780E+02	2.780E+02	2.780E+02	2.780E+02
446	447	448	449	450
2.780E+02	2.780E+02	2.780E+02	2.780E+02	2.780E+02
451	452	453	454	455
2.780E+02	2.780E+02	2.780E+02	2.780E+02	2.780E+02
456	457	458	459	460
2.780E+02	2.780E+02	2.780E+02	2.780E+02	2.780E+02
461	462	463	464	465
2.780E+02	2.780E+02	2.780E+02	2.780E+02	2.780E+02
466	467	468	469	470
2.780E+02	2.780E+02	2.780E+02	2.780E+02	2.780E+02
471	472	473	474	475
2.780E+02	2.780E+02	2.780E+02	2.780E+02	2.780E+02
476	477	478	479	480
2.780E+02	2.780E+02	2.780E+02	2.780E+02	2.780E+02
481	482	483	484	485
2.780E+02	2.780E+02	2.780E+02	2.780E+02	2.780E+02
486	487	488	489	490
2.780E+02	2.780E+02	2.780E+02	2.780E+02	2.780E+02
491	492	493	494	495
2.780E+02	2.780E+02	2.780E+02	2.780E+02	2.780E+02
496	497	498	499	500
2.780E+02	2.780E+02	2.780E+02	2.780E+02	2.780E+02
501	502	503	504	505
2.780E+02	2.780E+02	2.780E+02	2.780E+02	2.780E+02
506	507	508	509	510
2.780E+02	2.780E+02	2.780E+02	2.780E+02	2.780E+02
511	512	513	514	515
2.780E+02	2.780E+02	2.780E+02	2.780E+02	2.780E+02
516	517	518	519	520
2.780E+02	2.780E+02	2.780E+02	2.780E+02	2.780E+02
521	522	523	524	525
2.780E+02	2.780E+02	2.780E+02	2.780E+02	2.780E+02
526	527	528	529	530
2.780E+02	2.780E+02	2.780E+02	2.780E+02	2.780E+02
531	532	533	534	535
2.780E+02	2.780E+02	2.780E+02	2.780E+02	2.780E+02
536	537	538	539	540
2.780E+02	2.780E+02	2.780E+02	2.780E+02	2.780E+02
541	542	543	544	545
2.780E+02	2.780E+02	2.780E+02	2.780E+02	2.780E+02
546	547	548	549	550

2.780E+02	2.780E+02	2.780E+02	2.780E+02	2.780E+02
551	552	553	554	555
2.780E+02	2.780E+02	2.780E+02	2.780E+02	2.780E+02
556	557	558	559	560
2.780E+02	2.780E+02	2.780E+02	2.780E+02	2.780E+02
561	562	563	564	565
2.780E+02	2.780E+02	2.780E+02	2.780E+02	2.780E+02
566	567	568	569	570
2.780E+02	2.780E+02	2.780E+02	2.780E+02	2.780E+02
571	572	573	574	575
2.780E+02	2.780E+02	2.780E+02	2.780E+02	2.780E+02
576	577	578	579	580
2.780E+02	2.780E+02	2.780E+02	2.780E+02	2.780E+02
581	582	583	584	585
2.780E+02	2.780E+02	2.780E+02	2.780E+02	2.780E+02
586	587	588	589	590
2.780E+02	2.780E+02	2.780E+02	2.780E+02	2.780E+02
591	592	593	594	595
2.780E+02	2.780E+02	2.780E+02	2.780E+02	2.780E+02
596	597	598	599	600
2.780E+02	2.780E+02	2.780E+02	2.780E+02	2.780E+02
601	602	603	604	605
2.780E+02	2.780E+02	2.780E+02	2.780E+02	2.780E+02
606	607	608	609	610
2.780E+02	2.780E+02	2.780E+02	2.780E+02	2.780E+02
611	612	613	614	615
2.780E+02	2.780E+02	2.780E+02	2.780E+02	2.780E+02
616	617	618	619	620
2.780E+02	2.780E+02	2.780E+02	2.780E+02	2.780E+02
621	622	623	624	625
2.780E+02	2.780E+02	2.780E+02	2.780E+02	2.780E+02
626	627	628	629	630
2.780E+02	2.780E+02	2.780E+02	2.780E+02	2.780E+02
631	632	633	634	635
2.780E+02	2.780E+02	2.780E+02	2.780E+02	2.780E+02
636	637	638	639	640
2.780E+02	2.780E+02	2.780E+02	2.780E+02	2.780E+02
641	642	643	644	645
2.780E+02	2.780E+02	2.780E+02	2.780E+02	2.780E+02
646	647	648	649	650
2.780E+02	2.780E+02	2.780E+02	2.780E+02	2.780E+02
651	652	653	654	655
2.780E+02	2.780E+02	2.780E+02	2.780E+02	2.780E+02
656	657	658	659	660
2.780E+02	2.780E+02	2.780E+02	2.780E+02	2.780E+02
661	662	663	664	665
2.780E+02	2.780E+02	2.780E+02	2.780E+02	2.780E+02
666	667	668	669	670
2.780E+02	2.780E+02	2.780E+02	2.780E+02	2.780E+02
671	672	673	674	675
2.780E+02	2.780E+02	2.780E+02	2.780E+02	2.780E+02
676	677	678	679	680
2.780E+02	2.780E+02	2.780E+02	2.780E+02	2.780E+02
681	682	683	684	685
2.780E+02	2.780E+02	2.780E+02	2.780E+02	2.780E+02
686	687	688	689	690
2.780E+02	2.780E+02	2.780E+02	2.780E+02	2.780E+02
691	692	693	694	695
2.780E+02	2.780E+02	2.780E+02	2.780E+02	2.780E+02
696	697	698	699	700
2.780E+02	2.780E+02	2.780E+02	2.780E+02	2.780E+02
701	702	703	704	705
2.780E+02	2.780E+02	2.780E+02	2.780E+02	2.780E+02
706	707	708	709	710
2.780E+02	2.780E+02	2.780E+02	2.780E+02	2.780E+02
711	712	713	714	715
2.780E+02	2.780E+02	2.780E+02	2.780E+02	2.780E+02
716	717	718	719	720
2.780E+02	2.780E+02	2.780E+02	2.780E+02	2.780E+02
721	722	723	724	725
2.780E+02	2.780E+02	2.780E+02	2.780E+02	2.780E+02
726	727	728	729	730
2.780E+02	2.780E+02	2.780E+02	2.780E+02	2.780E+02
731	732	733	734	735
2.780E+02	2.780E+02	2.780E+02	2.780E+02	2.780E+02

736	737	738	739	740
2.780E+02	2.780E+02	2.780E+02	2.780E+02	2.780E+02
741	742	743	744	745
2.780E+02	2.780E+02	2.780E+02	2.780E+02	2.780E+02
746	747	748	749	750
2.780E+02	2.780E+02	2.780E+02	2.780E+02	2.780E+02
751	752	753	754	755
2.780E+02	2.780E+02	2.780E+02	2.780E+02	2.780E+02
756	757	758	759	760
2.780E+02	2.780E+02	2.780E+02	2.780E+02	2.780E+02
761	762	763	764	765
2.780E+02	2.780E+02	2.780E+02	2.780E+02	2.780E+02
766	767	768	769	770
2.780E+02	2.780E+02	2.780E+02	2.780E+02	2.780E+02
771	772	773	774	775
2.780E+02	2.780E+02	2.780E+02	2.780E+02	2.780E+02
776	777	778	779	780
2.780E+02	2.780E+02	2.780E+02	2.780E+02	2.780E+02
781	782	783	784	785
2.780E+02	2.780E+02	2.780E+02	2.780E+02	2.780E+02
786	787	788	789	790
2.780E+02	2.780E+02	2.780E+02	2.780E+02	2.780E+02
791	792	793	794	795
2.780E+02	2.780E+02	2.780E+02	2.780E+02	2.780E+02
796	797	798	799	800
2.780E+02	2.780E+02	2.780E+02	2.780E+02	2.780E+02
801	802	803	804	805
2.780E+02	2.780E+02	2.780E+02	2.780E+02	2.780E+02
806	807	808	809	810
2.780E+02	2.780E+02	2.780E+02	2.780E+02	2.780E+02
811	812	813	814	815
2.780E+02	2.780E+02	2.780E+02	2.780E+02	2.780E+02
816	817	818	819	820
2.780E+02	2.780E+02	2.780E+02	2.780E+02	2.780E+02
821	822	823	824	825
2.780E+02	2.780E+02	2.780E+02	2.780E+02	2.780E+02
826	827	828	829	830
2.780E+02	2.780E+02	2.780E+02	2.780E+02	2.780E+02
831	832	833	834	835
2.780E+02	2.780E+02	2.780E+02	2.780E+02	2.780E+02
836	837	838	839	840
2.780E+02	2.780E+02	2.780E+02	2.780E+02	2.780E+02
841	842	843	844	845
2.780E+02	2.780E+02	2.780E+02	2.780E+02	2.780E+02
846	847	848	849	850
2.780E+02	2.780E+02	2.780E+02	2.780E+02	2.780E+02
851	852	853	854	855
2.780E+02	2.780E+02	2.780E+02	2.780E+02	2.780E+02
856	857	858	859	860
2.780E+02	2.780E+02	2.780E+02	2.780E+02	2.780E+02
861	862	863	864	865
2.780E+02	2.780E+02	2.780E+02	2.780E+02	2.780E+02
866	867	868	869	870
2.780E+02	2.780E+02	2.780E+02	2.780E+02	2.780E+02
871	872	873	874	875
2.780E+02	2.780E+02	2.780E+02	2.780E+02	2.780E+02
876	877	878	879	880
2.780E+02	2.780E+02	2.780E+02	2.780E+02	2.780E+02
881	882	883	884	885
2.780E+02	2.780E+02	2.780E+02	2.780E+02	2.780E+02
886	887	888	889	890
2.780E+02	2.780E+02	2.780E+02	2.780E+02	2.780E+02
891	892	893	894	895
2.780E+02	2.780E+02	2.780E+02	2.780E+02	2.780E+02
896	897	898	899	900
2.780E+02	2.780E+02	2.780E+02	2.780E+02	2.780E+02
901	902	903	904	905
2.780E+02	2.780E+02	2.780E+02	2.780E+02	2.780E+02
906	907	908	909	910
2.780E+02	2.780E+02	2.780E+02	2.780E+02	2.780E+02
911	912	913	914	915
2.780E+02	2.780E+02	2.780E+02	2.780E+02	2.780E+02
916	917	918	919	920
2.780E+02	2.780E+02	2.780E+02	2.780E+02	2.780E+02
921	922	923	924	925

2.780E+02	2.780E+02	2.780E+02	2.780E+02	2.780E+02
926	927	928	929	930
2.780E+02	2.780E+02	2.780E+02	2.780E+02	2.780E+02
931	932	933	934	935
2.780E+02	2.780E+02	2.780E+02	2.780E+02	2.780E+02
936	937	938	939	940
2.780E+02	2.780E+02	2.780E+02	2.780E+02	2.780E+02
941	942	943	944	945
2.780E+02	2.780E+02	2.780E+02	2.780E+02	2.780E+02
946	947	948	949	950
2.780E+02	2.780E+02	2.780E+02	2.780E+02	2.780E+02
951	952	953	954	955
2.780E+02	2.780E+02	2.780E+02	2.780E+02	2.780E+02
956	957	958	959	960
2.780E+02	2.780E+02	2.780E+02	2.780E+02	2.780E+02
961	962	963	964	965
2.780E+02	2.780E+02	2.780E+02	2.780E+02	2.780E+02
966	967	968	969	970
2.780E+02	2.780E+02	2.780E+02	2.780E+02	2.780E+02
971	972	973	974	975
2.780E+02	2.780E+02	2.780E+02	2.780E+02	2.780E+02
976	977	978	979	980
2.780E+02	2.780E+02	2.780E+02	2.780E+02	2.780E+02
981	982	983	984	985
2.780E+02	2.780E+02	2.780E+02	2.780E+02	2.780E+02
986	987	988	989	990
2.780E+02	2.780E+02	2.780E+02	2.780E+02	2.780E+02
991	992	993	994	995
2.780E+02	2.780E+02	2.780E+02	2.780E+02	2.780E+02
996	997	998	999	1000
2.780E+02	2.780E+02	2.780E+02	2.780E+02	2.780E+02
1001	1002	1003	1004	1005
2.780E+02	2.780E+02	2.780E+02	2.780E+02	2.780E+02
1006	1007	1008	1009	1010
2.780E+02	2.780E+02	2.780E+02	2.780E+02	2.780E+02
1011	1012	1013	1014	1015
2.780E+02	2.780E+02	2.780E+02	2.780E+02	2.780E+02
1016	1017	1018	1019	1020
2.780E+02	2.780E+02	2.780E+02	2.780E+02	2.780E+02
1021	1022	1023	1024	1025
2.780E+02	2.780E+02	2.780E+02	2.780E+02	2.780E+02
1026	1027	1028	1029	1030
2.780E+02	2.780E+02	2.780E+02	2.780E+02	2.780E+02
1031	1032	1033	1034	1035
2.780E+02	2.780E+02	2.780E+02	2.780E+02	2.780E+02
1036	1037	1038	1039	1040
2.780E+02	2.780E+02	2.780E+02	2.780E+02	2.780E+02
1041	1042	1043	1044	1045
2.780E+02	2.780E+02	2.780E+02	2.780E+02	2.780E+02
1046	1047	1048	1049	1050
2.780E+02	2.780E+02	2.780E+02	2.780E+02	2.780E+02
1051	1052	1053	1054	1055
2.780E+02	2.780E+02	2.780E+02	2.780E+02	2.780E+02
1056	1057	1058	1059	1060
2.780E+02	2.780E+02	2.780E+02	2.780E+02	2.780E+02
1061	1062	1063	1064	1065
2.780E+02	2.780E+02	2.780E+02	2.780E+02	2.780E+02
1066	1067	1068	1069	1070
2.780E+02	2.780E+02	2.780E+02	2.780E+02	2.780E+02
1071	1072	1073	1074	1075
2.780E+02	2.780E+02	2.780E+02	2.780E+02	2.780E+02
1076	1077	1078	1079	1080
2.780E+02	2.780E+02	2.780E+02	2.780E+02	2.780E+02
1081	1082	1083	1084	1085
2.780E+02	2.780E+02	2.780E+02	2.780E+02	2.780E+02
1086	1087	1088	1089	1090
2.780E+02	2.780E+02	2.780E+02	2.780E+02	2.780E+02
1091	1092	1093	1094	1095
2.780E+02	2.780E+02	2.780E+02	2.780E+02	2.780E+02
1096	1097	1098	1099	1100
2.780E+02	2.780E+02	2.780E+02	2.780E+02	2.780E+02
1101	1102	1103	1104	1105
2.780E+02	2.780E+02	2.780E+02	2.780E+02	2.780E+02
1106	1107	1108	1109	1110
2.780E+02	2.780E+02	2.780E+02	2.780E+02	2.780E+02

1111	1112	1113	1114	1115
2.780E+02	2.780E+02	2.780E+02	2.780E+02	2.780E+02
1116	1117	1118	1119	1120
2.780E+02	2.780E+02	2.780E+02	2.780E+02	2.780E+02
1121	1122	1123	1124	1125
2.780E+02	2.780E+02	2.780E+02	2.780E+02	2.780E+02
1126	1127	1128	1129	1130
2.780E+02	2.780E+02	2.780E+02	2.780E+02	2.780E+02
1131	1132	1133	1134	1135
2.780E+02	2.780E+02	2.780E+02	2.780E+02	2.780E+02
1136	1137	1138	1139	1140
2.780E+02	2.780E+02	2.780E+02	2.780E+02	2.780E+02
1141	1142	1143	1144	1145
2.780E+02	2.780E+02	2.780E+02	2.780E+02	2.780E+02
1146	1147	1148	1149	1150
2.780E+02	2.780E+02	2.780E+02	2.780E+02	2.780E+02
1151	1152	1153	1154	1155
2.780E+02	2.780E+02	2.780E+02	2.780E+02	2.780E+02
1156	1157	1158	1159	1160
2.780E+02	2.780E+02	2.780E+02	2.780E+02	2.780E+02
1161	1162	1163	1164	1165
2.780E+02	2.780E+02	2.780E+02	2.780E+02	2.780E+02
1166	1167	1168	1169	1170
2.780E+02	2.780E+02	2.780E+02	2.780E+02	2.780E+02
1171	1172	1173	1174	1175
2.780E+02	2.780E+02	2.780E+02	2.780E+02	2.780E+02
1176	1177	1178	1179	1180
2.780E+02	2.780E+02	2.780E+02	2.780E+02	2.780E+02
1181	1182	1183	1184	1185
2.780E+02	2.780E+02	2.780E+02	2.780E+02	2.780E+02
1186	1187	1188	1189	1190
2.780E+02	2.780E+02	2.780E+02	2.780E+02	2.780E+02
1191	1192	1193	1194	1195
2.780E+02	2.780E+02	2.780E+02	2.780E+02	2.780E+02
1196	1197	1198	1199	1200
2.780E+02	2.780E+02	2.780E+02	2.780E+02	2.780E+02
1201	1202	1203	1204	1205
2.780E+02	2.780E+02	2.780E+02	2.780E+02	2.780E+02
1206	1207	1208	1209	1210
2.780E+02	2.780E+02	2.780E+02	2.780E+02	2.780E+02
1211	1212	1213	1214	1215
2.780E+02	2.780E+02	2.780E+02	2.780E+02	2.780E+02
1216	1217	1218	1219	1220
2.780E+02	2.780E+02	2.780E+02	2.780E+02	2.780E+02
1221	1222	1223	1224	1225
2.780E+02	2.780E+02	2.780E+02	2.780E+02	2.780E+02
1226	1227	1228	1229	1230
2.780E+02	2.780E+02	2.780E+02	2.780E+02	2.780E+02
1231	1232	1233	1234	1235
2.780E+02	2.780E+02	2.780E+02	2.780E+02	2.780E+02
1236	1237	1238	1239	1240
2.780E+02	2.780E+02	2.780E+02	2.780E+02	2.780E+02
1241	1242	1243	1244	1245
2.780E+02	2.780E+02	2.780E+02	2.780E+02	2.780E+02
1246	1247	1248	1249	1250
2.780E+02	2.780E+02	2.780E+02	2.780E+02	2.780E+02
1251	1252	1253	1254	1255
2.780E+02	2.780E+02	2.780E+02	2.780E+02	2.780E+02
1256	1257	1258	1259	1260
2.780E+02	2.780E+02	2.780E+02	2.780E+02	2.780E+02
1261	1262	1263	1264	1265
2.780E+02	2.780E+02	2.780E+02	2.780E+02	2.780E+02
1266	1267	1268	1269	1270
2.780E+02	2.780E+02	2.780E+02	2.780E+02	2.780E+02
1271	1272	1273	1274	1275
2.780E+02	2.780E+02	2.780E+02	2.780E+02	2.780E+02
1276	1277	1278	1279	1280
2.780E+02	2.780E+02	2.780E+02	2.780E+02	2.780E+02
1281	1282	1283	1284	1285
2.780E+02	2.780E+02	2.780E+02	2.780E+02	2.780E+02
1286	1287	1288	1289	1290
2.780E+02	2.780E+02	2.780E+02	2.780E+02	2.780E+02
1291	1292	1293	1294	1295
2.780E+02	2.780E+02	2.780E+02	2.780E+02	2.780E+02
1296	1297	1298	1299	1300

2.780E+02	2.780E+02	2.780E+02	2.780E+02	2.780E+02
1301	1302	1303	1304	1305
2.780E+02	2.780E+02	2.780E+02	2.780E+02	2.780E+02
1306	1307	1308	1309	1310
2.780E+02	2.780E+02	2.780E+02	2.780E+02	2.780E+02
1311	1312	1313	1314	1315
2.780E+02	2.780E+02	2.780E+02	2.780E+02	2.780E+02
1316	1317	1318	1319	1320
2.780E+02	2.780E+02	2.780E+02	2.780E+02	2.780E+02
1321	1322	1323	1324	1325
2.780E+02	2.780E+02	2.780E+02	2.780E+02	2.780E+02
1326	1327	1328	1329	1330
2.780E+02	2.780E+02	2.780E+02	2.780E+02	2.780E+02
1331	1332	1333	1334	1335
2.780E+02	2.780E+02	2.780E+02	2.779E+02	2.780E+02
1336	1337	1338	1339	1340
2.780E+02	2.780E+02	2.780E+02	2.780E+02	2.780E+02
1341	1342	1343	1344	1345
2.780E+02	2.780E+02	2.780E+02	2.780E+02	2.780E+02
1346	1347	1348	1349	1350
2.780E+02	2.780E+02	2.780E+02	2.780E+02	2.780E+02
1351	1352	1353	1354	1355
2.780E+02	2.780E+02	2.780E+02	2.780E+02	2.780E+02
1356	1357	1358	1359	1360
2.780E+02	2.780E+02	2.780E+02	2.780E+02	2.780E+02
1361	1362	1363	1364	1365
2.780E+02	2.780E+02	2.780E+02	2.780E+02	2.780E+02
1366	1367	1368	1369	1370
2.780E+02	2.780E+02	2.780E+02	2.780E+02	2.780E+02
1371	1372	1373	1374	1375
2.780E+02	2.780E+02	2.780E+02	2.780E+02	2.780E+02
1376	1377	1378	1379	1380
2.780E+02	2.780E+02	2.780E+02	2.780E+02	2.780E+02
1381	1382	1383	1384	1385
2.780E+02	2.780E+02	2.780E+02	2.780E+02	2.780E+02
1386	1387	1388	1389	1390
2.780E+02	2.780E+02	2.780E+02	2.780E+02	2.780E+02
1391	1392	1393	1394	1395
2.780E+02	2.780E+02	2.780E+02	2.780E+02	2.780E+02
1396	1397	1398	1399	1400
2.780E+02	2.780E+02	2.780E+02	2.780E+02	2.780E+02
1401	1402	1403	1404	1405
2.780E+02	2.780E+02	2.780E+02	2.780E+02	2.780E+02
1406	1407	1408	1409	1410
2.780E+02	2.780E+02	2.780E+02	2.780E+02	2.780E+02
1411	1412	1413	1414	1415
2.780E+02	2.780E+02	2.780E+02	2.780E+02	2.780E+02
1416	1417	1418	1419	1420
2.780E+02	2.780E+02	2.780E+02	2.780E+02	2.780E+02
1421	1422	1423	1424	1425
2.780E+02	2.780E+02	2.780E+02	2.780E+02	2.780E+02
1426	1427	1428	1429	1430
2.780E+02	2.880E+02	2.784E+02	2.826E+02	2.875E+02
1431	1432	1433	1434	1435
2.879E+02	2.879E+02	2.879E+02	2.879E+02	2.879E+02
1436	1437	1438	1439	1440
2.879E+02	2.879E+02	2.879E+02	2.879E+02	2.879E+02
1441	1442	1443	1444	1445
2.879E+02	2.879E+02	2.879E+02	2.879E+02	2.879E+02
1446	1447	1448	1449	1450
2.879E+02	2.879E+02	2.879E+02	2.880E+02	2.780E+02
1451	1452	1453	1454	1455
2.880E+02	2.880E+02	2.880E+02	2.880E+02	2.880E+02
1456	1457	1458	1459	1460
2.880E+02	2.880E+02	2.880E+02	2.879E+02	2.878E+02
1461	1462	1463	1464	1465
2.877E+02	2.877E+02	2.876E+02	2.876E+02	2.875E+02
1466	1467	1468	1469	1470
2.875E+02	2.875E+02	2.874E+02	2.874E+02	2.874E+02
1471	1472	1473	1474	1475
2.872E+02	2.872E+02	2.870E+02	2.851E+02	2.821E+02
1476	1477	1478	1479	1480
2.789E+02	2.781E+02	2.780E+02	2.780E+02	2.780E+02
1481	1482	1483	1484	1485
2.780E+02	2.780E+02	2.780E+02	2.780E+02	2.780E+02

1486	1487	1488	1489	1490
2.780E+02	2.780E+02	2.780E+02	2.780E+02	2.780E+02
1491	1492	1493	1494	1495
2.780E+02	2.780E+02	2.780E+02	2.780E+02	2.780E+02
1496	1497	1498	1499	1500
2.780E+02	2.780E+02	2.780E+02	2.780E+02	2.780E+02
1501	1502	1503	1504	1505
2.780E+02	2.780E+02	2.780E+02	2.780E+02	2.780E+02
1506	1507	1508	1509	1510
2.780E+02	2.780E+02	2.780E+02	2.780E+02	2.780E+02
1511	1512	1513	1514	1515
2.780E+02	2.780E+02	2.780E+02	2.780E+02	2.780E+02
1516	1517	1518	1519	1520
2.780E+02	2.780E+02	2.780E+02	2.780E+02	2.780E+02
1521	1522	1523	1524	1525
2.780E+02	2.780E+02	2.780E+02	2.780E+02	2.780E+02
1526	1527	1528	1529	1530
2.780E+02	2.780E+02	2.780E+02	2.780E+02	2.780E+02
1531	1532	1533	1534	1535
2.841E+02	2.785E+02	2.781E+02	2.780E+02	2.780E+02
1536	1537	1538	1539	1540
2.780E+02	2.780E+02	2.780E+02	2.780E+02	2.780E+02
1541	1542	1543	1544	1545
2.780E+02	2.780E+02	2.780E+02	2.780E+02	2.780E+02
1546	1547	1548	1549	1550
2.780E+02	2.780E+02	2.780E+02	2.780E+02	2.780E+02
1551	1552	1553	1554	1555
2.780E+02	2.780E+02	2.780E+02	2.780E+02	2.780E+02
1556	1557	1558	1559	1560
2.780E+02	2.780E+02	2.780E+02	2.780E+02	2.877E+02
1561	1562	1563	1564	1565
2.874E+02	2.797E+02	2.787E+02	2.783E+02	2.781E+02
1566	1567	1568	1569	1570
2.780E+02	2.780E+02	2.780E+02	2.780E+02	2.780E+02
1571	1572	1573	1574	1575
2.780E+02	2.780E+02	2.780E+02	2.780E+02	2.780E+02
1576	1577	1578	1579	1580
2.780E+02	2.780E+02	2.780E+02	2.780E+02	2.780E+02
1581	1582	1583	1584	1585
2.780E+02	2.780E+02	2.780E+02	2.780E+02	2.780E+02
1586	1587	1588	1589	1590
2.780E+02	2.780E+02	2.780E+02	2.879E+02	2.877E+02
1591	1592	1593	1594	1595
2.847E+02	2.808E+02	2.795E+02	2.787E+02	2.782E+02
1596	1597	1598	1599	1600
2.780E+02	2.780E+02	2.780E+02	2.780E+02	2.780E+02
1601	1602	1603	1604	1605
2.780E+02	2.780E+02	2.780E+02	2.780E+02	2.780E+02
1606	1607	1608	1609	1610
2.780E+02	2.780E+02	2.780E+02	2.780E+02	2.780E+02
1611	1612	1613	1614	1615
2.780E+02	2.780E+02	2.780E+02	2.780E+02	2.780E+02
1616	1617	1618	1619	1620
2.780E+02	2.780E+02	2.879E+02	2.878E+02	2.877E+02
1621	1622	1623	1624	1625
2.874E+02	2.832E+02	2.807E+02	2.793E+02	2.785E+02
1626	1627	1628	1629	1630
2.781E+02	2.780E+02	2.780E+02	2.780E+02	2.780E+02
1631	1632	1633	1634	1635
2.780E+02	2.780E+02	2.780E+02	2.780E+02	2.780E+02
1636	1637	1638	1639	1640
2.780E+02	2.780E+02	2.780E+02	2.780E+02	2.780E+02
1641	1642	1643	1644	1645
2.780E+02	2.780E+02	2.780E+02	2.780E+02	2.780E+02
1646	1647	1648	1649	1650
2.780E+02	2.879E+02	2.879E+02	2.878E+02	2.877E+02
1651	1652	1653	1654	1655
2.856E+02	2.841E+02	2.815E+02	2.798E+02	2.787E+02
1656	1657	1658	1659	1660
2.782E+02	2.780E+02	2.780E+02	2.780E+02	2.780E+02
1661	1662	1663	1664	1665
2.780E+02	2.780E+02	2.780E+02	2.780E+02	2.780E+02
1666	1667	1668	1669	1670
2.780E+02	2.780E+02	2.780E+02	2.780E+02	2.780E+02
1671	1672	1673	1674	1675

2.780E+02	2.780E+02	2.780E+02	2.780E+02	2.780E+02
1676	1677	1678	1679	1680
2.879E+02	2.879E+02	2.878E+02	2.878E+02	2.877E+02
1681	1682	1683	1684	1685
2.867E+02	2.849E+02	2.822E+02	2.803E+02	2.790E+02
1686	1687	1688	1689	1690
2.783E+02	2.780E+02	2.780E+02	2.780E+02	2.780E+02
1691	1692	1693	1694	1695
2.780E+02	2.780E+02	2.780E+02	2.780E+02	2.780E+02
1696	1697	1698	1699	1700
2.780E+02	2.780E+02	2.780E+02	2.780E+02	2.780E+02
1701	1702	1703	1704	1705
2.780E+02	2.780E+02	2.780E+02	2.780E+02	2.879E+02
1706	1707	1708	1709	1710
2.879E+02	2.878E+02	2.878E+02	2.877E+02	2.877E+02
1711	1712	1713	1714	1715
2.865E+02	2.854E+02	2.826E+02	2.807E+02	2.792E+02
1716	1717	1718	1719	1720
2.783E+02	2.780E+02	2.780E+02	2.780E+02	2.780E+02
1721	1722	1723	1724	1725
2.780E+02	2.780E+02	2.780E+02	2.780E+02	2.780E+02
1726	1727	1728	1729	1730
2.780E+02	2.780E+02	2.780E+02	2.780E+02	2.780E+02
1731	1732	1733	1734	1735
2.780E+02	2.780E+02	2.780E+02	2.879E+02	2.879E+02
1736	1737	1738	1739	1740
2.879E+02	2.878E+02	2.877E+02	2.877E+02	2.876E+02
1741	1742	1743	1744	1745
2.868E+02	2.858E+02	2.830E+02	2.809E+02	2.794E+02
1746	1747	1748	1749	1750
2.784E+02	2.780E+02	2.780E+02	2.780E+02	2.780E+02
1751	1752	1753	1754	1755
2.780E+02	2.780E+02	2.780E+02	2.780E+02	2.780E+02
1756	1757	1758	1759	1760
2.780E+02	2.780E+02	2.780E+02	2.780E+02	2.780E+02
1761	1762	1763	1764	1765
2.780E+02	2.780E+02	2.879E+02	2.879E+02	2.879E+02
1766	1767	1768	1769	1770
2.878E+02	2.878E+02	2.877E+02	2.877E+02	2.876E+02
1771	1772	1773	1774	1775
2.865E+02	2.859E+02	2.832E+02	2.812E+02	2.795E+02
1776	1777	1778	1779	1780
2.784E+02	2.780E+02	2.780E+02	2.780E+02	2.780E+02
1781	1782	1783	1784	1785
2.780E+02	2.780E+02	2.780E+02	2.780E+02	2.780E+02
1786	1787	1788	1789	1790
2.780E+02	2.780E+02	2.780E+02	2.780E+02	2.780E+02
1791	1792	1793	1794	1795
2.780E+02	2.879E+02	2.879E+02	2.879E+02	2.878E+02
1796	1797	1798	1799	1800
2.878E+02	2.877E+02	2.877E+02	2.877E+02	2.876E+02
1801	1802	1803	1804	1805
2.866E+02	2.860E+02	2.834E+02	2.813E+02	2.796E+02
1806	1807	1808	1809	1810
2.784E+02	2.780E+02	2.780E+02	2.780E+02	2.780E+02
1811	1812	1813	1814	1815
2.780E+02	2.780E+02	2.780E+02	2.780E+02	2.780E+02
1816	1817	1818	1819	1820
2.780E+02	2.780E+02	2.780E+02	2.780E+02	2.780E+02
1821	1822	1823	1824	1825
2.879E+02	2.879E+02	2.879E+02	2.878E+02	2.878E+02
1826	1827	1828	1829	1830
2.877E+02	2.877E+02	2.877E+02	2.877E+02	2.876E+02
1831	1832	1833	1834	1835
2.866E+02	2.861E+02	2.835E+02	2.814E+02	2.796E+02
1836	1837	1838	1839	1840
2.783E+02	2.780E+02	2.780E+02	2.780E+02	2.780E+02
1841	1842	1843	1844	1845
2.780E+02	2.780E+02	2.780E+02	2.780E+02	2.780E+02
1846	1847	1848	1849	1850
2.780E+02	2.780E+02	2.780E+02	2.780E+02	2.879E+02
1851	1852	1853	1854	1855
2.879E+02	2.879E+02	2.878E+02	2.878E+02	2.878E+02
1856	1857	1858	1859	1860
2.877E+02	2.877E+02	2.877E+02	2.876E+02	2.876E+02

1861	1862	1863	1864	1865
2.867E+02	2.861E+02	2.836E+02	2.815E+02	2.796E+02
1866	1867	1868	1869	1870
2.783E+02	2.780E+02	2.780E+02	2.780E+02	2.780E+02
1871	1872	1873	1874	1875
2.780E+02	2.780E+02	2.780E+02	2.780E+02	2.780E+02
1876	1877	1878	1879	1880
2.780E+02	2.780E+02	2.780E+02	2.879E+02	2.879E+02
1881	1882	1883	1884	1885
2.879E+02	2.879E+02	2.878E+02	2.878E+02	2.877E+02
1886	1887	1888	1889	1890
2.877E+02	2.877E+02	2.877E+02	2.876E+02	2.876E+02
1891	1892	1893	1894	1895
2.872E+02	2.861E+02	2.837E+02	2.815E+02	2.795E+02
1896	1897	1898	1899	1900
2.783E+02	2.780E+02	2.780E+02	2.780E+02	2.780E+02
1901	1902	1903	1904	1905
2.780E+02	2.780E+02	2.780E+02	2.780E+02	2.780E+02
1906	1907	1908	1909	1910
2.780E+02	2.780E+02	2.879E+02	2.879E+02	2.879E+02
1911	1912	1913	1914	1915
2.879E+02	2.878E+02	2.878E+02	2.877E+02	2.877E+02
1916	1917	1918	1919	1920
2.877E+02	2.877E+02	2.876E+02	2.876E+02	2.876E+02
1921	1922	1923	1924	1925
2.875E+02	2.861E+02	2.837E+02	2.815E+02	2.795E+02
1926	1927	1928	1929	1930
2.782E+02	2.780E+02	2.780E+02	2.780E+02	2.780E+02
1931	1932	1933	1934	1935
2.780E+02	2.780E+02	2.780E+02	2.780E+02	2.780E+02
1936	1937	1938	1939	1940
2.780E+02	2.879E+02	2.879E+02	2.879E+02	2.879E+02
1941	1942	1943	1944	1945
2.878E+02	2.878E+02	2.878E+02	2.877E+02	2.877E+02
1946	1947	1948	1949	1950
2.877E+02	2.877E+02	2.876E+02	2.876E+02	2.876E+02
1951	1952	1953	1954	1955
2.875E+02	2.861E+02	2.837E+02	2.815E+02	2.794E+02
1956	1957	1958	1959	1960
2.782E+02	2.780E+02	2.780E+02	2.780E+02	2.780E+02
1961	1962	1963	1964	1965
2.780E+02	2.780E+02	2.780E+02	2.780E+02	2.780E+02
1966	1967	1968	1969	1970
2.879E+02	2.879E+02	2.879E+02	2.879E+02	2.878E+02
1971	1972	1973	1974	1975
2.878E+02	2.878E+02	2.877E+02	2.877E+02	2.877E+02
1976	1977	1978	1979	1980
2.877E+02	2.876E+02	2.876E+02	2.876E+02	2.876E+02
1981	1982	1983	1984	1985
2.875E+02	2.860E+02	2.838E+02	2.815E+02	2.793E+02
1986	1987	1988	1989	1990
2.781E+02	2.780E+02	2.780E+02	2.780E+02	2.780E+02
1991	1992	1993	1994	1995
2.780E+02	2.780E+02	2.780E+02	2.780E+02	2.879E+02
1996	1997	1998	1999	2000
2.879E+02	2.879E+02	2.879E+02	2.878E+02	2.878E+02
2001	2002	2003	2004	2005
2.878E+02	2.878E+02	2.877E+02	2.877E+02	2.877E+02
2006	2007	2008	2009	2010
2.877E+02	2.876E+02	2.876E+02	2.876E+02	2.875E+02
2011	2012	2013	2014	2015
2.875E+02	2.861E+02	2.838E+02	2.815E+02	2.792E+02
2016	2017	2018	2019	2020
2.781E+02	2.780E+02	2.780E+02	2.780E+02	2.780E+02
2021	2022	2023	2024	2025
2.780E+02	2.780E+02	2.780E+02	2.879E+02	2.879E+02
2026	2027	2028	2029	2030
2.879E+02	2.879E+02	2.879E+02	2.878E+02	2.878E+02
2031	2032	2033	2034	2035
2.878E+02	2.877E+02	2.877E+02	2.877E+02	2.877E+02
2036	2037	2038	2039	2040
2.876E+02	2.876E+02	2.876E+02	2.875E+02	2.875E+02
2041	2042	2043	2044	2045
2.875E+02	2.862E+02	2.838E+02	2.815E+02	2.791E+02
2046	2047	2048	2049	2050

```
    2.781E+02   2.780E+02   2.780E+02   2.780E+02   2.780E+02
     2051        2052        2053        2054        2055
    2.780E+02   2.780E+02   2.879E+02   2.879E+02   2.879E+02
     2056        2057        2058        2059        2060
    2.879E+02   2.879E+02   2.878E+02   2.878E+02   2.878E+02
     2061        2062        2063        2064        2065
    2.878E+02   2.877E+02   2.877E+02   2.877E+02   2.876E+02
     2066        2067        2068        2069        2070
    2.876E+02   2.876E+02   2.875E+02   2.875E+02   2.875E+02
     2071        2072        2073        2074        2075
    2.875E+02   2.863E+02   2.840E+02   2.814E+02   2.790E+02
     2076        2077        2078        2079        2080
    2.781E+02   2.780E+02   2.780E+02   2.780E+02   2.780E+02
     2081        2082        2083        2084        2085
    2.780E+02   2.879E+02   2.879E+02   2.879E+02   2.879E+02
     2086        2087        2088        2089        2090
    2.879E+02   2.879E+02   2.878E+02   2.878E+02   2.878E+02
     2091        2092        2093        2094        2095
    2.878E+02   2.877E+02   2.877E+02   2.876E+02   2.876E+02
     2096        2097        2098        2099        2100
    2.876E+02   2.875E+02   2.875E+02   2.875E+02   2.875E+02
     2101        2102        2103        2104        2105
    2.874E+02   2.866E+02   2.841E+02   2.814E+02   2.789E+02
     2106        2107        2108        2109        2110
    2.781E+02   2.780E+02   2.780E+02   2.780E+02   2.780E+02
     2111        2112        2113        2114        2115
    2.880E+02   2.879E+02   2.879E+02   2.879E+02   2.879E+02
     2116        2117        2118        2119        2120
    2.879E+02   2.879E+02   2.879E+02   2.878E+02   2.878E+02
     2121        2122        2123        2124        2125
    2.877E+02   2.877E+02   2.876E+02   2.876E+02   2.876E+02
     2126        2127        2128        2129        2130
    2.875E+02   2.875E+02   2.875E+02   2.874E+02   2.874E+02
     2131        2132        2133        2134        2135
    2.874E+02   2.869E+02   2.846E+02   2.817E+02   2.789E+02
     2136        2137        2138        2139
    2.781E+02   2.780E+02   2.780E+02   2.780E+02
1      Position of the Interface Toe at t=0 min. Without Subsurface Barrier
OFLOTRAN   2.1a                          CPU                        06/13/94 22:23:


          Calculations required   552.50     CPU seconds


          Total CPU seconds =   554.11
```

APPENDIX 3

LIST OPTIMIZATION SETS FROM SET 1 TO SET 11, AND SHOW ONLY OPTIMIZATION PARAMETERS

	SET 1 (INFEASIBLE)	SET 2 (FEASIBLE)	SET 3 (FEASIBLE)	SET 4 (FEASIBLE)	SET 5 (INFEASIBLE)
TNODE2	> 283.74	281.19	280.45	280.91	> 278.02
LOCA	0.79124	0.80779	0.82930	0.83263	0.88312
WID	0.45352E-01	0.44818E-01	0.45395E-01	0.45450E-01	0.44419E-01
C	0.68043E+10	0.69509E+10	0.65585E+10	0.64389E+10	0.60237E+10
DENSUM	0.21178E+07	0.21176E+07	0.21174E+07	0.21174E+07	0.21167E+07

	SET 6 (INFEASIBLE)	SET 7 (INFEASIBLE)	SET 8 (FEASIBLE)	SET 9 (INFEASIBLE)	SET 10 (FEASIBLE)
TNODE2	> 278.97	> 278.00	280.50	> 278.36	282.56
LOCA	0.84350	0.88093	0.85685	0.88738	0.85116
WID	0.45909E-01	0.46534E-01	0.45361E-01	0.47337E-01	0.44404E-01
C	0.68056E+10	0.74555E+10	0.62804E+10	0.58207E+10	0.61050E+10
DENSUM	0.21173E+07	0.21165E+07	0.21173E+07	0.21170E+07	0.21174E+07

	SET 11 (FEASIBLE)
TNODE2	281.41
LOCA	0.88312
WID	0.49568E-01
C	0.51549E+10
DENSUM	0.21172E+07

SELECT AND SAVE THE BEST 6 DESIGN SETS FOR SUBSEQUENT OPTIMIZATION LOOPING

REMOVED DESIGN SET 1 (DENSUM = 0.21178E+07)

REMOVED DESIGN SET 2 (DENSUM = 0.21176E+07)

REMOVED DESIGN SET 3 (DENSUM = 0.21174E+07)

REMOVED DESIGN SET 4 (DENSUM = 0.21174E+07)

REMOVED DESIGN SET 10 (DENSUM = 0.21174E+07)

LIST OPTIMIZATION SETS FROM SET 1 TO SET 13, AND SHOW ONLY OPTIMIZATION PARAMETERS

	SET 1 (INFEASIBLE)	SET 2 (INFEASIBLE)	SET 3 (INFEASIBLE)	SET 4 (FEASIBLE)	SET 5 (INFEASIBLE)
TNODE2	> 278.02	> 278.97	> 278.00	280.50	> 278.36
LOCA	0.88312	0.84350	0.88093	0.85685	0.88738
WID	0.44419E-01	0.45909E-01	0.46534E-01	0.45361E-01	0.47337E-01
C	0.60237E+10	0.68056E+10	0.74555E+10	0.62804E+10	0.58207E+10
DENSUM	0.21167E+07	0.21173E+07	0.21165E+07	0.21173E+07	0.21170E+07

	SET 6 (FEASIBLE)	SET 7 (INFEASIBLE)	SET 8 (INFEASIBLE)	SET 9 (INFEASIBLE)	SET 10 (INFEASIBLE)
TNODE2	281.41	> 285.15	> 279.39	> 278.01	> 278.00
LOCA	0.88312	0.85580	0.89331	0.88630	0.89676
WID	0.49568E-01	0.51045E-01	0.20251E-01	0.47977E-01	0.45849E-01
C	0.51549E+10	0.47602E+10	0.12217E+11	0.62562E+10	0.10698E+11
DENSUM	0.21172E+07	0.21176E+07	0.21166E+07	0.21168E+07	0.21161E+07

	SET 11 (INFEASIBLE)	SET 12 (INFEASIBLE)	SET 13 (INFEASIBLE)
TNODE2	> 278.00	> 278.00	> 278.00
LOCA	0.88668	0.74557	0.86032
WID	0.56351E-01	0.61936E-01	0.53664E-01
C	0.57825E+10	0.16802E+11	0.67440E+10
DENSUM	0.21167E+07	0.21172E+07	0.21168E+07

SELECT AND SAVE THE BEST 6 DESIGN SETS FOR SUBSEQUENT OPTIMIZATION LOOPING

REMOVED DESIGN SET 8 (DENSUM = 0.21166E+07)

REMOVED DESIGN SET 12 (DENSUM = 0.21172E+07)

REMOVED DESIGN SET 11 (DENSUM = 0.21167E+07)

REMOVED DESIGN SET 2 (DENSUM = 0.21173E+07)

```
REMOVED DESIGN SET   1 (DENSUM  = 0.21167E+07)

REMOVED DESIGN SET  10 (DENSUM  = 0.21161E+07)

REMOVED DESIGN SET   4 (DENSUM  = 0.21173E+07)

SELECT AND SAVE THE BEST   6 DESIGN SETS FOR SUBSEQUENT OPTIMIZATION LOOPING

REMOVED DESIGN SET   9 (DENSUM  = 0.21205E+07)

REMOVED DESIGN SET  19 (DENSUM  = 0.21169E+07)

REMOVED DESIGN SET  18 (DENSUM  = 0.21169E+07)

REMOVED DESIGN SET  12 (DENSUM  = 0.21217E+07)

REMOVED DESIGN SET  17 (DENSUM  = 0.21170E+07)

REMOVED DESIGN SET  16 (DENSUM  = 0.21171E+07)

REMOVED DESIGN SET  13 (DENSUM  = 0.21166E+07)

REMOVED DESIGN SET  14 (DENSUM  = 0.21170E+07)

REMOVED DESIGN SET   6 (DENSUM  = 0.21179E+07)

REMOVED DESIGN SET  15 (DENSUM  = 0.21178E+07)

REMOVED DESIGN SET  11 (DENSUM  = 0.21180E+07)

REMOVED DESIGN SET  10 (DENSUM  = 0.21226E+07)

REMOVED DESIGN SET   3 (DENSUM  = 0.21230E+07)

REMOVED DESIGN SET   5 (DENSUM  = 0.21243E+07)

REMOVED DESIGN SET   4 (DENSUM  = 0.21235E+07)

REMOVED DESIGN SET   8 (DENSUM  = 0.21202E+07)

REMOVED DESIGN SET  21 (DENSUM  = 0.21203E+07)

REMOVED DESIGN SET  26 (DENSUM  = 0.21221E+07)

REMOVED DESIGN SET  22 (DENSUM  = 0.21214E+07)

REMOVED DESIGN SET  24 (DENSUM  = 0.21221E+07)

REMOVED DESIGN SET   7 (DENSUM  = 0.21214E+07)

 BEST VARIABLES ARE

            SET  3
         (FEASIBLE)
TNODE2       280.53
LOCA        0.54000
WID         0.50000E-01
DENSUM      0.21169E+07

******  SUMMARY OF CONSTRAINTS (IF ANY) EVALUATED AT THE CURRENT OPTIMAL SOLUTION  ******


******  DESIGN SENSITIVITY SUMMARY TABLE  ******

   DERIVATIVES ARE EVALUATED AT THE CURRENT OPTIMAL DESIGN VECTOR


              DENSUM       TNODE2
 LOCA      -0.3093E+06  -581.6
 WID            0.      -634.6
```

```
LIST OPTIMIZATION SETS FROM SET   1 TO SET   7, AND SHOW ONLY OPTIMIZATION PARAMETERS

            SET  1        SET  2        SET  3        SET  4        SET  5
         (INFEASIBLE)  (INFEASIBLE)  (FEASIBLE)    (INFEASIBLE)  (INFEASIBLE)
TNODE2   >  287.97     >  287.97        280.53     >  287.97     >  287.97
LOCA       0.54000       0.54000       0.54000       0.52201       0.51885
WID        0.50000E-01   0.50000E-01   0.50000E-01   0.49615E-01   0.50640E-01
DENSUM     0.21215E+07   0.21215E+07   0.21169E+07   0.21218E+07   0.21218E+07

            SET  6        SET  7
         (INFEASIBLE)  (INFEASIBLE)
TNODE2   >  287.97     >  287.98
LOCA       0.50597       0.46543
WID        0.50360E-01   0.57657E-01
DENSUM     0.21220E+07   0.21221E+07

SELECT AND SAVE THE BEST   6 DESIGN SETS FOR SUBSEQUENT OPTIMIZATION LOOPING

REMOVED DESIGN SET   6 (DENSUM  = 0.21220E+07)


LIST OPTIMIZATION SETS FROM SET   1 TO SET   7, AND SHOW ONLY OPTIMIZATION PARAMETERS

            SET  1        SET  2        SET  3        SET  4        SET  5
         (INFEASIBLE)  (INFEASIBLE)  (FEASIBLE)    (INFEASIBLE)  (INFEASIBLE)
TNODE2   >  287.97     >  287.97        280.53     >  287.97     >  287.97
LOCA       0.54000       0.54000       0.54000       0.52201       0.51885
WID        0.50000E-01   0.50000E-01   0.50000E-01   0.49615E-01   0.50640E-01
DENSUM     0.21215E+07   0.21215E+07   0.21169E+07   0.21218E+07   0.21218E+07

            SET  6        SET  7
         (INFEASIBLE)  (INFEASIBLE)
TNODE2   >  287.98     >  287.98
LOCA       0.46543       0.47732
WID        0.57657E-01   0.43399E-01
DENSUM     0.21221E+07   0.21233E+07

SELECT AND SAVE THE BEST   6 DESIGN SETS FOR SUBSEQUENT OPTIMIZATION LOOPING

REMOVED DESIGN SET   6 (DENSUM  = 0.21221E+07)


 BEST VARIABLES ARE

            SET  3
         (FEASIBLE)
TNODE2      280.53
LOCA       0.54000
WID        0.50000E-01
DENSUM     0.21169E+07


******  SUMMARY OF CONSTRAINTS (IF ANY) EVALUATED AT THE CURRENT OPTIMAL SOLUTION  ******


******  DESIGN SENSITIVITY SUMMARY TABLE  ******

   DERIVATIVES ARE EVALUATED AT THE CURRENT OPTIMAL DESIGN VECTOR


             DENSUM      TNODE2
 LOCA     -0.1046E+06  -5521.
 WID           0.      0.1179E+05

LIST OPTIMIZATION SETS FROM SET   1 TO SET   7, AND SHOW ONLY OPTIMIZATION PARAMETERS

            SET  1        SET  2        SET  3        SET  4        SET  5
         (INFEASIBLE)  (INFEASIBLE)  (FEASIBLE)    (INFEASIBLE)  (INFEASIBLE)
TNODE2   >  287.97     >  287.97        280.53     >  287.97     >  287.97
LOCA       0.54000       0.54000       0.54000       0.52201       0.51885
WID        0.50000E-01   0.50000E-01   0.50000E-01   0.49615E-01   0.50640E-01
DENSUM     0.21215E+07   0.21215E+07   0.21169E+07   0.21218E+07   0.21218E+07
```

```
            SET  6          SET  7
          (INFEASIBLE)  (INFEASIBLE)
TNODE2    >  287.98     >  287.97
LOCA        0.47732       0.54224
WID         0.43399E-01   0.48604E-01
DENSUM      0.21233E+07   0.21216E+07


***** ROUTINE COMPLETED *****  CP =       1935.560

LIST OPTIMIZATION SETS FROM SET   1 TO SET   6, AND SHOW ONLY OPTIMIZATION PARAMETERS

            SET  1          SET  2          SET  3          SET  4          SET  5
          (INFEASIBLE)  (INFEASIBLE)  (FEASIBLE)    (INFEASIBLE)  (INFEASIBLE)
TNODE2    >  287.97     >  287.97       280.53      >  287.97     >  287.97
LOCA        0.54000       0.54000       0.54000       0.52201       0.51885
WID         0.50000E-01   0.50000E-01   0.50000E-01   0.49615E-01   0.50640E-01
DENSUM      0.21215E+07   0.21215E+07   0.21169E+07   0.21218E+07   0.21218E+07

            SET  6
          (INFEASIBLE)
TNODE2    >  287.97
LOCA        0.50597
WID         0.50360E-01
DENSUM      0.21220E+07

*** EXIT FROM ANSYS DESIGN OPTIMIZATION (/OPT) ***


***** ROUTINE COMPLETED *****  CP =          1.490


LIST OPTIMIZATION SETS FROM SET   1 TO SET  15, AND SHOW ONLY OPTIMIZATION PARAMETERS

            SET  1          SET  2          SET  3          SET  4          SET  5
          (INFEASIBLE)  (INFEASIBLE)  (FEASIBLE)    (FEASIBLE)    (FEASIBLE)
TNODE2    >  278.00     >  278.00       281.75        282.28        281.75
LOCA        0.50000       0.50000       0.87000       0.89000       0.54000
WID         0.60000E-01   0.60000E-01   0.40000E-01   0.40000E-01   0.56000E-01
C           0.12000E+11   0.12000E+11   0.65700E+10   0.60000E+10   0.98300E+10
DENSUM      0.21192E+07   0.21192E+07   0.21172E+07   0.21171E+07   0.21196E+07

            SET  6          SET  7          SET  8          SET  9          SET 10
          (INFEASIBLE)  (INFEASIBLE)  (INFEASIBLE)  (FEASIBLE)    (INFEASIBLE)
TNODE2    >  278.00     >  278.00     >  278.01       280.08      >  279.61
LOCA        0.80830       0.71542       0.80871       0.89675       0.89823
WID         0.40145E-01   0.44566E-01   0.15183E-01   0.41279E-01   0.41337E-01
C           0.39023E+11   0.61556E+11   0.46972E+11   0.60355E+10   0.60794E+10
DENSUM      0.21168E+07   0.21174E+07   0.21168E+07   0.21170E+07   0.21169E+07

            SET 11          SET 12          SET 13          SET 14          SET 15
          (INFEASIBLE)  (INFEASIBLE)  (INFEASIBLE)  (INFEASIBLE)  (INFEASIBLE)
TNODE2    >  279.97     >  279.79     >  279.78     >  279.41     >  279.97
LOCA        0.89745       0.89820       0.89723       0.89810       0.89715
WID         0.41281E-01   0.41284E-01   0.41276E-01   0.41259E-01   0.41268E-01
C           0.60422E+10   0.60649E+10   0.60413E+10   0.60519E+10   0.60458E+10
DENSUM      0.21169E+07   0.21169E+07   0.21169E+07   0.21169E+07   0.21169E+07
***** ROUTINE COMPLETED *****  CP =        244.230

LIST OPTIMIZATION SETS FROM SET   1 TO SET  15, AND SHOW ONLY OPTIMIZATION PARAMETERS

            SET  1          SET  2          SET  3          SET  4          SET  5
          (INFEASIBLE)  (INFEASIBLE)  (INFEASIBLE)  (INFEASIBLE)  (INFEASIBLE)
TNODE2    >  278.00     >  278.00     >  287.90     >  278.00     >  278.00
LOCA        0.35000       0.35000       0.87000       0.32000       0.84000
WID         0.64000E-01   0.64000E-01   0.20000E-01   0.65000E-01   0.26000E-01
C           0.32000E+11   0.32000E+11   0.65700E+10   0.62000E+11   0.95300E+11
DENSUM      0.21196E+07   0.21196E+07   0.21187E+07   0.21197E+07   0.21166E+07

            SET  6          SET  7          SET  8          SET  9          SET 10
          (INFEASIBLE)  (INFEASIBLE)  (INFEASIBLE)  (INFEASIBLE)  (INFEASIBLE)
TNODE2    >  278.00     >  278.00     >  278.01     >  278.00     >  278.00
LOCA        0.80830       0.71542       0.80871       0.87099       0.85848
WID         0.40145E-01   0.44566E-01   0.15183E-01   0.19661E-01   0.19902E-01
C           0.39023E+11   0.61556E+11   0.46972E+11   0.47342E+11   0.47231E+11
```

```
DENSUM      0.21168E+07   0.21174E+07   0.21168E+07   0.21164E+07   0.21165E+07
             SET 11        SET 12        SET 13        SET 14        SET 15
          (INFEASIBLE)  (INFEASIBLE)  (INFEASIBLE)  (INFEASIBLE)  (INFEASIBLE)
TNODE2    >  278.00     >  278.01     >  278.01     >  278.01     >  278.01
LOCA        0.83996       0.76105       0.79210       0.78114       0.78066
WID         0.17733E-01   0.15122E-01   0.15165E-01   0.15121E-01   0.15167E-01
C           0.46222E+11   0.75063E+11   0.46861E+11   0.47003E+11   0.47049E+11
DENSUM      0.21167E+07   0.21172E+07   0.21169E+07   0.21170E+07   0.21170E+07

SELECT AND SAVE THE BEST  15 DESIGN SETS FOR SUBSEQUENT OPTIMIZATION LOOPING

LIST OPTIMIZATION SETS FROM SET   1 TO SET  11, AND SHOW ONLY OPTIMIZATION PARAMETERS

             SET  1        SET  2        SET  3        SET  4        SET  5
          (FEASIBLE)    (FEASIBLE)    (INFEASIBLE)  (INFEASIBLE)  (INFEASIBLE)
TNODE2      280.41        280.41     >  278.89     >  279.82     >  286.13
LOCA        0.54000       0.54000       0.54000       0.45000       0.44000
WID         0.50000E-01   0.50000E-01   0.35000E-01   0.45000E-01   0.40000E-01
C           0.11300E+11   0.11300E+11   0.17000E+11   0.15000E+11   0.15300E+11
DENSUM      0.21194E+07   0.21194E+07   0.21192E+07   0.21199E+07   0.21203E+07

             SET  6        SET  7        SET  8        SET  9        SET 10
          (INFEASIBLE)  (FEASIBLE)    (INFEASIBLE)  (FEASIBLE)    (FEASIBLE)
TNODE2    >  278.96       281.56     >  283.74       280.27        281.19
LOCA        0.75348       0.60092       0.79124       0.65404       0.80779
WID         0.46364E-01   0.48817E-01   0.45352E-01   0.49207E-01   0.44818E-01
C           0.81771E+10   0.10162E+11   0.68043E+10   0.92967E+10   0.69509E+10
DENSUM      0.21179E+07   0.21191E+07   0.21178E+07   0.21187E+07   0.21176E+07

             SET 11
          (INFEASIBLE)
TNODE2    >  278.06
LOCA        0.87957
WID         0.48236E-01
C           0.52832E+10
DENSUM      0.21169E+07

SELECT AND SAVE THE BEST   6 DESIGN SETS FOR SUBSEQUENT OPTIMIZATION LOOPING

REMOVED DESIGN SET   5 (DENSUM  = 0.21203E+07)

REMOVED DESIGN SET   4 (DENSUM  = 0.21199E+07)

REMOVED DESIGN SET   3 (DENSUM  = 0.21192E+07)

REMOVED DESIGN SET   1 (DENSUM  = 0.21194E+07)

REMOVED DESIGN SET   2 (DENSUM  = 0.21194E+07)


DESIGN SET   5  IS THE BEST DESIGN WITH DENSUM  = 0.21176E+07 (FEASIBLE)

STATE VARIABLE VIOLATION FOR DESIGN SET   6 (TNODE2  =  278.062    )

LIST OPTIMIZATION SETS FROM SET   1 TO SET  10, AND SHOW ONLY OPTIMIZATION PARAMETERS

             SET  1        SET  2        SET  3        SET  4        SET  5
          (INFEASIBLE)  (FEASIBLE)    (INFEASIBLE)  (FEASIBLE)    (FEASIBLE)
TNODE2    >  278.96       281.56     >  283.74       280.27        281.19
LOCA        0.75348       0.60092       0.79124       0.65404       0.80779
WID         0.46364E-01   0.48817E-01   0.45352E-01   0.49207E-01   0.44818E-01
C           0.81771E+10   0.10162E+11   0.68043E+10   0.92967E+10   0.69509E+10
DENSUM      0.21179E+07   0.21191E+07   0.21178E+07   0.21187E+07   0.21176E+07

             SET  6        SET  7        SET  8        SET  9        SET 10
          (INFEASIBLE)  (INFEASIBLE)  (FEASIBLE)    (INFEASIBLE)  (FEASIBLE)
TNODE2    >  278.06     >  278.06       280.45     >  285.07       280.91
LOCA        0.87957       0.87957       0.82930       0.87908       0.83263
WID         0.48236E-01   0.48236E-01   0.45395E-01   0.38254E-01   0.45450E-01
C           0.52832E+10   0.52832E+10   0.65585E+10   0.49843E+10   0.64389E+10
DENSUM      0.21169E+07   0.21169E+07   0.21174E+07   0.21174E+07   0.21174E+07
```